

EXTREME SEA LEVELS AROUND THE COAST OF SOUTHERN AFRICA

SARAH SEARSON

A Thesis submitted to the Faculty of Science at the University of Cape Town in
fulfillment of the requirements for the degree of Master of Science

June 1994

The University of Cape Town has been given
the right to reproduce this thesis in whole
or in part. Copyright is held by the author.

The copyright of this thesis vests in the author. No quotation from it or information derived from it is to be published without full acknowledgement of the source. The thesis is to be used for private study or non-commercial research purposes only.

Published by the University of Cape Town (UCT) in terms of the non-exclusive license granted to UCT by the author.

CONTENTS

	Page
Abstract	i
List of figures	ii
List of tables	iv
CHAPTER 1 INTRODUCTION	1
CHAPTER 2 TIDES	16
2.1 TIDE PRODUCING FORCES	16
2.2 TIDAL CYCLES	19
2.3 HARMONIC ANALYSIS	24
2.4 OBSERVED RESPONSES	25
CHAPTER 3 DATA AND METHODS	27
3.1 DATA COLLECTION	27
3.2 QUALITY CONTROL	30
3.3 PRELIMINARY PROCESSING	34
3.3.1 Tides	
a) Analysis	
b) Prediction	
3.3.2 Residuals	
3.3.3 Basic statistics	
3.4 METHODS	40
3.4.1 Extremes	
a) Time series analysis	
b) Composition of high sea levels	
c) Specific events	

d) Averaged monthly maxima

3.4.2 Predictive methods

CHAPTER 4 RESULTS	46
4.1 EXPLORATORY STATISTICS	46
4.1.1 Levels	
4.1.2 Residuals	
4.1.3 Tides	
4.2 EXTREMES	53
4.2.1 Time series	
4.2.2 Composition of high sea levels	
4.2.3 Specific events	
4.2.4 Averaged monthly maxima	
4.3 EXTREME VALUE ANALYSIS AND EMPIRICAL DISTRIBUTION	64
4.3.1 a) Simon's Bay	
b) Other ports	
CHAPTER 5 DISCUSSION	75
REFERENCES	95
Acknowledgements	100

ABSTRACT

Tide gauge data from ten ports around the coast of Southern Africa are used to study the nature and behaviour of extreme high sea levels with a view towards predicting the likelihood of extremes occurring in the future.

A recorded sea level height can be thought of as a combination of an astronomical tide and a weather determined component. In Southern Africa tides are typically 2 to 2.5 metres in range and the non-tidal residual accounts for up to 50 cm. Sea level is governed by local tides and local meteorology and there is great similarity in the magnitudes and timing at all ports.

However tides are found to be the dominant contribution to extreme levels, hence the long term character of tidal variations is important in Southern African extremes. The fortnightly, equinoctial and 4.4 year tidal cycles determine the expected sea level extremes.

A prediction technique developed here makes use of the tidal dominance by calculating the likelihood of exceedance for a specific month in a particular year. For any month the highest tide is known and an extreme will depend on the necessary surge occurring. Probability is derived from the surge distribution for that month, carried out for each month in a year, and the results presented as an exceedance chart.

LIST OF FIGURES

Figure

- 2.1 Tide producing forces as a resultant of attracting and centrifugal forces along a meridional section through the earth.
- 2.2 Diurnal tide generation (after Pugh 1987, p.82).
- 2.3 Basis of spring-neap tidal variation.
- 2.4 Perigee-syzygy alignments at new and full moon.
- 2.5 Regression of the moon's ascending node.
- 2.6 Example of some tidal characteristics, for February 1993 at Simon's Bay.
- 3.1 Map of Southern Africa showing sites of mechanical tide gauges and AWLR's.
- 3.2 a&b a) Year of hourly true residuals and b) low pass filtered equivalent, for Walvis Bay 1982.
- 4.1 Regional variation of some statistics at ten ports.
- 4.2 Frequency distribution of observed levels at six ports.
- 4.3 Frequency distribution of residuals at six ports.
- 4.4 Frequency distribution of tides at six ports.
- 4.5 a,b&c Monthly maxima from Simon's Bay, a) residuals b) tides and c) observed levels.
- 4.6 Monthly maxima of observed levels at four ports.
- 4.7 Monthly maxima of residuals at four ports.
- 4.8 Tide versus residual for each extreme event at six ports.
- 4.9 a Seven highest surge events at Simon's Bay.
- 4.9 b Seven highest observed events at Simon's Bay.
- 4.9 c Five highest surge events at Port Elizabeth.
- 4.9 d Five highest observed events at Port Elizabeth.

- 4.10 a,b&c Average monthly maxima for five ports, a) observed levels b) tides and c) residuals.
- 4.11 Empirical distributions and Gumbel and GEV asymptotes for thirty annual maxima from Simon's Bay.
- 4.12 Gumbel empirical distributions for three sub-sets of Simon's Bay data: Annual maxima 1960-1990, monthly maxima 1960-1990 and monthly maxima 1980-1990.
- 4.13 Port Diagrams.
- 5.1 Difference in time of arrival of the higher spring high tide of February 9th 1993, from 1993 South African Tide Tables.
- 5.2 Tidal chart of Atlantic and Indian oceans for M_2 , after Cartwright et al 1988.
- 5.3 a&b Simon's Bay: a) Annual maxima observed and annual maxima tidal values and b) long term sea level variation and trend (after Hughes et al 1991).
- 5.4 Monthly maxima tidal predictions for 1993 at Simon's Bay using four different analysis periods and South African Tide Table.
- 5.5 Monthly maxima in predicted tides from 1990-1998 at Simon's Bay.
- 5.6 a,b&c Exceedance charts for a) a 'high' year: 1993 b) an 'average' year and c) a 'low' year: 1995.

LIST OF TABLES

Table

- 3.1 Locations and gauge makes for tide gauge data used in this thesis.
- 3.2 Missing data for Southern African ports by year.
- 3.3 Example of harmonic constituent output from TOGA analysis programs.
- 4.1 Statistics for ten Southern African ports.
- 5.1 Timing of the higher spring high tide of February 9th 1993.
- 5.2 An arbitrary selection of twenty two of the larger constituents and variations in the estimates of their amplitude with analysis year at Simon's Bay.
- 5.3 Percentage likelihood of exceeding HAT (220 cm above CD) for each month 1990-1998 at Simon's Bay.

Chapter 1

INTRODUCTION

The storm of May 1984 is remembered as being particularly destructive on the south and west coasts of South Africa. Substantial damage occurred as a result of high winds, large waves and considerable storm surge (Jury et al 1986). Sea levels were particularly high due to the storm coinciding with spring high tides. A series of lesser storms during the winter of 1989 stripped many beaches of sand (although this was replenished the following summer) and left the Green Point sewage outfall in Cape Town permanently wrecked (Brundrit and Shannon 1989). Excessive rainfall may also create havoc as with Cyclone Domoina in January 1984 which caused extensive damage and loss of life in Natal by the ensuing river floods. Tides had just passed neaps, otherwise coastal damage would have been more severe.

Extreme high sea levels have the potential to cause much environmental and economic damage even in the absence of a severe storm, because smaller waves superimposed on a high background sea level will have a similar effect to larger waves on a lower background level. Both lead to overtopping of defences and the flooding of low lying areas.

Any hard structure situated near the high water mark or on low lying land may be vulnerable, e.g. harbours, houses and roads. Hughes and Brundrit (1992), in providing a Coastal Vulnerability Index (CVI) for the impacts of sea level rise, showed that the greatest hazard in South Africa is from extreme events and

flooding. The CVI depends on local infrastructure and coastal morphology and particularly vulnerable for example is the railway in southern Natal that closely follows the shoreline and private homes on the shores of lagoons and estuaries on the Cape south coast.

Buildings need to be designed and built to survive these extreme conditions. Engineers and planners therefore require estimates of the high sea levels likely to be experienced during the lifetime of the structure in order to incorporate reasonable design protection.

Knowledge of extreme sea level behaviour is not only useful in terms of hazard protection for construction, it may be required in relation to other human activity e.g. harbour management, salvage work, mariculture enterprises or for recreational purposes. From the scientific viewpoint, 'storminess' can also be used as one of the ever increasing number of environmental variables being employed as indicators of global change.

So how can extreme high sea levels be predicted? In order to make future estimates of the recurrence of extremes past data must be analysed, the greater the length of available data the greater the accuracy of the estimates. There are established methods that use a statistical approach to obtain estimates of return periods. Typically the estimated level corresponding to the 1-in-50 year return period is used, i.e. the level that will occur, on average, once every fifty years. These methods require a greater amount of data (twenty-five years) than is generally available at the Southern African sites. Nevertheless, even in the absence of sufficiently long records much useful information on behaviour, cycles and processes involved can still be obtained through a detailed and thorough examination of the sea level record.

Sea level records in Southern Africa consist of hourly data recorded at tide gauges sited at the ports shown in fig. 1.1. The amount of data per port is variable and intermittent but on average spans eleven years. An investigation of the available records can be undertaken with the overall aim of increasing the understanding of extreme sea level behaviour in Southern Africa. Before setting out

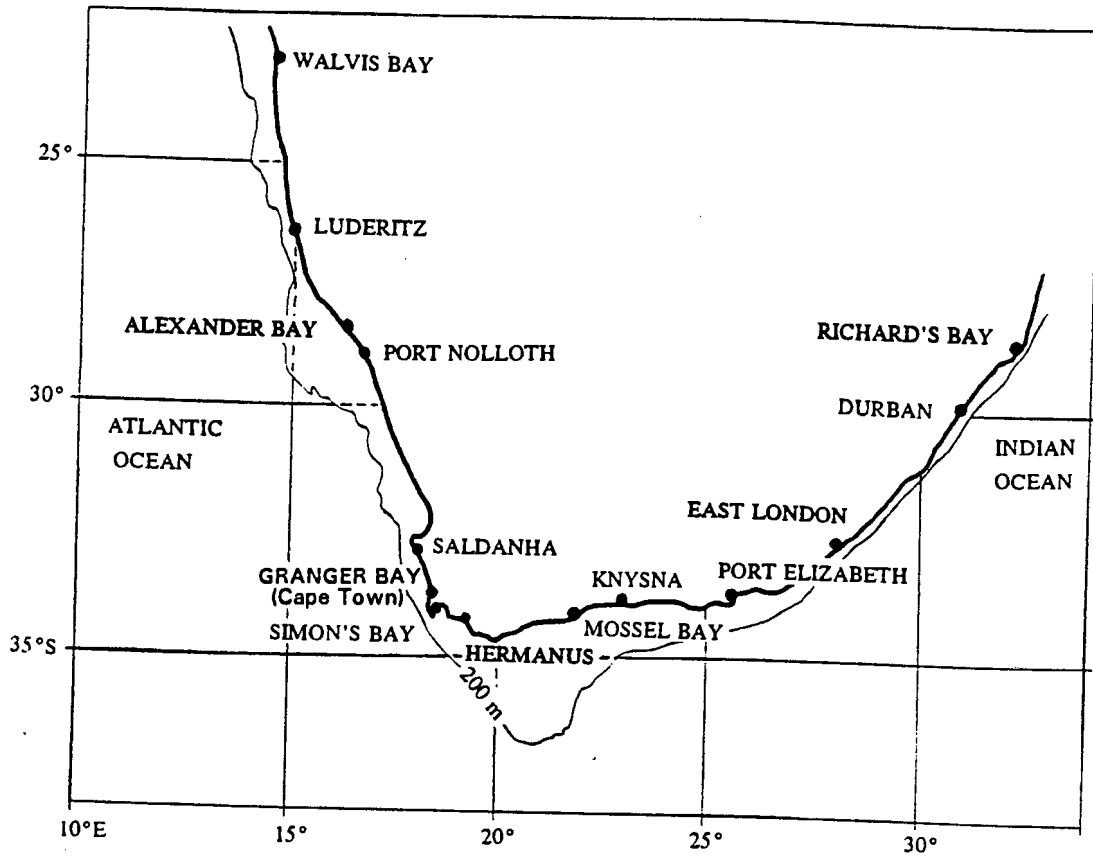


FIG. 1.1 Map of Southern Africa showing tide gauge sites.

the detailed objectives some necessary background information must be provided on sea levels, from both general and specifically Southern African perspectives.

As the first part of the background study the development of tidal knowledge, from ancient beliefs to an increased scientific understanding to the ability to interpret and predict observed behaviour, is put into historical perspective (Cartwright 1980, Deacon 1971, Pugh 1987 and Smith 1973).

Observing and explaining the rise and fall of the sea has been a perplexing problem for centuries. Many ancient civilizations accumulated practical knowledge of tidal patterns for the benefit of primitive fishermen and sea faring people. Some had ingenious explanations to account for their observations, early Arabic belief supposed tides to be due to the warming and expansion of the sea by the moon's rays and the resultant waves rolling towards shore. The earliest hard evidence of the practical application of tidal knowledge comes from the remains of an Harappan tidal dockyard on the river Indus which dates back to 2450 BC. And although an understanding of fundamental causes is not implicit, later Indian societies of the Vedic period (2000-1400 BC) undoubtedly did know of the link between the cycles of the moon and tidal fluctuations (Markanday and Srivastava 1980).

The essence of tides was known to the Greeks and Romans, but generally Mediterranean peoples did not have the motivation of practical necessity to investigate in detail, with the tidal range of water in this land-locked sea being only in the order of 30 cm. However, due to some well travelled philosophers much was known of tides elsewhere. Alexander the Great and his army encountered large tides in the Indus estuary (329-325 BC) and Herodotus (in about 450 BC) noted tidal variations in the Gulf of Suez. Pytheus described the twice daily tides he encountered in the North Atlantic on his trips to Great Britain in about 320 BC. He is credited with making the first systematic observations of tides as well as being the first to relate alternation of spring and neap cycles to the phases of the moon. Aristotle, who died in 322 BC, was unable to explain the tidal currents that ran at Euripus but did know of the coincidence of tides with the phases of the moon.

Although much of the classical writings and postulations are now known to be correct there was also much in error. Pliny the Elder (23-79 AD) who recognised the concepts of age of the tide and equinoctial cycles, also supposed that animals without blood felt the influence of the moon most strongly, whilst Aristotle had proposed that all animals die on the ebbing tide.

There was a decline in critical thinking during the Dark Ages when much classical knowledge of all kinds was lost, but with a few exceptions. Notably the Venerable Bede (circa 720 AD) who conscientiously recorded the tidal fluctuations along the Northumbrian coast of England and Gerald of Wales (1146-1220) who recorded observations of tides adjacent to the Irish Sea.

The arrival of the Renaissance brought renewed attempts at explaining tidal phenomena. The link between the moon and tides was investigated by many during the mid-seventeenth century, including Galileo (who suggested the sea bed induced tidal modifications resulting from the annual and daily rotations of the earth), Descartes (who proposed that the invisible ether of space was compressed under the passage of the moon giving rise to tides) and Kepler who originated the idea of the moon attracting the waters of the earth. But it was Newton, in 1687, who made the major advance in scientific understanding by developing Kepler's laws of planetary motion, establishing the concept of gravitational attraction and proposing the 'Equilibrium Theory of Tides'. The tide producing forces were thus broadly explained using the premise of an ideal earth, completely covered with water and undergoing no inertial effects. However the actual response of the oceans to even this simplified system of forces is still a complicated problem.

Early in the nineteenth century Laplace (1749-1827) laid the foundations for much of the later work by considering the earth's rotation and inertia on a globe covered by water of uniform depth. His treatment of tides as fluids in motion led to the introduction of the Dynamic Theory of Tides in 1775 and with which he progressed some way towards a general solution although it has still not yet been fully achieved.

Compilation of tide predicting tables requires detailed understanding of the relation between water level and phase of the moon and times of high tide to local meridional transit of the moon. The earliest recorded attempts at formulating tidal predictions are Chinese tables dating back to AD 1056 (Zuonsheng Yang et al 1989) and were probably used to assist ancient tourists witness the spectacular river bores near Hangzhou and as an aid to shipping. In Europe in the late twelfth century times of high water at London bridge were given by a simple table consisting of the age of the moon and a corresponding time of high tide, this work was credited to the Abbot of St. Albans John Wallingford who died in 1213. By about 1683 tables were regularly compiled for London and a few other ports, but the assorted methods were often well kept family secrets handed down to each new generation. Until in 1883, the Hydrographic Office of the British Admiralty took over and began to regularly publish national Tide Tables. At present the longest continuous record of sea level is that for the port of Brest, northern France, where tidal heights have been measured since 1806.

The method of harmonic analysis of a series of observations, that of decomposing a tidal record into astronomical components and then recombining them for any future time was developed by Lord Kelvin in about 1867 and this work furthered by, among others, Professor William Ferrel (1817-1891) and Sir George Darwin (1841-1912). The harmonic methods in use today are described in detail by Doodson and Warburg (1941) and further details of the harmonic analysis and prediction used in this thesis is given in Chapter Three, section 3.3.1.

Since the advent of computers tidal harmonic analysis and prediction has been quickly and efficiently performed, but even with precise forecasts of tide the actual sea level differs from that predicted. This non-tidal residual is most often a response to local meteorology, but may in rare instances be due to tsunamis. Depending on local conditions (meteorology, bathymetry, etc.) the magnitude of the non-tidal residual may be up to several metres in extreme cases but is more commonly of the order of up to half a metre.

Tsunamis result from sea floor disturbances such as earthquakes and landslides and are a more common problem in, for example, particular areas of the Pacific Ocean prone to seismic activity. Even without established local 'sources' tsunamis may be experienced far from their point of origin. The effects of the Krakatoa explosion in 1883 were recorded in Port Elizabeth with oscillations ranging five feet (Gill 1883). Tsunamis occur only rarely and little information is known about these events around Southern Africa, hence they are not considered to have direct bearing on the non-tidal component in this thesis.

Thus the observed sea level recorded at a tide gauge in Southern Africa can be thought of as two independent components superimposed on a long term mean sea level: the predictable astronomical tide and a weather determined component. Details of background theory and some relevant observations of the meteorological element are now given.

There are three main elements of meteorology that influence any given sea level: air pressure, wind stress and waves (Pugh 1987, ch. 6). Simultaneous records reveal an inverse relationship between sea level and atmospheric pressure, the theoretical response of sea level is that of an inverted barometer (Robinson 1964), where 1 mb of pressure decrease is equivalent to a 1.01 cm rise in the sea surface. For a typical mid-latitude depression of 980 mb, 33 mb below a Standard Atmosphere of 1013 mb, the implied increase in sea level is 33.3 cm.

Wind stress on a sea surface acts in the direction of the wind and is inversely proportional to water depth. It will therefore be most important when the wind blows over extensive regions of shallow water. There is a transfer of momentum and energy to the surface water which produces a sea surface slope and current. If a component of the wind stress is parallel to a coastline the longshore currents and Ekman transport that are produced lead to further changes in the water level. Briefly, Ekman transport is a net movement of water to the left of wind stress in the Southern Hemisphere (and to the right in the Northern Hemisphere) and depends on such factors as wind strength, latitude (coriolis

parameter) and water depth. Thus Ekman transport due to a longshore wind adjacent to a land mass may pile up water onto the coast or move water offshore (coastal upwelling) depending on wind direction relative to land, and hemisphere, with either transport being in geostrophic equilibrium with the longshore current.

Waves moving from deep water towards a shore also create apparent changes in the mean water level. For a suitably gentle sloping beach i.e. with no wave reflection, it can be shown that outside the line of breakers mean level is depressed. This wave set down is a maximum as the wave breaks, subsequently the surface gradient increases as the wave shoals (wave set up) due to dissipation of the wave energy. These two wave effects are unlikely to be recorded at tide gauges as the recorders are usually sited at locations deliberately protected from wave conditions within harbours. Pugh (1987, p. 228) suggests wave set up may be experienced in some harbours together with the possibility of a disparity between its magnitude at high and low waters, further investigation here is beyond the scope of this thesis.

Observations reveal that atmospheric pressure, wind and sea level are all closely linked. Thus it is not easy to be able to identify the effects of air pressure alone as related wind stresses are also present. Therefore the inverted barometer factor includes a wind stress component so that the theoretical 1.01 cm/mb is not often realised but generally ranges from approximately 0.5 to 2 cm/mb. This under or over compensation depends on time scales and location. At high frequencies (corresponding to periods of minutes) pressure changes are dominant as there is a short response time in the sea level, sometimes these may resonate and become exaggerated producing long period edge waves (Shillington 1984). On longer time scales (days to months) wind stress becomes more important as its response time is longer.

The greatest responses are associated with the deepest depressions which with many close isobars indicates high geostrophic winds, e.g. small intense tropical cyclones. Larger and slower moving mid-latitude depressions are less severe but have an added effect due to their longer lifetime. The local synoptic

situation is clearly important in the character of the weather determined component.

To introduce a Southern African perspective, historical and current knowledge is examined in terms of both the tidal and weather determined components. The work done on sea level extremes follows from this, and as there has not been a great amount of investigation in Southern Africa, an account of international research and application is also presented.

In South Africa the first tidal observations were made at Simon's Bay and Granger Bay between 1835 and 1837 under the direction of the astronomer Sir John Herschel, using tide gauges of his own design (Warner and Warner 1984). Together with similar observations made at twenty-eight sites in the North and South Atlantic Oceans, he and William Whewell (1794-1866) disproved the popular theory that tidal generation occurred solely in the Southern Ocean and subsequently propagated northwards, by showing Cape Town tides to be simultaneous with those on the coast of Portugal.

The British Admiralty measured South African sea levels from the late 1880's and were followed by the South African Railways and Harbours Authority. The South African Navy took over in 1957 and at present the Naval Hydrographer has original tidal charts dating back to the 1930's and all digitised records from the late 1950's. Unfortunately the earlier marigrams were transferred back with the British Admiralty and the Railways and Harbours gauges were neither calibrated or levelled in.

Recent tidal research includes Merry (1982), who assessed the spatial and temporal variations of mean sea level around South Africa with particular attention to the reference of Land Levelling Datum. Rosenthal and Grant (1989) proposed a simplification for the prediction of South African tides using only ten constituents as an easy alternative for the use of researchers.

In the main, sea level research in Southern Africa has tended to target characteristics within the observed and particularly the weather determined

component record. The synoptic coastal weather cycles are known to be important and have been extensively studied in relation to Southern African sea levels, many features in the non-tidal signals have been identified.

Mid-latitude depressions have greatest effect on the coastline during winter when the northward shift of the high pressure zones allows them to pass closer to the sub-continent (De Cuevas 1985). Most ports exhibit a response to this feature and the signal may be followed from port to port as the depression moves along the coast, although it is less prominent at the northern ports of Walvis Bay, Luderitz and Durban. A typical mid-latitude storm may increase sea levels by up to 35-50 cm.

Locally tropical cyclones develop in a region to the northeast of Madagascar then track down the Mozambique Channel. They rarely make landfall and are in general weak by the time they reach South African waters. Hence the only records that should be affected are Durban and Richard's Bay, but evidence of their passage in the sea level record alone is not clear.

Coastal trapped or shelf waves have been examined in detail and several comprehensive accounts of their occurrence, generation and propagation have been written (Schumann 1983, De Cuevas 1985, Schumann and Brink 1990). Generally amplitudes range from 10-50 cm on a time scale of 2-20 days and travelling with speeds of around 5 m/s. Due to seasonal changes in the prevailing synoptic weather conditions there are seasonal differences in shelf waves. During winter such a wave is likely to travel from Walvis Bay to Port Elizabeth forced by the eastward passage of a mid-latitude depression and a coastal low, further propagation is inhibited by interaction with the Agulhas Current (Brink 1990). In summer a coastal trapped wave rarely reaches Port Elizabeth due to a lack of forcing, as the dominant regional meteorology becomes predominantly south/southeasterly winds characteristic of the South Atlantic high.

The seasonal change in prevailing winds also dictates the seasonal presence of upwelling, albeit a negative feature and not directly influential to high extremes in sea level. Winter upwelling is characteristic of the west coast (Walvis Bay and

Luderitz) as the southeasterly winds here are seasonally intensified. On the south coast upwelling generally occurs in summer.

As a point of interest, the examination of long term sea level trends on the west coast led to the discovery of an El Nino type phenomena in the South Atlantic and other environmental variables such as sea surface temperatures and salinities confirmed its presence in the Northern Benguela region (Shannon et al 1986).

Engineers have specific requirements concerning the information needed in regard of marine structures. Design levels and design wave heights are two components of expected conditions likely to be experienced during a structures lifetime. Wijnberg (1993) provided a methodology to obtain estimates of regional design sea levels, whereby the statistical characteristics of sea level were established at three sites (Port Nolloth, Mossel Bay and Richard's Bay representing west, south and east coasts respectively) and applied to a simulation model. From the synthetic results annual maxima and minima were extracted and estimations of extreme sea levels made directly.

Engineering assessments on the extreme design sea levels were compiled for the construction of Koeberg Nuclear power station near Cape Town (WHP 1976), and Dames and Moore (1979) provided the project with estimates of design tsunami levels. Other than these engineering motivated approaches there has been little work carried out on extremes in Southern Africa, however much investigation has been done elsewhere.

Since the early sixties research on the estimation of return periods for high sea levels has concentrated on the coasts of Britain, initiated by the great susceptibility of much of this coastline to disastrous flooding.

Gumbel (1958) and Jenkinson (1955) provided the necessary foundations of theory in Extreme Value and Generalised Extreme Value analysis respectively, which have since been used as the basic means of calculating return periods and the standard by which to judge other methods. Further details are provided in Chapter Three, section 3.4.2.

Lennon (1963) made comparison of six different statistical techniques including Gumbel and Jenkinson's GEV, applied to ports on the west coast of Britain. Suthons (1963) employed only Jenkinson's GEV to data from eleven ports on the south and east coasts of Britain to provide estimates of highest levels to be expected up to 2060. In addition at eight of the sites where maxima showed a rising tendency, he introduced the effects of a long term trend of one foot per century by standardising the observed maxima to a 'standard epoch', 1960. This spate of research was initiated in part by a particularly destructive storm which hit the east coast in the winter of 1953.

Blackman and Graff (1978) updated the work of Lennon (1963) and Suthons (1963) for ten south coast ports on the British coast by making revised estimates of secular trends and this was further expanded to sixty-seven ports in a comprehensive cover of the British Isles by Graff (1981). Graff also extended the original GEV by solving parameters by maximum likelihood and attempted to account for the time dependence (the length and period of data under consideration) of the frequency statistics by compiling partial frequency curves.

Smith (1986) extended the classical analysis of Gumbel to include the use of r largest events per year for sea level data from Venice, a city especially vulnerable to the sea. Parameters of distribution were estimated by an adaptation of a method of maximum likelihood and problems of trend and periodicity within the observed sequence were addressed. Similarly Tawn (1988a) refined the GEV for the r largest events per year. He accounted for dependence in the series of observations based on the concept of standard storm length to 'filter' events such that only independent extremes are obtained.

As development and construction becomes more frequently sited in coastal areas remote from long established tidal sites and hence where annual maxima methods are precluded, there is an increasing need to yield results from short records. A more recent alternative approach has been to consider the sea level sequence as an independent statistical combination of (deterministic) tide and (stochastic) surge. In this way Ackers and Ruxton (1975) calculated combined

probabilities of extreme levels to aid in the design of coastal works in Essex. Furthermore, the effect of wave heights a necessary consideration for the practicalities of coastal development were also incorporated into their determinations of return periods for extreme high sea levels.

Two further methods evolved from this approach: the Extreme Probability Method of Middleton and Thompson (1986) (also used by Hamon and Middleton (1989) on data from Sydney) and the Revised Joint Probabilities Method of Tawn and Vassie (1989). Several problems arising from the latter, namely tide-surge interaction and inclusion of historical data were dealt with by Tawn (1988 b). However the basic limitation is that of using a short data set to represent the distribution of extremes, hence Tawn and Vassie (1990) tested the feasibility of using a site's tidal distribution and transferring a larger surge data set from a nearby location.

From the foregoing summary of past and present Southern African sea level knowledge and the review of extreme sea level research, the objectives of this thesis can now be put into context:

1. To undertake a basic exploration of sea level, tidal and residual data from all possible Southern African locations using standard statistical indicators. Although the primary concern of this thesis is extremes it will be necessary to provide the general setting of sea level, tidal and residual characteristics.
2. To complete a thorough study of the monthly maxima of the sea levels, tides and residuals in order to better understand the structure and behaviour of extremes.
3. To compile Port Diagrams (sea level height versus return period) for the empirical distributions of extremes at all possible Southern African ports. Because of data

limitation, the standard extrapolation methods of Gumbel and Jenkinson can only be applied to Simon's Bay.

To fulfil these goals, and present the results and the ensuing discussion, the thesis is structured in the following manner:

Tides will be shown to be the determining factor in sea levels and sea level extremes, thus the necessary tidal background is given in Chapter Two. This establishes a foundation of pertinent information and terminology which will be required in later chapters.

Chapter Three, Data and Methods, covers details of the raw data, from the collection by the Navy and quality control measures to the generation of simultaneous tidal and residual series. The processes of computer tidal analysis and prediction are presented, with particular attention to detail of the TOGA software package used. The choice of the Doodson filter to obtain residual values, its advantages and disadvantages under available conditions is described. The final preliminary processing is the calculation of basic statistics for each of the three, hourly data sets from all sites.

The methods of analysing the data further fell into two categories, graphical and theoretical. Graphical presentations of monthly observed, residual and tidal maxima facilitate the additional understanding of the behaviour of extremes in observed, tides and residuals. For example, cycles and circumstance of extreme events, and the relative effects of each component in a high sea level. The standard theoretical methods estimate return periods of extreme sea levels from the distribution of annual maxima, they are the Extreme Value and Generalised Extreme Value methods of Gumbel and Jenkinson.

Chapter Four shows the results of the basic statistical and monthly maxima analyses; to aid in the presentation of these results only a representative selection of ports is given. The long term predictions of extremes at Simon's Bay and empirical distributions of all other ports are also displayed.

The results of the previous chapter are collated and commented upon in the discussion, Chapter Five. Three key points emerge:

- There is a large degree of similarity around the coast in the structure of sea levels, and its tidal and weather determined components.
 - The tidal character is of prime importance in the hourly and extreme sea levels.
 - And, over and above set objectives, an alternative means of prediction becomes apparent using particular tidal cycles important in the occurrence of extremes.
- Exceedance charts are constructed to obtain monthly probabilities for extreme high sea levels.

Chapter 2

TIDES

It will become apparent in this thesis that tides are particularly important in the structure of Southern African sea levels and extremes, hence some of the terminology and tidal phenomena will now be introduced in detail as a foundation for work that is utilised and developed in later chapters. Newton's Equilibrium Theory of Tides provides the framework for describing fundamental forces driving various cycles in tides. An account of basic tidal behaviour in terms of the tide producing forces, the concept of harmonic analysis and some observed coastal responses are presented in the following sections.

2.1 TIDE PRODUCING FORCES.

The gravitational attraction of the moon and sun on the earth and the rotational forces involved in the earth moon system, is the primary cause of ocean tides. More specifically it is the different degrees of gravitational attraction experienced at various points on the earth's surface that gives rise to tide producing forces (King 1962, Dietrich et al 1980, Doodson and Warburg 1941). The complexity of the actual and relative motions of the three orbiting bodies are regular and well known which enables the tide producing forces (TPF's) to be

predicted with some assurance. However, the response of the oceans to these forces is not so well understood.

Newton was the first to explain the TPF's in terms of the gravitational attraction of the sun, moon and earth. He developed a theory of equilibrium tide, that which would occur on an ideal earth, completely covered in water and omitting inertial effects. Although only providing a broad description of the TPF's Newton's equilibrium tide succeeds in explaining many of the main lunar and solar cycles and is useful in gaining insight into the general behaviour of tidal phenomena.

Gravitational attraction provides the centripetal force necessary for rotation and is exactly balanced by a centrifugal force, in order to maintain an orbit of stable equilibrium. These total forces are in balance at the common centre of gravity of the earth-moon system which actually lies within the earth. The centrifugal force necessary for any particle on the earth is always the same, as all points describe circles of the same radius about the common centre. It always acts in a direction away from the moon and parallel to a line joining the centres of the two bodies.

Gravitational attraction varies slightly in magnitude and direction with distance from the moon so there will exist an imbalance of forces on the surface of the earth. For points nearer to the moon than the centre of the earth the gravitational attraction will be greater than that necessary to maintain the orbit. For those points further from the moon the centrifugal forces will be greater than the gravitational forces. The differences between the attractive forces necessary for orbit and those actually experienced are the tide producing forces and shown schematically in fig. 2.1.

It can be shown (Pugh 1987 p.63), using G = gravitational constant, a = acceleration due to gravity, M_m = mass of the moon, m = mass of a particle and R = distance between their centres, that the TPF's at P_1 , P_2 and P_3 in fig. 2.1 are given by:

$$\text{TPF at } P_1 = \frac{2 G M_m m a}{R^3}$$

$$\text{TPF at } P_2 = - \frac{2 G M_m m a}{R^3}$$

$$\text{TPF at } P_3 = \frac{G M_m m a}{R^3}$$

So particles at P_1 and P_2 are displaced away from the centre of the earth and those at P_3 towards it, hence an equilibrium shape is maintained assuming static conditions for a fluid earth. It can also be seen that the impact of the sun, some twenty-five million times more massive than the moon has a much reduced effect due to the R^3 term resulting in solar tidal forces being a factor of 0.46 weaker than the moon.

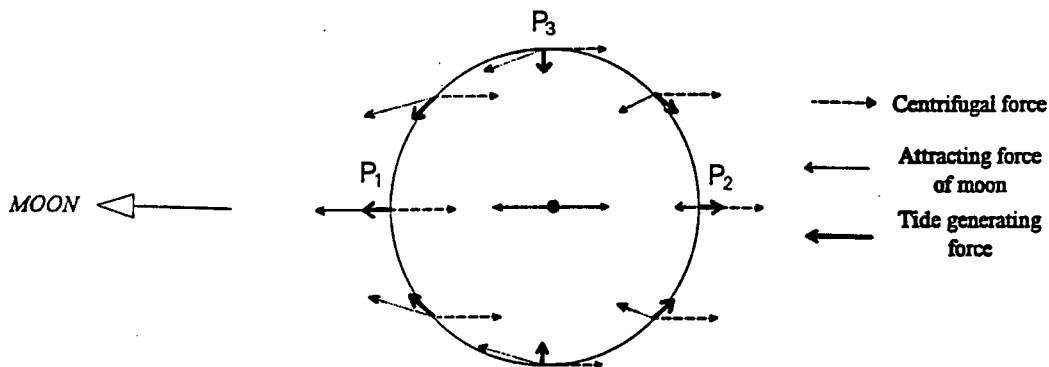


FIG. 2.1 Tide producing forces as a resultant of attracting and centrifugal forces along a meridional section through the earth.

For any point selected at random on the surface of the earth the disturbing force acts at some angle, hence this force may be resolved into horizontal and vertical components. The tide producing forces are very small in magnitude compared with gravitational forces but when they are resolved into vertical and horizontal components, these horizontal 'tractive' forces are of the same order of magnitude as other horizontal forces in the ocean and are crucial in the movement

of water by tidal currents. Whereas the vertical components are overwhelmed by the gravitational attraction of the earth.

Considering the earth as a whole, centrifugal and gravitational forces are in balance and the total TPF is zero, but at no one point is the TPF zero. This tractive (tangential to the earth's surface) force varies and is a maximum at forty-five degrees from the equator. A detailed mathematical analysis is given by Doodson and Warburg (1941).

2.2 TIDAL CYCLES.

If a rotation of the moon around the earth is now introduced in the plane of the equator the system of forces is fixed in relation to the direction of the moon. The effect experienced at any fixed point on the equator is that the TPF's become periodic and produce a twice daily symmetric rise and fall of sea levels as the point moves underneath the envelope of water. This is the basic 12 hour 25 minute oscillation of semi-diurnal tides corresponding to the period of the lunar day.

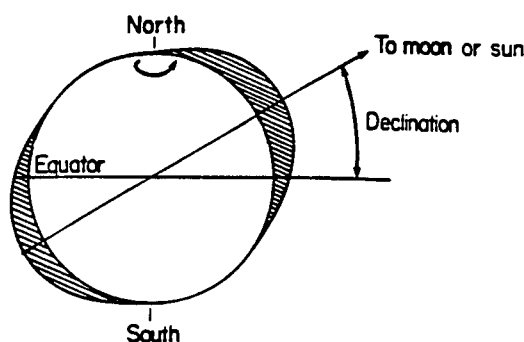


FIG. 2.2 Diurnal tide generation (after Pugh 1987 p.82).

The moon is not always overhead at the equator, but constantly moving north and south in its orbit and more often positioned directly above some other

latitude. Due to this angle of declination measured from the earth's equatorial plane, the bulges are not centred on the equator and successive tides experienced are therefore asymmetric (fig. 2.2). This diurnal (daily) inequality of tidal heights increases with lunar declination and is zero when the moon is overhead at the equator. The equilibrium tide is composed of semi-diurnal and diurnal parts. The diurnal part increases with declination and equals zero at zero declination (the equator), the semi-diurnal part decreases with declination. Pure diurnal tides are not common but in regions where diurnal components are able to dominate or resonate, declinational cycles are important.

A further important characteristic in tidal phenomena is the spring neap cycle which is dependent on the relative positions of the earth, moon and sun and is a semi-monthly variation (fig. 2.3). Spring tides (those with maximum tidal range) arise when all three are aligned in celestial longitude as at New or Full moon and solar and lunar TPF's are compounded. This alignment or syzygy occurs twice in 29.53 days and is a synodic month. Both configurations, the moon 'in front of' or 'behind' the earth lead to spring tides. At first and third quarters the moon and sun are at right angles and the resultant force reduced leading to neap tides (those with small tidal range).

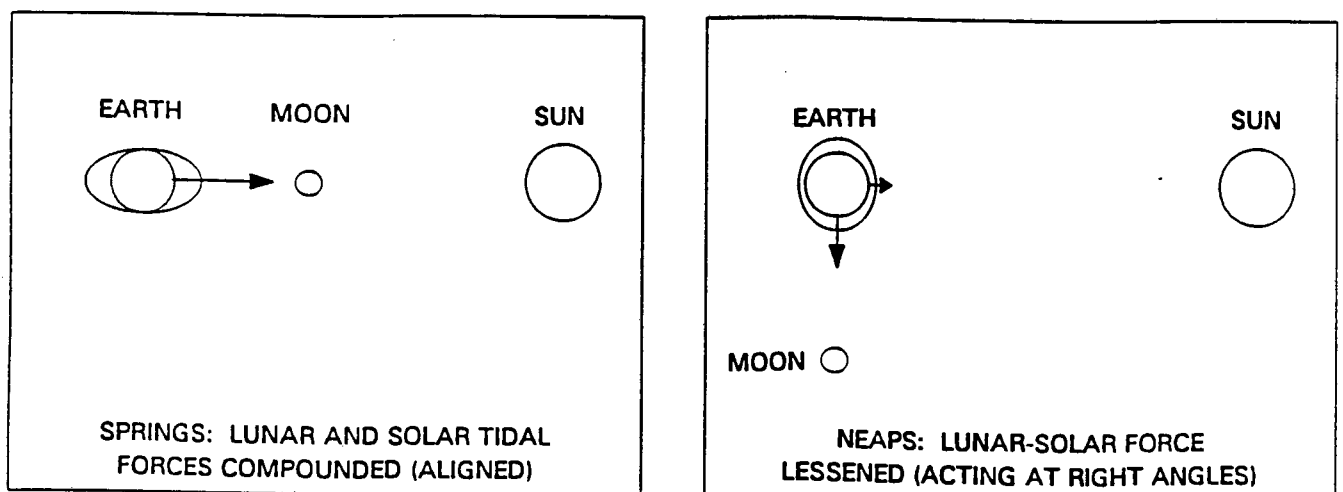


FIG. 2.3 Basis of spring-neap tidal variation. Not to scale.

The moon moves in an elliptic path, the position of it's closest approach to the earth (the perigee), also rotates around the earth. One cycle of the moon from perigee to perigee occurs every 27.55 days or an anomalistic month, compared to a synodic month of 29.53 days. Both motions are 'anti-clockwise' (in fig. 2.4) along the lunar orbit due to the additional movements of the earth's rotation around the sun requiring an extra distance to be covered for the New moon to New moon cycle. A true or sidereal month measured by consecutive conjunctions with a distant, fixed star is 27.32 days. The position of perigee completes one full revolution around the earth in 8.8 years. The two diagrams in fig. 2.4 show two possible configurations of syzygy coincident with perigee, and is based on Wood (1986) figs. 2A and 2B.

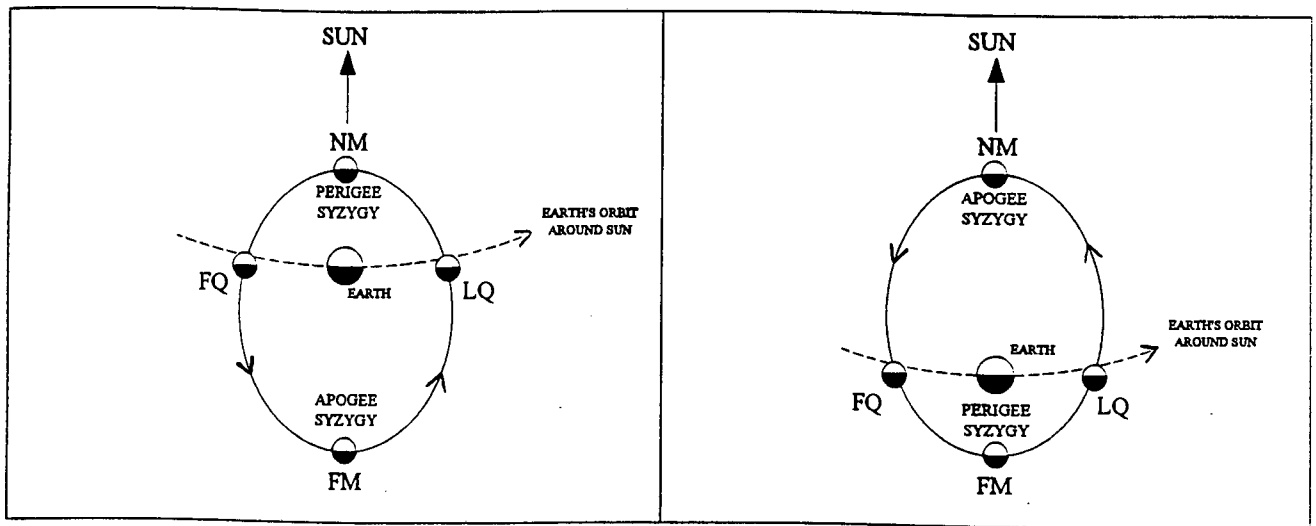


FIG. 2.4 Perigee-syzygy alignments at new and full moon. Elliptical eccentricity and scales have been exaggerated for clarity. NM = new moon, FQ = first quarter, FM = full moon, LQ = last quarter.

The ecliptic plane is defined relative to the earth as the plane of apparent motion of the sun and varies from $+23^{\circ}27'$ to $-23^{\circ}27'$ over half a year. The plane of rotation of the moon is at a constant angle of $5^{\circ}09'$ to the ecliptic but is slowly

rotating westward with a period of 18.6 years. The standard reference point, 'fixed' with respect to the stellar background is usually taken as the vernal equinox also known as the First Point of Aries. The moon's ascending node is that point where the ecliptic is crossed from south to north (i.e. P). These two points and two planes of movement are shown schematically in fig. 2.5a. Beginning with the ascending node at the First Point of Aries, it will slowly move 'backwards' (clockwise) around the ecliptic until it returns to the First Point of Aries 18.6 years later (fig. 2.5b). This movement is generally known as the precession of the moon's ascending node or the Saros Cycle. Hence the maximum angle of declination of the moon relative to the earth can vary from $(23^{\circ}27' + 5^{\circ}09') = 28^{\circ}36'$ to $(23^{\circ}27' - 5^{\circ}09') = 18^{\circ}18'$ over 9.3 years. This cycle will be pronounced in observed tides where diurnal components are able to dominate.

Apparent solar movements have similar, but usually reduced influence. There are diurnal and semi-diurnal factors as for the moon, but with periods related to the solar day. Times of zero solar declination occur at the March and September equinoxes when solar diurnal components are diminished and semi-diurnal components enhanced. There are two further solar variations which have little impact on present day tides but reflect the same orbital characteristics as the moon. They are the precession of the vernal equinox relative to the fixed stellar background which has a period of 26,000 years and the position of closest approach or perihelion (at present January 2nd) which is rotating with a period 20,940 years.

As an example, fig. 2.6 shows some features of the tide experienced at Simon's Bay during February in 1993 together with the corresponding phases of the moon.

One important aspect of observed phenomena is the time lag or age of the tide. The maximum effects of all the above mentioned cycles are observed at some time after the occurrence of maximum TPF's. This is a dynamic response as the equilibrium theory assumes instantaneous reaction of water to the applied forces and does not take into account inertia or frictional effects. The lag may be a few

hours or several days depending on location, and for Simon's Bay is about two days.

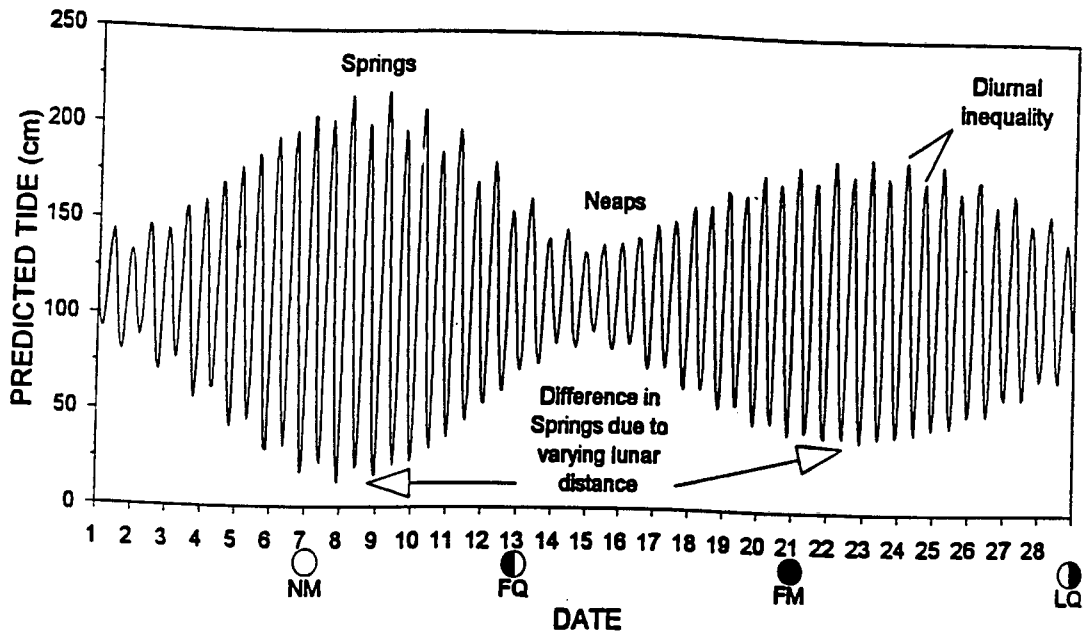


FIG. 2.6 Example of some tidal characteristics, for February 1993 at Simon's Bay. NM = new moon, FQ = first quarter, FM = full moon, LQ = last quarter.

Newton's ideal ocean and equilibrium tide, although greatly simplified explains many features of the tides. In 1775 Laplace introduced the dynamic theory of tides and included the effects of inertia of ocean waters and the earth's rotation. Additional complexity is added by irregular coastlines, alternation of land masses, the varying depth of water, Coriolis and frictional forces. His general equations of dynamic theory have still not been solved.

2.3 HARMONIC ANALYSIS.

The tide can be thought of as the total effect of a large number of regular variations in the motions and positions of the moon and sun, each described by a harmonic constituent with a specific amplitude and phase, of the form:

$$H_n \cos(\sigma_n t - g_n)$$

where H_n is an amplitude, g_n a phase lag on the equilibrium tide at Greenwich, and σ_n an angular speed of the n th constituent. The frequencies of all constituents are well known. Least squares fitting harmonic analysis is carried out on a sufficiently long series of observations in order to calculate the site specific phases and amplitudes of each constituent. In the analysis long term variations (8.8 and 18.6 year cycles) unable to be resolved in the analysis of one years observations are represented by small adjustment factors or nodal corrections, f and u . Each constituent is then represented by:

$$H_n f_n \cos [\sigma_n t - g_n + (V_n + u_n)]$$

where f_n is the nodal factor, u_n the nodal angle and V_n the phase at a specified time zero. Distortions in shallow water can also be expressed as harmonic terms with angular speeds of either sums, differences, or multiples of the speeds of standard constituents.

Once the sea level record has been resolved into a number of harmonics calculation of the astronomical tide can be readily made for any time in the past or future by summing the appropriate contributions from each of the constituents for that hour. There are many constituents available for use, the South African Navy uses 51 in its analysis and prediction of tides, 68 are employed by the software package used in this thesis (further details are found in Chapter Three, section 3.3.1).

2.4 OBSERVED RESPONSES.

Tides vary in character from place to place. Features may be present due to local conditions affecting a particular response to the TPF's. Such local conditions may be bottom topography, shore configuration, gulf or basin shape and size,

friction at sea bed, and areas of shallow water all of which strongly influence the observed tides (e.g. Doodson and Warburg 1941, Pugh 1987).

Double high- or low- waters occur at several locations around the English Channel and North Sea. They are due to shallow water distortions of tidal propagation and the beating of particular constituents' amplitudes and phases.

In more than a dozen estuaries around the world the incoming tide may rush up the river as a wall of water. The better known river bores being of the Severn in the Bristol channel, the Amazon, and the Chien tang kiang river in China. A tidal wave propagating into a narrowing, shoaling estuary tends to increase in amplitude as an effect of the reduction in cross-section i.e. decrease in depth and width (Pugh 1987 p.249-255). Clearly river morphology is a key factor and any alteration due to dredging or silting may cause the occurrence of bores to disappear as happened in the Seine estuary.

In certain seas, for example the Gulf of Mexico and the Java Sea, the diurnal tide is reinforced by resonance within the boundaries to such an extent that it predominates, producing regular tidal curves with one high and one low water every 24 hours 50 minutes. Mixed tides at some Pacific Islands are a broad response of the Pacific as a whole to the diurnal components being large enough to respond better to the diurnal TPF's. Tides of the Atlantic are dominated by semi-diurnal variations suggesting that it is better suited to respond to the semi-diurnal TPF's.

In Tahiti, high tides are observed to occur at the same time each day although the total range is not great. This can be explained if an amphidrome of lunar TPF's (a point in the sea of zero lunar tidal amplitude due to 'cancelling' of lunar constituents) is situated nearby so that solar constituents are able to dominate.

Chapter 3

DATA AND METHODS

3.1 DATA COLLECTION.

Hourly sea level data were obtained from the South African Navy on magnetic tape and floppy disc, for mechanical tide gauges maintained by the Navy's Hydrographic Office. At present the Navy manages mechanical tide gauges at the thirteen ports around South Africa and Namibia shown in fig. 3.1. All thirteen sites are working harbours and the Navy uses the sea level data to update tidal predictions for publication in the annual South African Tide Tables. However only ten ports are used in this thesis mainly because of data availability, these ten locations and the type of tide gauge used at each are given in table 3.1.

Mechanical tide gauges make use of a vertically moving float working within a stilling well. A pen attached to the float continuously records sea level heights on a rotating drum chart which turns once in twenty-four hours. These charts are replaced weekly, then later digitised by visually reading the height off the drum chart trace at hourly intervals, to the nearest centimetre. Sea access to the well is through a small hole below the water line which damps out the effect of external short period fluctuations (ten to twenty second wind-induced waves). The gauges are situated within harbours thereby providing additional shelter from the exposure to wind waves and from the wave set-up experienced on beaches.

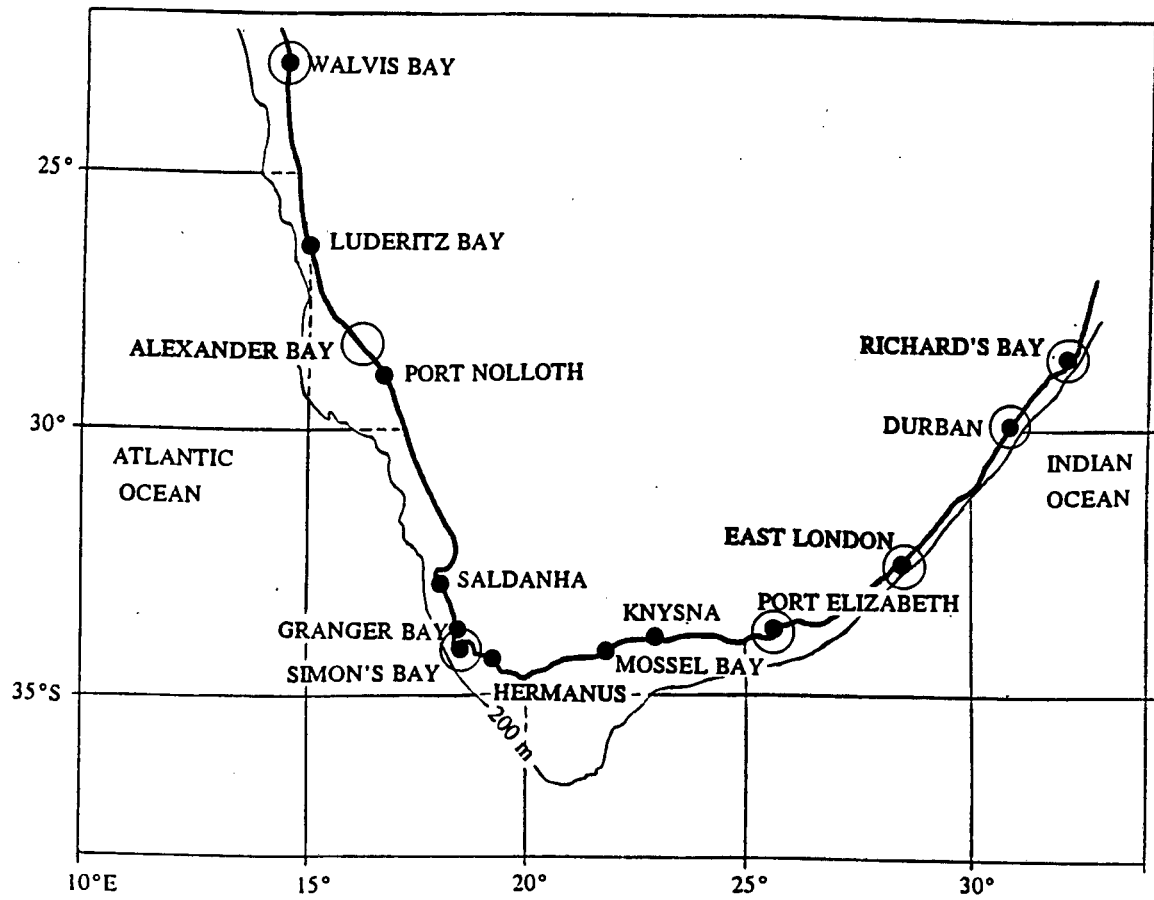


FIG. 3.1 Map of Southern Africa showing sites of mechanical tide gauges (●) and AWLR's (○).

PORT	ID	LOCATION	GAUGE MAKE
Walvis Bay	WB	22°57'S 014°30'E	AOTT
Luderitz	LB	26°39'S 015°09'E	KENT
Port Nolloth	PN	29°15'S 016°52'E	KENT
Saladanha	SA	33°05'S 018°00'E	SAIP
Granger Bay	GB	33°54'S 018°25'E	KENT
Simon's Bay	SB	34°11'S 018°26'E	LEA
Mossel Bay	MB	34°11'S 022°09'E	KENT
Knysna	KN	34°05'S 023°04'E	KENT
Port Elizabeth	PE	33°58'S 025°38'E	AOTT
Durban	DU	29°53'S 031°03'E	KENT

TABLE 3.1 Locations and gauge makes for tide gauge data used in this thesis.

Modern acoustic water level recorders (AWLR) are being phased in and are at present at seven locations: Walvis Bay, Alexander Bay, Simon's Bay, Port Elizabeth, East London, Durban and Richard's Bay. AWLR's utilise timed sound pulses (four per second) to measure the mean height of water in a stilling well, the levels are recorded as one minute means, and stored electronically within the gauge. Time, barometric pressure and sea temperature are also recorded. Each week the information is downloaded via telephone straight to the Hydrographic Office. Acoustic gauges have potential for greater accuracy, time-resolution and accessibility, but problems associated with the large diurnal temperature changes have so far resulted in a lack of reliability and consistency.

Both types of gauge require periodic maintenance, calibration and checks on reference to datum and benchmarks, all of which are carried out every four to six months by the Hydrographic Office. Since 1979, all sea level heights are measured relative to Chart Datum (CD), which is -0.900m from Land Levelling Datum (LLD), except at Luderitz (-0.865m) and Port Nolloth (-0.718m). The results of some later analyses are given using observed levels referenced to LLD to allow direct comparisons between ports to be made.

Digitised historical records exist from the late 1950's and in a few cases back to the late 1930's. However unknown calibrations and many gaps usually mean these early records are inappropriate for analysis. The entire records for East London (1965-1990) and Richard's Bay (1980-1983) were found to contain too many gaps and with too many unknown shifts in datum to be of research quality use and were therefore not included. Hermanus data was not available.

The data used in this thesis are given in table 3.2 for each port by year, with information on the amount missing per year. 100% missing data indicates a data file exists but no 'good' data was recorded. Gaps in table 3.2 indicate that no data was available. Generally, digitised hourly records extend from 1980-1990 except in two cases where they go back further: Port Elizabeth 1979-1990 and Simon's Bay where although existent from 1958 the years 1958, 1959 and 1979 had to be discarded due to unknown datum shifts. There is much missing data at all ports, often worsening towards the late eighties. Good continuous records of sea level are not available, hence data sets are analysed typically including many gaps.

3.2 QUALITY CONTROL.

A simple method of error detection within a time series is to test each value against a linear estimate lying between the values immediately prior to and following the point under consideration. The observed data series were checked for obvious outliers by two Lagrangian formulae suggested by Lennon (1965), which work on observations according to a pre-defined tolerance limit of, in this case, 20 cm. These erroneous points were then interpolated where graphical inspection proved it to be justified. In order to try and improve continuity of the series, any gaps of a few hours or less were also interpolated where appropriate, but as at peak high or low tides where estimation of correct sea level height was deemed unreliable, gaps were left untreated. Nothing was done to longer periods of no

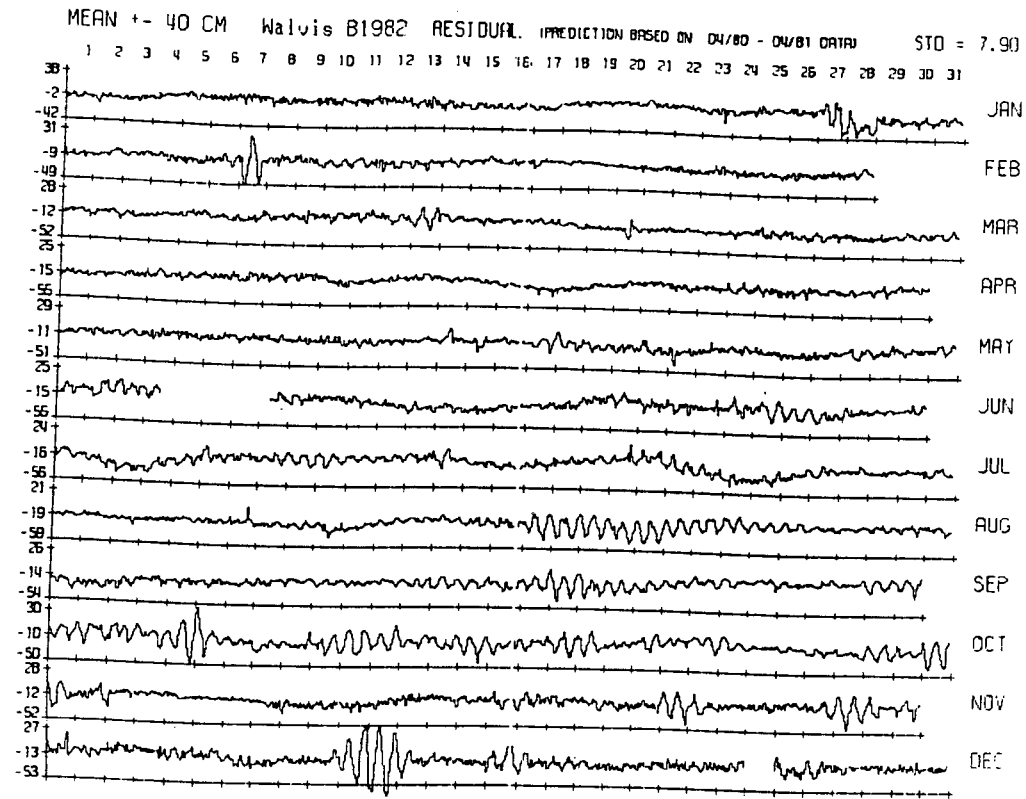
P O R T										
YEAR	WB	LB	PN	SA	GB	SB	MB	KN	PE	DU
1990	100.0	9.7	26.7	0.6	38.0	7.4	1.2		68.3	57.7
1989	74.0	7.5	16.5	5.1	16.6	38.5	3.5		30.0	17.6
1988	35.8	34.8	12.6	8.6	27.8	41.8	27.9		14.9	42.0
1987	28.8	11.1	0.5	5.8	19.2	17.7	4.9		10.6	17.1
1986	12.6	0.7	0.0	11.5	5.3	3.3	0.06		2.2	22.4
1985	3.3	0.0	0.03	0.0	0.0	14.5	0.0	0.0	0.0	53.8
1984	5.0	3.9	3.9	14.9	3.3	6.9	7.5	3.6	3.8	13.9
1983	3.8	5.2	3.0	11.1	3.4	17.8	44.5	3.0	3.6	2.0
1982	1.3	1.0	0.5	44.1	11.5	1.4	0.0	74.4	3.1	0.0
1981	20.5	0.8	8.0	66.6	16.4	0.0	4.4	0.01	11.0	50.0
1980	0.6	9.8	7.9	20.3	8.0	0.3	0.5	0.4	2.9	0.2
1979						100.0			16.0	
1978						0.0				
1977						0.0				
1976						0.0				
1975						0.0				
1974						0.0				
1973						0.0				
1972						0.0				
1971						0.0				
1970						0.0				
1969						0.0				
1968						0.0				
1967						0.0				
1966						0.0				
1965						0.0				
1964						0.0				
1963						0.0				
1962						0.0				
1961						0.0				
1960						0.0				

TABLE 3.2 Missing data for Southern African ports by year. Hours missing as a percentage of total possible hours for that year, gaps indicate no data.

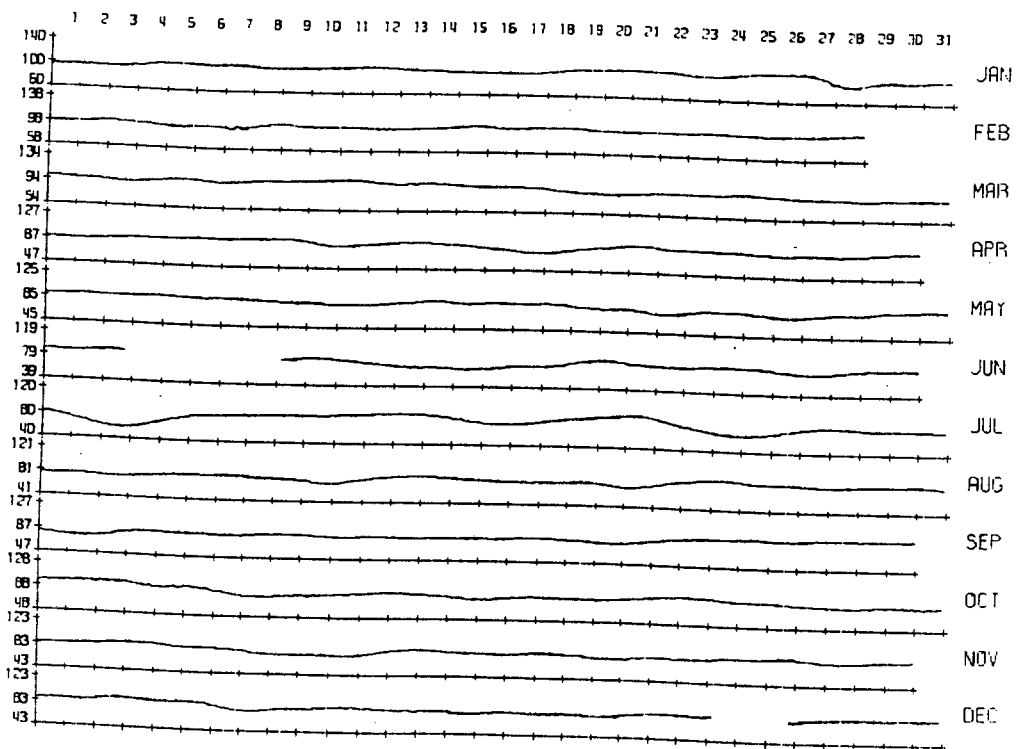
data. Percentages of total missing data varied from 7.24% at Port Nolloth to 25.74% at Walvis Bay. A final visual examination was carried out using computer software which plots the simultaneous data from any three usually adjacent ports. This comparison facilitates the detection of less obvious errors such as phase changes.

Mechanical errors arising from the gauge itself are generally easy to detect, e.g. equipment malfunction, stuck or dry pen, stopped chart drive. Through the digitisation process human errors may result from single values having been miss-read or miss-keyed, or the wrong trace on the marigram followed. These inaccuracies can easily be rectified or deleted. However, timing errors (such as chart not zeroed or secured on the drum correctly, clock running down) are not usually so obvious and get lost in the relatively large variation of the tide. If the tidal prediction is removed from the observed level leaving the 'true' residual, these timing errors of perhaps only a couple of minutes become more apparent. Most ports show sporadic periods of the resulting pseudo semi-diurnal tides in this more sensitive residual record, Middleton and Thompson (1986) noted this same 'residual tide'. Nothing is done to these periods as much data would be lost and in the observed series they are almost undetectable for although the time factor is in slight error the absolute values of observed sea level are not. Furthermore to obtain a more useful residual record a low-pass filter is used to produce a smoother series, and reduce the amount of 'noise'. An example of a particularly bad true residual record and its low pass filtered equivalent are shown in fig. 3.2 a&b for Walvis Bay, 1981.

The two basic problems with using this tide gauge sea level data are the lack of high research quality mostly apparent in the true residual record and the lack of adequate record length or continuity necessary for confident time series analysis. These are two common problems when dealing with physical variables being measured in a harsh environment. The quality of the data must therefore be borne in mind when examining the results of the analysis of the data and the extremes.



a)



b)

FIG. 3.2 a) Year of true residuals and b) low pass filtered equivalent, for Walvis Bay 1982.

3.3 PRELIMINARY PROCESSING.

The hourly sea level data is used to derive two parallel data sets, the simultaneous predicted tidal values and the weather determined variation or residual values.

3.3.1 Tides.

Tidal predictions were made using an interactive software package developed at the TOGA Sea Level Center in collaboration with the National Oceanographic Data Center (Patrick Caldwell (NODC) and Bernard Kilonsky (TSLC), 1988). The package facilitates the use of the tidal prediction programs of the Institute of Ocean Sciences, Victoria, British Columbia and includes a graphics display capability which allows the plotting of any (single) year of hourly observed, predicted or true residual values. An account of the separate analysis and prediction sections in the package is given below, further detailed information on the methods of analysis and a thorough description of programs used is provided by Foreman (1977).

a) Analysis.

The tidal analysis program determines the harmonic constituents for a particular sea level record, which can then be used for the generation of past and future astronomical tides at that site. Three hundred and sixty-six days of apparently good data is recommended, and the selection of a suitable window is aided by the plotting of all available observed data. Gaps are acceptable but should be minimised.

There are two types of constituents, main and shallow water, each treated separately within the program. Processing of main constituents makes use of the concept of satellite components. Each constituent is composed of a major component and one or more satellites, all with similar phase but too close in frequency to be resolved by a year of data. It is assumed that the ratio of satellite amplitude to major component amplitude is equal to the equilibrium ratios, and that each satellite component has the same phase lag relative to the equilibrium tide as

the major component. In this manner, the main component is corrected to obtain the amplitude and phase that would be fitted if the satellites were resolved. Satellites also provide a means for making an adjustment for long term or nodal factors.

The forty-four main constituents may be further divided; the subscript to a designated name of 0, 1 or 2 denotes long period, diurnal and semi-diurnal species (this notation is also extended to higher species). Satellites are not present in any of the seven long period constituents or T_2 , hence in total there are sixty-eight satellite components to thirty-six main constituents.

Shallow water constituents account for the modification of the tidal profile caused by physical processes in shallow water such as bottom friction and depth limitations. These non-astronomical distortions can be expressed by simple harmonics themselves, with angular speeds which are multiples, sums or differences of the speeds of one or more of the main constituents. There are twenty-four shallow water constituents.

Appropriate constituent frequencies are selected for fitting to the data according to the Rayleigh criteria, which requires that constituents be separated by at least a complete period from their neighbours over the length of data used for analysis (the long period constituents are automatically included). Of the sixty-nine constituents in the package, sixty-eight are found to be useable for the Southern African ports.

A least squares fit is made on the observed time series using sines and cosines of constituent frequencies as fitting functions. The Cholesky method of solving symmetric positive definite matrices, with regard to linear least squares problems, is used (Wilkinson 1966).

An output listings file (table 3.3) gives for each constituent uncorrected amplitudes (AL) and phases (GL), corrected amplitudes (A) and phases (G), and the phase relative to the Greenwich meridian (GNWCH) which removes the effect of using local time. All calculated phases are relative to the reference point 0000 01 Jan 1976. The example given is for the period 1/1/81 to 2/1/82 at Simon's Bay.

Simon's Bay Units in CM
 STATION 221 TIME ZONE = 30, LATITUDE = 3411, LONGITUDE = 1826
 NUMBER OF VALID DATA = 8807 AVERAGE =109.10 STANDARD DEVIATION = 43.05
 THEORETICAL RMS = 9.23 MATRIX CONDITION = .82
 ANALYSIS OF HOURLY TIDAL HEIGHTS STN 221 1H 1/1/81 TO 24H 2/1/82
 NO.OBS.= 8808 NO.PTS.ANAL.= 8808 MIDPT=12H 3/7/81 SEPARATION =1.00

NAME	FREQUENCY	STN	M-Y	M-Y	AL	GL	A	G	GNWCH
1 Z0	0.000000	221	181	182	109.0712	360.00	109.0712	360.00	360.00
2 SA	0.000114	221	181	182	1.2645	191.08	1.2645	9.89	11.12
3 SSA	0.000228	221	181	182	1.6499	72.84	1.6499	275.70	278.17
4 MSM	0.001310	221	181	182	0.8463	156.08	0.8463	122.51	136.66
5 MM	0.001512	221	181	182	0.8562	262.84	0.8562	330.71	347.04
6 MSF	0.002822	221	181	182	0.8666	135.53	0.8666	169.83	200.31
7 MF	0.003050	221	181	182	0.6871	188.97	0.6871	66.13	99.07
8 ALP1	0.034397	221	181	182	0.1188	309.51	0.1287	172.15	183.63
9 2Q1	0.035706	221	181	182	0.1513	38.70	0.1624	228.22	253.84
10 SIG1	0.035909	221	181	182	0.1095	305.65	0.1192	235.51	263.33
11 Q1	0.037219	221	181	182	0.7447	357.44	0.8070	254.26	296.22
12 RHO1	0.037421	221	181	182	0.0656	264.95	0.0705	259.20	303.34
13 O1	0.038731	221	181	182	1.4771	292.84	1.6171	257.10	315.40
14 TAU1	0.038959	221	181	182	0.1061	345.17	0.0946	326.99	27.75
15 BET1	0.040040	221	181	182	0.0261	87.57	0.0291	200.52	272.96
16 NO1	0.040269	221	181	182	0.4885	285.86	0.4801	194.05	268.95
17 CHI1	0.040471	221	181	182	0.0638	56.52	0.0693	88.49	165.58
18 PI1	0.041439	221	181	182	0.0135	182.44	0.0135	351.83	79.36
19 P1	0.041553	221	181	182	1.4943	155.42	1.4853	143.34	232.11
20 S1	0.041667	221	181	182	0.1213	266.68	0.1694	113.28	203.28
21 K1	0.041781	221	181	182	5.7339	141.10	6.0493	144.43	235.67
22 PSI1	0.041895	221	181	182	0.2631	280.05	0.2658	109.37	201.84
23 PHI1	0.042009	221	181	182	0.0527	237.83	0.0526	91.83	185.53
24 THE1	0.043091	221	181	182	0.2066	181.80	0.2171	148.35	253.73
25 J1	0.043293	221	181	182	0.6064	104.74	0.6393	170.22	277.79
26 SO1	0.044603	221	181	182	0.1328	197.09	0.1455	232.93	354.63
27 OO1	0.044831	221	181	182	0.3483	353.99	0.4515	197.51	321.68
28 UPS1	0.046343	221	181	182	0.1266	286.70	0.1661	203.40	343.91
29 OQ2	0.075975	221	181	182	0.2852	281.15	0.2501	46.46	146.99
30 EPS2	0.076177	221	181	182	0.6359	191.86	0.6026	55.90	158.62
31 2N2	0.077487	221	181	182	1.8150	239.53	1.6712	71.23	188.09
32 MU2	0.077689	221	181	182	1.9798	133.20	1.9225	63.43	182.47
33 N2	0.078999	221	181	182	11.7516	191.19	11.4845	87.08	220.27
34 NU2	0.079202	221	181	182	1.9086	79.63	1.8690	77.22	212.60
35 H1	0.080397	221	181	182	0.5024	212.23	0.4826	176.15	324.44
36 M2	0.080511	221	181	182	52.6032	128.93	51.5211	92.79	242.31
37 H2	0.080625	221	181	182	0.5189	281.64	0.5128	65.11	215.87
38 MKS2	0.080740	221	181	182	1.2523	201.10	1.4252	352.00	143.99
39 LDA2	0.081821	221	181	182	0.2452	32.14	0.2392	142.16	305.83
40 L2	0.082024	221	181	182	1.3535	237.02	1.3496	77.31	243.17
41 T2	0.083219	221	181	182	1.1731	288.49	1.1731	109.68	288.45
42 S2	0.083333	221	181	182	23.2077	114.33	23.2332	114.44	294.44
43 R2	0.083447	221	181	182	0.2953	197.42	0.2387	201.89	23.12
44 K2	0.083561	221	181	182	5.6142	279.44	6.5164	106.58	289.05
45 MSN2	0.084845	221	181	182	0.3107	188.47	0.2977	256.55	92.88
46 ETA2	0.085074	221	181	182	0.3519	228.56	0.3973	110.66	309.45
47 MO3	0.119242	221	181	182	0.0885	153.94	0.0948	82.07	289.88
48 M3	0.120767	221	181	182	0.6024	65.11	0.5839	11.02	235.31
49 SO3	0.122064	221	181	182	0.0317	334.26	0.0347	298.63	176.92
50 MK3	0.122292	221	181	182	0.0341	333.52	0.0353	300.71	181.46
51 SK3	0.125114	221	181	182	0.2260	138.63	0.2387	142.07	53.30
52 MN4	0.159511	221	181	182	0.3609	257.87	0.3454	117.62	40.33
53 M4	0.161023	221	181	182	0.6605	243.99	0.6336	171.71	110.75
54 SN4	0.162333	221	181	182	0.0264	76.37	0.0258	332.37	285.56
55 MS4	0.163845	221	181	182	0.4743	270.09	0.4651	234.06	203.58
56 MK4	0.164073	221	181	182	0.1141	97.29	0.1297	248.30	220.29
57 S4	0.166667	221	181	182	0.1230	312.26	0.1232	312.47	312.47
58 SK4	0.166895	221	181	182	0.0813	79.80	0.0945	267.05	269.51
59 2MK5	0.202804	221	181	182	0.0842	131.39	0.0852	62.44	92.72
60 2SK5	0.208447	221	181	182	0.0386	311.57	0.0408	315.11	46.35
61 2MN6	0.240022	221	181	182	0.0423	213.06	0.0396	36.67	108.91
62 M6	0.241534	221	181	182	0.0903	142.01	0.0848	33.59	122.16
63 2MS6	0.244356	221	181	182	0.1455	205.25	0.1397	133.08	252.13
64 2MK6	0.244584	221	181	182	0.0269	299.88	0.0300	54.75	176.26
65 2SM6	0.247178	221	181	182	0.0217	169.01	0.0213	133.08	282.60
66 MSK6	0.247406	221	181	182	0.0214	213.84	0.0243	4.96	156.94
67 3MK7	0.283315	221	181	182	0.0352	243.36	0.0349	138.28	318.08
68 M8	0.322046	221	181	182	0.0900	85.21	0.0828	300.66	178.75

TABLE 3.3 Example of harmonic constituent output from TOGA analysis programs. Derived from the period 1/1/81 to 2/1/82 at Simon's Bay.

Long term modulations which cannot be resolved as independent constituents from one year of data are represented as nodal factors f and u , so that the harmonic expansion is written as:

$$AL_n f_n \cos [\sigma_n t - GNWCH_n + (V_n + u_n)]$$

where

f_n is the nodal factor,

u_n the nodal angle,

V_n the astronomical argument adjustment for phase at the specified time zero
0000 01 Jan 1976,

AL_n the amplitude of constituent n ,

$GNWCH_n$ a phase lag on the equilibrium tide at the Greenwich meridian,

and σ_n is the angular speed in degrees.

Angular speeds converted to radians per unit time using $(2 \sigma_n) / 360 = \omega_n$
have the general form:

$$\omega_n = i_a \omega_1 + i_b \omega_2 + i_c \omega_3 + i_d \omega_4 + i_e \omega_5 + i_f \omega_6$$

where ω_{1-6} are the angular speeds calculated from astronomical arguments with known rates of change and the coefficients i_{a-f} are small integers known as the Doodson numbers, the value of i_a defining the species.

The angular speeds ω_{1-6} are the mean rates of change with time of the astronomical coordinates TAU, SO, HO, PO, ENPO and PPO, where:

TAU is the lunar time,

SO the mean longitude of the moon relative to 0000 1/1/76 (i.e. a tropical month
27.32 days),

HO the mean longitude of the sun (a tropical year 365.24 days),

PO the mean longitude of the lunar perigee (8.8 years),

ENPO (negative of) the mean longitude of the ascending lunar node (18.6 years),

and PPO the mean longitude of solar perihelion (20,940 years).

The Doodson numbers allocated to each constituent therefore allow for the inclusion of the long term cycles into the harmonic equation as nodal factors.

Satellite information provided in the package includes the changes to the last three Doodson numbers i_{d-f} of its main constituent, thus a factor may be present in a main or satellite component or both. The ENPO factor (18.6 year variation) is not present in any main constituent (Doodson numbers i_e all 0), but is contained in at least one satellite of each main constituent, hence this factor is incorporated into a total of thirty-six main constituents. The PO factor (8.8 year variation) is accommodated in thirty-three main constituents, of which twelve are from satellite(s) only. The PPO modulation is represented in twelve constituents.

The nodal corrections and arguments are calculated for the mid-point of the analysis year relative to the time zero of 0000 01 Jan 1976 and then removed from each constituent. For the main constituents only V , the astronomical argument adjustment for phase is calculated. The nodal amplitude corrections, f and $(V + u)$ are calculated for all satellites and hence included into the main constituent. The shallow water term's nodal corrections are the combined factors of all its component main constituents, and all contain the ENPO and PO factors.

b) Prediction.

From the harmonics listing output of the analysis stage the corrected or base value of amplitude, A , and Greenwich phase lag, $GNWCH$, are used. Each constituent's contribution is summed to give a total tidal height:

$$T(t) = Z_0 + \sum AL_n f_n \cos [\sigma_n t - GNWCH_n + (V_n + u_n)]$$

where $T(t)$ is the total tide, Z_0 (the first constituent) is the mean level and the summation is for all constituents.

In the analytical stage the relevant factors (and the astronomical arguments) were calculated for the mid-point of the analysis year and then removed from the amplitude (AL) and phase (GL) of the constituent. These corrected values, A and G , are then used in the prediction stage to calculate a sea level, the factors (and

arguments) are recalculated for the sixteenth of each month of the year to be predicted and combined with the 'corrected' amplitude and phase, for each constituent, to give a total contribution. Phases are again calculated relative to 0000 01 Jan 1976.

The main requirement for the analysis and fitting of the harmonics was the need for as much data as possible within a twelve month period. A set of hourly predictions for 1970-1990 covering the long term nodal factor of 18.6 years was generated in order to obtain the full distribution of tidal values.

3.3.2 Residuals.

The true residual record is noisy as it is very sensitive to the quality of the observed record, especially timing errors from the tide gauge. A lot of this noise is spurious, hence in order to obtain a more useful record representative of the non-tidal residual, a low-pass numerical filter is used on the hourly observed levels to smooth out the series.

The procedure employed was the X_0 weighted numerical filter of Doodson and Warburg (1941), which uses only thirty-nine hours and applies weights of 0, 1, or 2 to each of the hourly values. When applied to the sea level sequence, this X_0 filter effectively averages out the main diurnal and semi-diurnal lunar and solar constituents. The series is then representative of the variation of the non-tidal or weather determined component. Residual values calculated by the Doodson filter are referenced the same as the observed levels which in this case is to local Chart Datum, absolute values necessary for direct comparisons are found by subtracting the port's (arithmetic) mean level.

The amplitude response function of the Doodson filter does not have as sharp a cut off as longer 72 or 168 hour filters, and contains finite values at a frequency equivalent to a period of 2.6 hours. However, although many filters exist which would more satisfactorily smooth the sea level series the Doodson filter is simple to apply and is most suitable for data containing gaps as only nineteen hours of data is lost at the beginning and end of a data series.

Further references to 'residuals' implies the values calculated from the Doodson filter, 'true residual' is the term used for the difference between the value of an observed sea level and that of the predicted tide. 'Surge' is sometimes used to indicate a single positive event in the residual series.

3.3.3 Basic Statistics.

For each port there exists a data set of the hourly observed sea level heights, and two simultaneous, derived data sets of hourly residual and hourly tidal values. A year consists of, on average, 8766 hours, a decade nearly ninety thousand. So in order to summarise and interpret this enormous amount of data for each port, and to enable comparisons to be drawn between sites, various statistics can be employed.

Frequency distributions of all hourly values are constructed in order to obtain measures of spread and central tendency for each data set. Fundamental statistics such as mean, standard deviation, maxima, minima, and range are also calculated.

3.4 METHODS.

3.4.1 Extremes.

In order to investigate the behaviour, occurrence and composition of the extreme high sea level events, the unwieldy amount of data can be greatly reduced by the use of monthly maxima. Historically annual maxima of observed sea levels were utilised in standard analyses such as that of Jenkinson (1955), but required a minimum of twenty-five years for significant results. Only Simon's Bay fulfills this requirement with a thirty year data set. Therefore monthly maxima are used to produce sets of extreme values and hence many more data points are available for the empirical analysis. These monthly maxima are checked for independence, such

that two consecutive extremes are not part of the same event from one month to the next.

Only the monthly maxima of observed sea levels are utilised in the determination of empirical distributions and production of Port Diagrams. However monthly maxima of residuals and tidal heights yield interesting, informative and relevant results. The different graphic displays allow alternative interpretations and comparisons to be made on the occurrence and composition of extremes.

a) Time series of monthly maxima.

For Simon's Bay the monthly and annual maxima records of observed sea levels, residuals and tidal values (1960-1990) are plotted. Four other representative ports are also highlighted showing observed and residual maxima; Walvis Bay (1980-1990), Saldanha (1980-1990), Port Elizabeth (1979-1990) and Durban (1980-1990).

b) Composition of high sea levels.

Values of predicted tide and corresponding residual for each observed monthly maxima event, gives an indication of the compositional variability within the data set of observed extremes. For six ports (Walvis Bay, Luderitz, Simon's Bay, Mossel Bay, Knysna and Port Elizabeth) the plots of tide versus residual are used to show the relative contributions to each observed monthly maxima.

c) Specific events.

Seven of the largest surge events at Simon's Bay are shown in detail, similarly the seven largest observed events are examined. A short time series of hourly observed and residual values spanning twenty days shows the context of the extreme, the state of tide, build up of surge and the consequent effect on the observed heights. A study of the five largest residual and observed events at Port Elizabeth is also carried out.

d) Averaged monthly maxima.

All values of monthly maxima for each particular month can be averaged enabling seasonal variations in the extremes to be identified. For six ports these profiles are plotted, January to December, for levels, residuals and tides.

2.4.2 Predictive Methods.

Theory is now given for the standard annual maxima analyses producing empirical distributions and two well-known extrapolation techniques. A fuller development of this extreme value theory is provided by Jenkinson (1955) and Gumbel (1958).

Given a set of annual maxima from a time series of an environmental variable such as rainfall, sea level or temperature, estimates of the extrapolated values of the maximum to be expected during some future period is often required. Gumbel provides the theoretical proof for the approximately linear x,y relation between increasing maximum value and the logarithm of the period.

For a return period of T years, the probability that a given high tide chosen at random will fail to reach a height χ is $1 - (1/705)^T$, (there are on average 705 tides per year). That all tides fail to reach χ is $(1 - (1/705)^T)^{705}$ which can be approximated to $e^{-1/T}$. The probability P that an annual maximum is less than χ , and the associated return period T of height χ are related by the following:

$$\begin{aligned} P &= e^{-1/T} \\ T &= -1 / \ln P \\ \ln T &= -\ln (-\ln P) \end{aligned} \tag{1}$$

These formulae enable the calculation of return periods, provided an acceptable frequency curve of annual maxima can be determined.

In general y will always be increasing with x, but the sign of the small rate of change dy/dx may be used to classify three types of curve; the linear relationship $dy/dx = 0$ being that of the Gumbel distribution (1958). Jenkinson

(1955) suggested a Generalised Extreme Value (GEV) solution to the functional equation of Fisher and Tippett (1928) for extreme values and which explains the nature of these three distributions:

$$x = a (1 - e^{-ky})$$

He showed that for different values of k , all three types of curvature may be described (see Jenkinson's fig. 1, 1955). For negative k , i.e. dy/dx decreasing with increasing x , x has a lower limit but can be considered 'uncontrolled' at the upper bound e.g. rainfall. This is referred to as a Type I curve. Gumbel's straight line is the special case of $k = 0$ (Type II). In nature, k positive (Type III) curves such as wind speeds and pressures are most common as maximum values can be seen to have an upper ceiling.

One of two extremal probabilities are usually chosen to represent the true cumulative frequency. Gumbel estimated the probability of an extreme, χ , being greater than or equal to the m th exceedance to be:

$$H(\chi) = 1 - \frac{m}{N + 1} \quad (2)$$

where N is the number of independent annual maxima, arranged in ascending order χ_m : $m = 1, N$. Jenkinson and others (Lennon 1963, Graff 1981) adopted the compromise frequency of Hazen (1930)

$$H(\chi) = 1 - \frac{m - 1/2}{N} \quad (3)$$

In order to fit a theoretical curve to the empirical points, a function of the probability is used. The reduced variate, $y = -\ln(-\ln P)$ has the advantage of opening out the two ends of the distribution so $y = -\infty$ to $+\infty$ rather than $P = 0$ to 1 . It should be remembered that the probability P of a level failing to reach χ , is equal to $1 - H$, where H is the probability of a level being greater than or equal to χ .

The extremal probability is then given as

$$H(x) = 1 - \exp[-\exp(-y)] \quad (4)$$

Gumbel uses :

$$y = \frac{x - \mu}{\beta} \quad (5)$$

and Jenkinson's GEV uses :

$$y = k \left[\frac{x - \mu}{\beta} \right]^{1/k} \quad (6)$$

where

μ = mode of extremes

β = 0.78 x standard deviation of extremes

$2^k = \sigma_1/\sigma_2$

σ_1 = standard deviation of annual maxima

σ_2 = standard deviation of biannual maxima

Simon's Bay is studied in detail, being the only Southern African port with a suitable length of data with which to apply the extrapolations of Gumbel and Jenkinson. Three data sets are utilised:

1. Annual maxima 1960 - 1990.
2. Monthly maxima 1960 - 1990.
3. Monthly maxima 1980 - 1990.

The annual maxima provide baseline results with which to compare the other two data sets. The long monthly maxima set is used in order to investigate

the possibility of obtaining many more extremes (data points) and the shorter eleven year data set is attempted as this is typical of other Southern African ports' data availability.

Empirical distributions of Gumbel (equation 2) and Hazen (equation 3) and the extrapolations according to Gumbel (equations 4 & 5) and Jenkinson's GEV (equations 4 & 6) are calculated. Results are given in the form of Port Diagrams, plots of sea level height versus return period (from equation 1).

Port Diagrams for the remaining sites are compiled using the empirical distribution of Gumbel. The extrapolation techniques are invalid for short data sets.

CHAPTER 4

RESULTS

To aid readability and reduce an otherwise repetitive presentation of data only a representative selection of ports are shown for each set of analyses, including at least one from each of west, south and east coasts.

4.1 EXPLORATORY STATISTICS.

Basic statistics and frequency distributions of the hourly series of levels, residuals and tides gives a general evaluation of the data. This information is tabulated in table 4.1 and a representation of the spatial variation of some of the statistics is given in fig. 4.1 in order to display broad regional characteristics.

4.1.1 Levels.

The frequency distribution graphs for six sites: Walvis Bay, Luderitz, Saldanha, Mossel Bay, Port Elizabeth and Durban (fig. 4.2) show a dominant bi-modal tidal signature within the observed signal for the west coast sites. This disappears gradually around the south and east coasts, until at Durban there is almost no bi-modal form in the distribution. The profile is particularly noisy at Port Elizabeth due to a change in the digitisation of charts before 1980 when levels were read to the nearest 3 cm.

OBSERVED SEA LEVELS (cm from Land Levelling Datum)										
		MAX	MIN	range	MEAN	STD	MODE	MEDIAN	no. hrs	% missing
Walvis Bay	WB	116	-109	225	2.8	40.17	-21	2	71609	25.74
Luderitz	LB	93	-111	204	-12.4	38.85	14	-13	87157	9.60
Port Nolloth	PN	152	-99	251	18.1	44.43	-8	18	89455	7.24
Saldanha	SA	135	-101	236	16.5	41.48	-6	15	77999	19.12
Granger Bay	GB	149	-110	259	14.9	41.05	-10	14	82677	14.26
Simon's Bay	SB	150	-100	250	17.0	42.26	-14	16/18	249884	8.06
Mossel Bay	MB	183	-116	299	22.0	49.92	28	21	88105	8.63
Knysna	KN	194	-93	287	28.4	46.53	19	28	45130	14.25
Port Elizabeth	PE	166	-101	267	25.7	44.61	26	25	92343	12.21
Durban	DU	159	-112	271	20.0	47.65	36	20	73101	24.19

DOODSON RESIDUAL (cm from mean observed level)										
		MAX	MIN	range	MEAN	STD	skewness	kurtosis	no. hrs	% missing
Walvis Bay	WB	33	-34	67	-0.03	8.64	0.04	-0.23	69182	28.28
Luderitz	LB	25	-32	57	-0.17	7.52	-0.37	0.31	84269	12.62
Port Nolloth	PN	36	-32	68	0.15	7.56	-0.14	1.37	84418	12.46
Saldanha	SA	33	-38	70	-0.09	9.75	-0.21	0.63	74869	22.36
Granger Bay	GB	35	-44	79	-0.18	9.45	-0.25	0.39	75888	21.32
Simon's Bay	SB	39	-38	77	0.01	8.22	-0.44	0.76	247071	9.08
Mossel Bay	MB	43	-39	82	-0.03	11.66	-0.01	0.21	85710	11.12
Knysna	KN	53	-42	95	0.00	12.16	0.29	0.70	44704	15.02
Port Elizabeth	PE	50	-40	90	-0.05	12.07	0.22	0.49	87547	16.77
Durban	DU	37	-47	84	0.03	10.32	0.20	0.64	70487	26.90

TOGA PREDICTED TIDES (1970-1990) (cm from Land Levelling Datum)										
(Mean, Standard Deviations, M2 and f factor are derived from the year of analysis)										
		MAX	MIN	range	MEAN	STD	M2	f factor		
Walvis Bay	WB	102	-93	195	1.8	39.01	50.17	0.093		
Luderitz	LB	91	-111	202	-13.5	38.88	49.36	0.097		
Port Nolloth	PN	136	-89	225	18.6	43.79	55.09	0.096		
Saldanha	SA	123	-88	211	15.1	41.71	51.76	0.100		
Granger Bay	GB	120	-88	208	15.0	41.17	51.19	0.100		
Simon's Bay	SB	130	-80	210	19.2	43.21	51.52	0.103		
Mossel Bay	MB	155	-102	257	23.9	49.89	59.82	0.103		
Knysna	KN	138	-82	220	29.1	46.46	54.75	0.106		
Port Elizabeth	PE	138	-83	221	24.7	44.02	52.29	0.094		
Durban	DU	139	-95	234	20.3	47.67	55.88	0.077		

SOUTH AFRICAN TIDE TABLES (cm from Land Levelling Datum)										
		LAT	MLWS	MLWN	ML	MHWN	MHWS	HAT	M2	f factor
Walvis Bay	WB	-95	-71	-31	0	31	71	102	49.71	0.095
Luderitz	LB	-107	-81	-43	-13	16	54	89	48.42	0.098
Port Nolloth	PN	-91	-63	-17	15	48	94	130	54.62	0.094
Saldanha	SA	-96	-64	-14	11	36	86	119	50.39	0.099
Granger Bay	GB	-81	-56	-12	15	43	86	120	49.68	0.099
Simon's Bay	SB	-83	-58	-12	16	44	90	124	51.29	0.103
Mossel Bay	MB	-91	-65	-6	23	51	110	152	58.77	0.104
Knysna	KN	-79	-54	0	26	53	106	141	53.99	0.101
Port Elizabeth	PE	-95	-61	-6	19	45	100	145	52.53	0.096
Durban	DU	-92	-66	-5	20	45	106	140	55.93	0.078

TABLE 4.1 Statistics for ten Southern African ports.

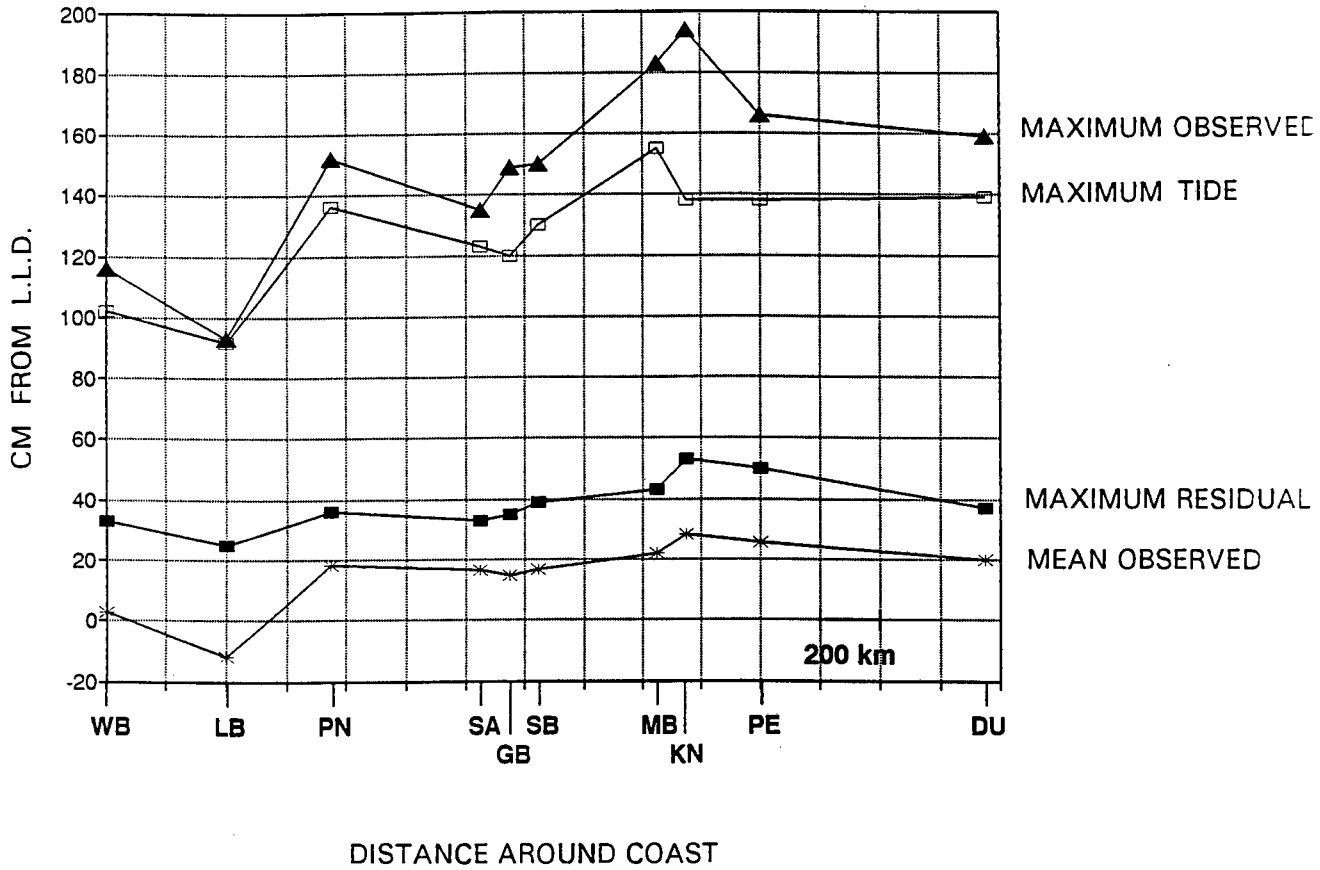


FIG. 4.1 Regional variation of some statistics at ten ports.

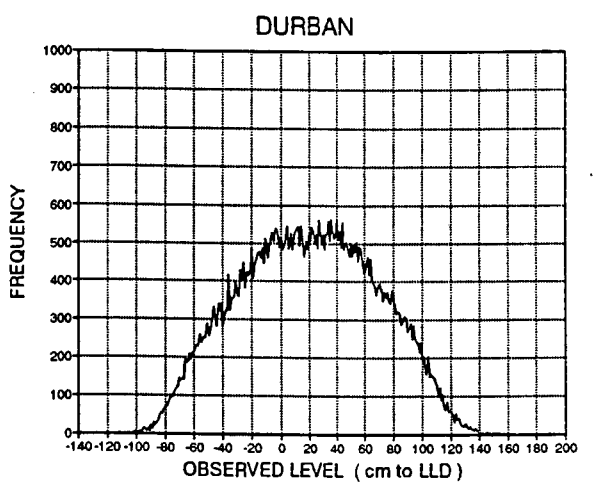
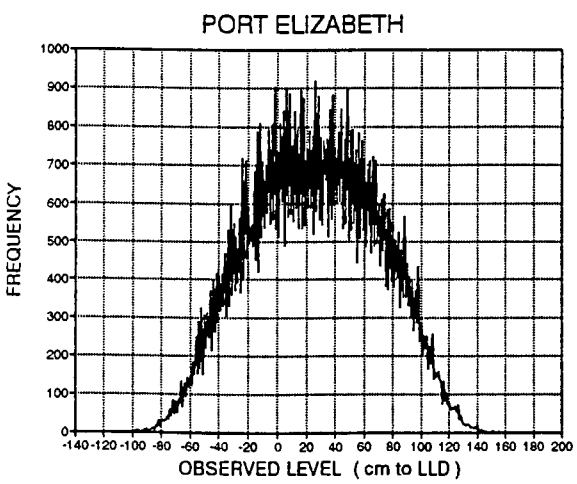
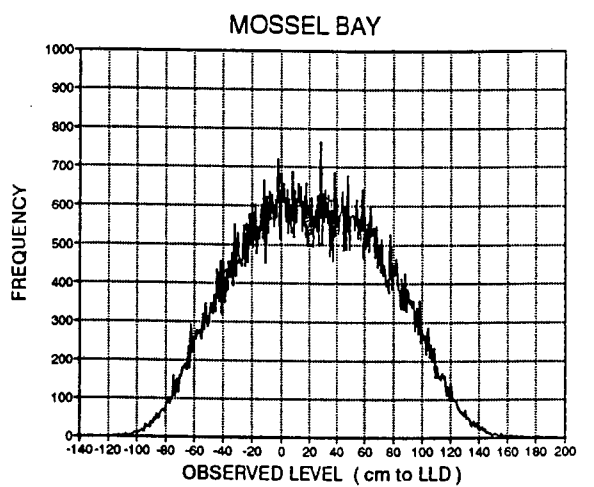
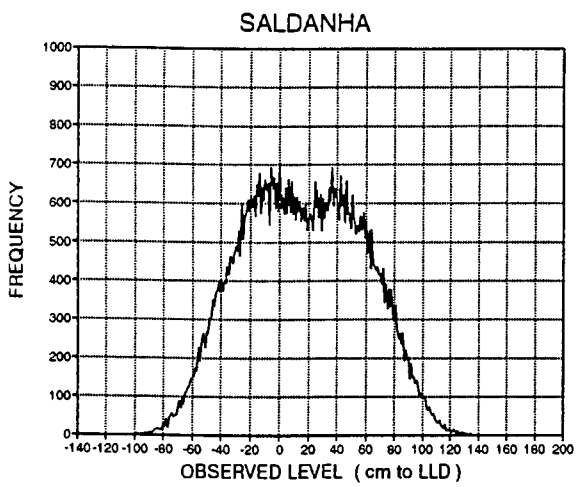
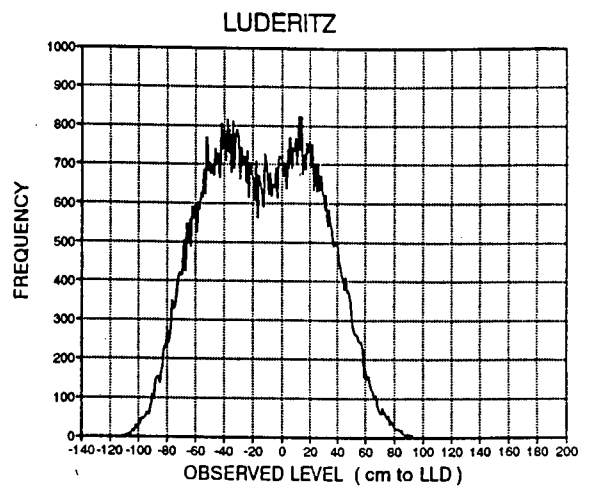
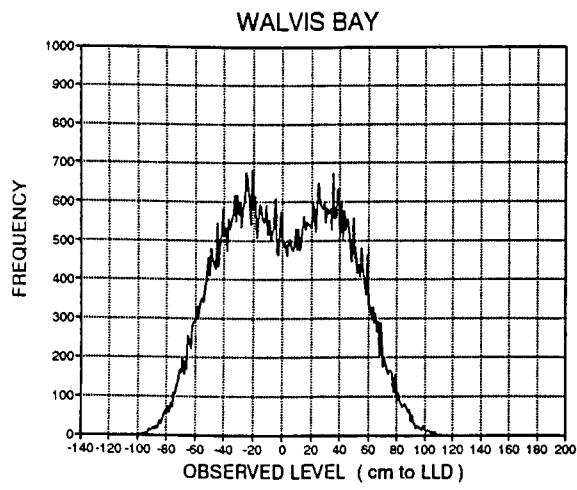


FIG. 4.2 Frequency distribution of observed levels at six ports.

4.1.2 Residuals.

Frequency distributions are shown for selected ports in fig. 4.3, they are normal distributions centred around the mean observed level and with some skewness. The slight differences in shape and spread reflect the changing meteorological influences around the coast. Also the number of data points used must be considered when directly comparing plots from each site.

Regional characteristics are again evident, distributions are somewhat sharper and with smaller range at the west coast sites, tending to become flatter but with an increased range along the south and east coasts.

4.1.3 Tides.

All tidal frequency distribution graphs (fig. 4.4) are bi-modal in form. This double peak occurs at high and low water neaps as heights of neaps are reached and exceeded during spring tides as well, and are therefore recorded more often. Mean level is not a peak because water is quickly rising or falling past this height, more time is registered at the level of neap tide as the changing water level has to slow and reverse direction. There is some irregular asymmetry between high and low neap peaks. Plots are derived from hourly predictions for 1970-1990 so highest astronomical tide (HAT) and lowest astronomical tide (LAT) are the points at each extreme end of the curves. Again the form of the distribution is sharper on the west coast and there is a distinct broadening in the distributions from west to east, particularly between Simon's Bay and Mossel Bay.

The Form Factor according to Defant (1961, p.306-308):

$$F = \frac{K_1 + O_1}{M_2 + S_2}$$

(i.e. the 'f factor' given in table 4.1) gives a measure of the tidal character by comparing the magnitude of the (two) main diurnal constituents to the (two) main semi-diurnal ones and where:

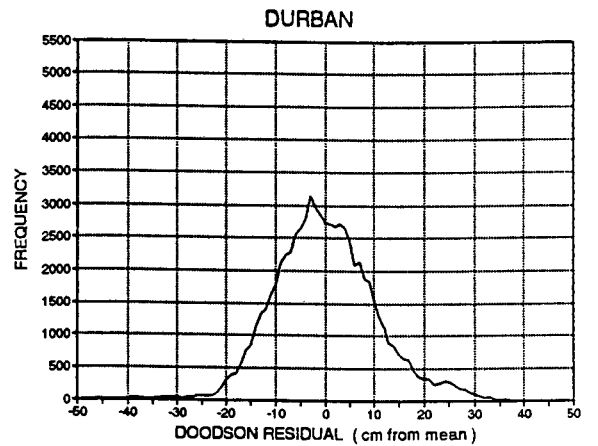
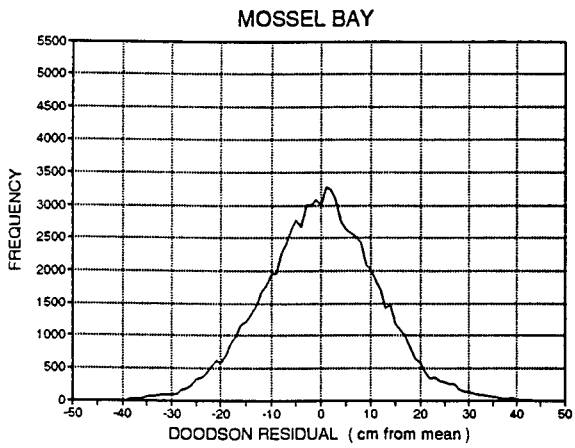
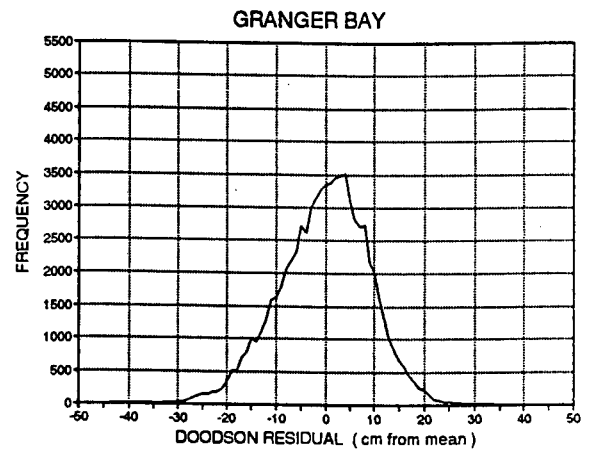
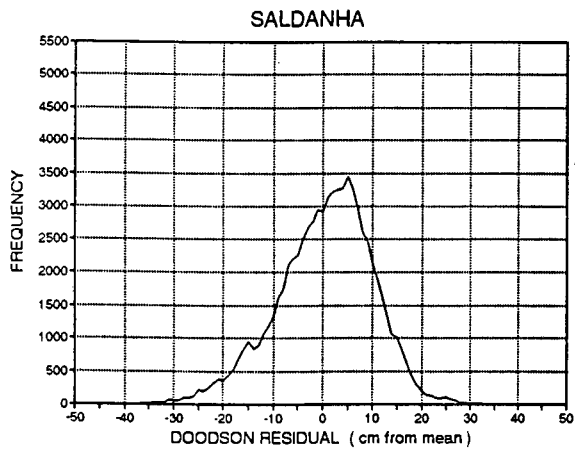
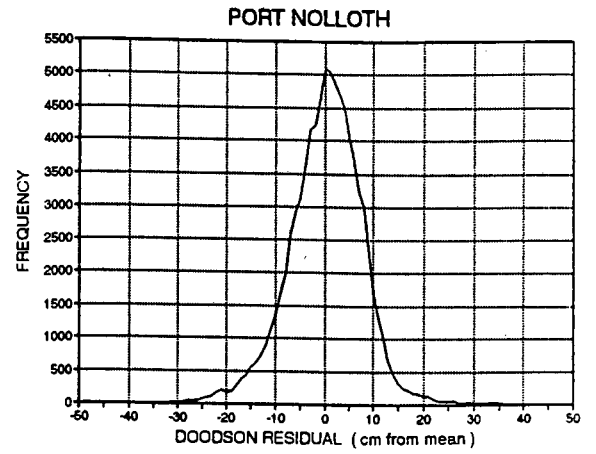
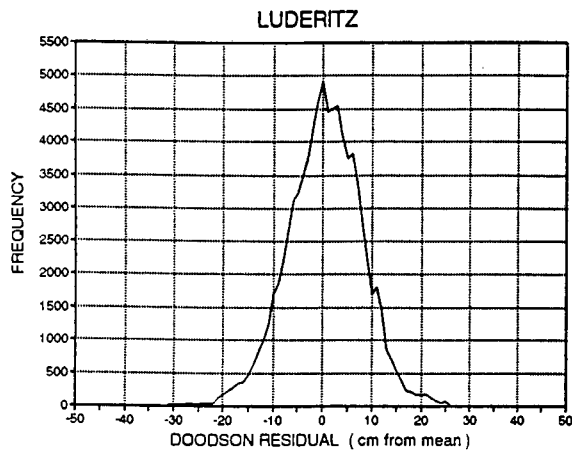


FIG. 4.3 Frequency distribution of residuals at six ports.

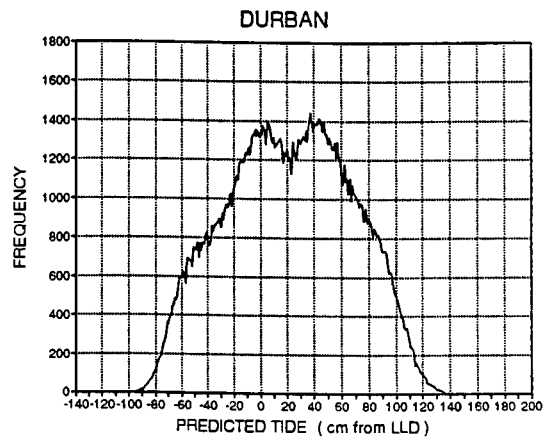
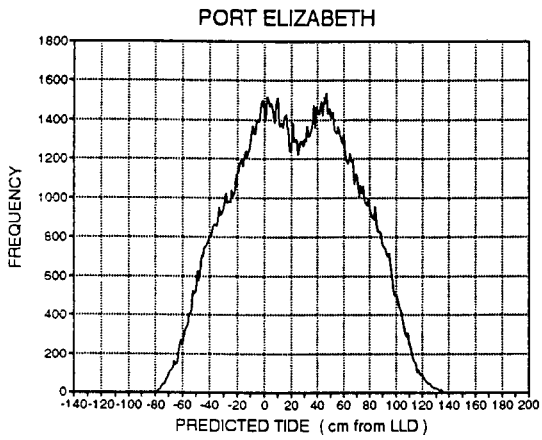
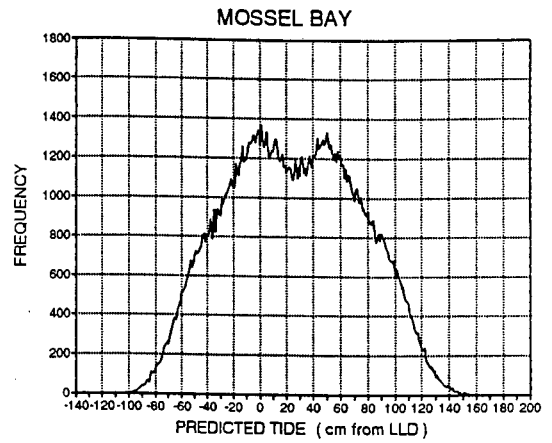
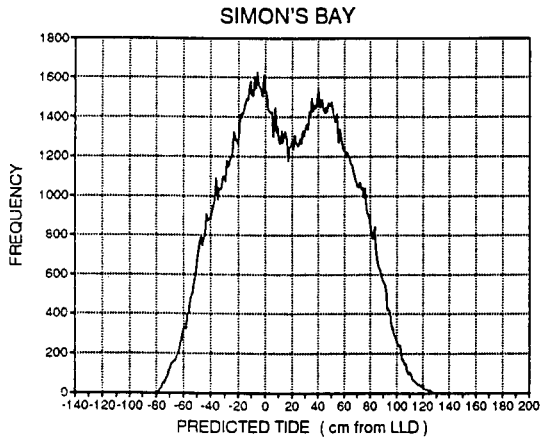
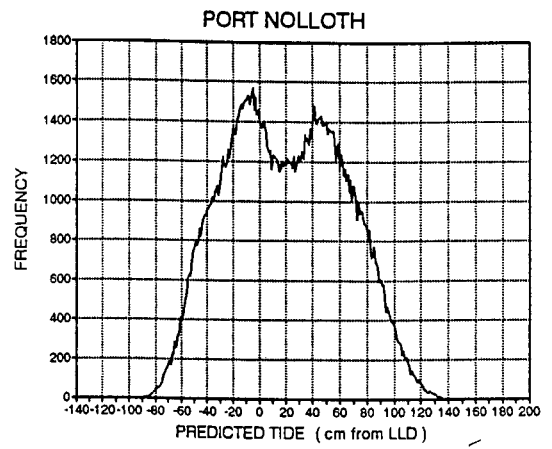
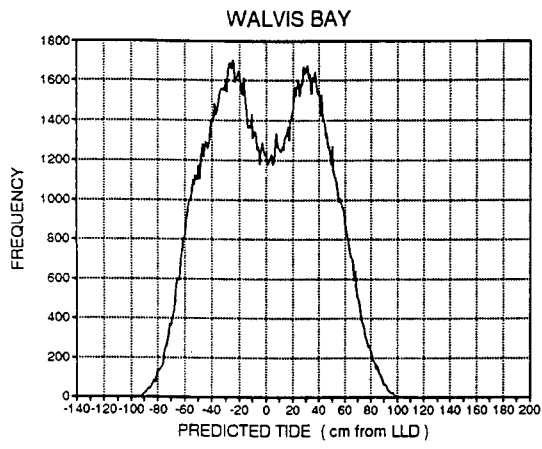


FIG. 4.4 Frequency distribution of tides at six ports.

- F = 0 – 0.25, semi-diurnal
- F = 0.25 – 1.50, mixed, mainly semi-diurnal
- F = 1.50 – 3.00, mixed, mainly diurnal
- F > 3.00, diurnal

There is a slight discrepancy between the f factors derived from TOGA constituents and those used by the Navy, nevertheless all Southern African ports are strongly semi-diurnal (largest F = 0.106 for Knysna using TOGA constituents). Minor variations are seen around the coast, the values increase from Walvis Bay to a peak at Mossel Bay/Knysna and from where it decreases to its lowest value at Durban.

The M_2 constituent (table 4.1) is the single largest contributor to the astronomical tide and peaks at Port Nolloth, Mossel Bay and Durban. There is no apparent trend and the range of values is approximately 12 cm.

4.2 EXTREMES.

Analyses of the monthly maxima gives insight into the temporal, spatial and compositional variability of extremes in the observed, residual and tidal series.

4.2.1 Time series of monthly maxima.

Simon's Bay: The most striking feature of a comparison of the thirty year record of monthly maxima of residuals (fig. 4.5a), tide (fig. 4.5b) and observed levels (fig. 4.5c) is the strong tidal signature within the observed series, particularly before the 1980's.

Tidal variations by their deterministic nature are easy to recognise, with two modulations being dominant on a long (greater than monthly) time scale. Equinoctial maxima occur in March and September, times of largest solar semi-diurnal forcing, and account for variations of between 10 and 40 cm. There is a

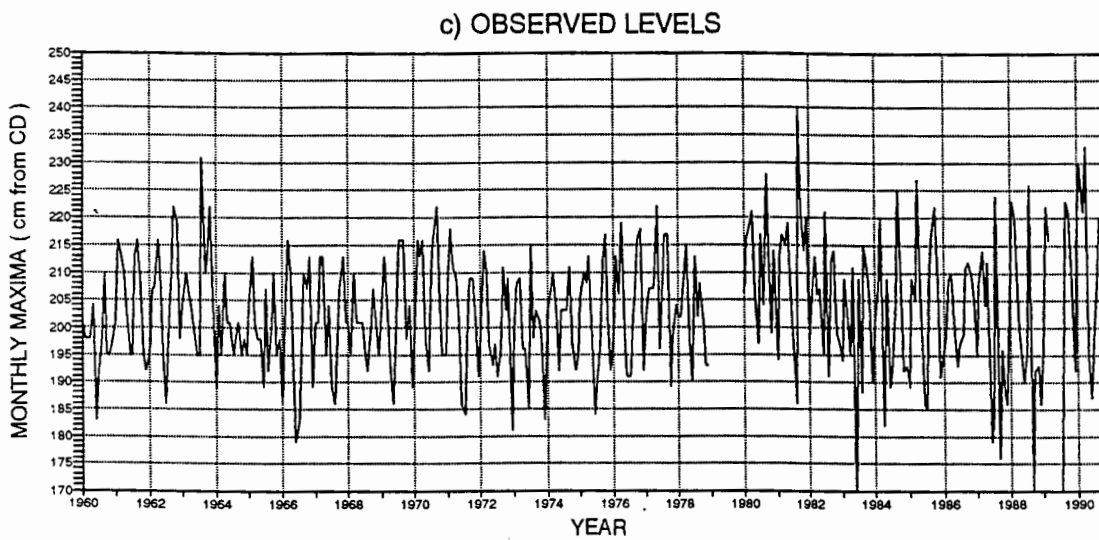
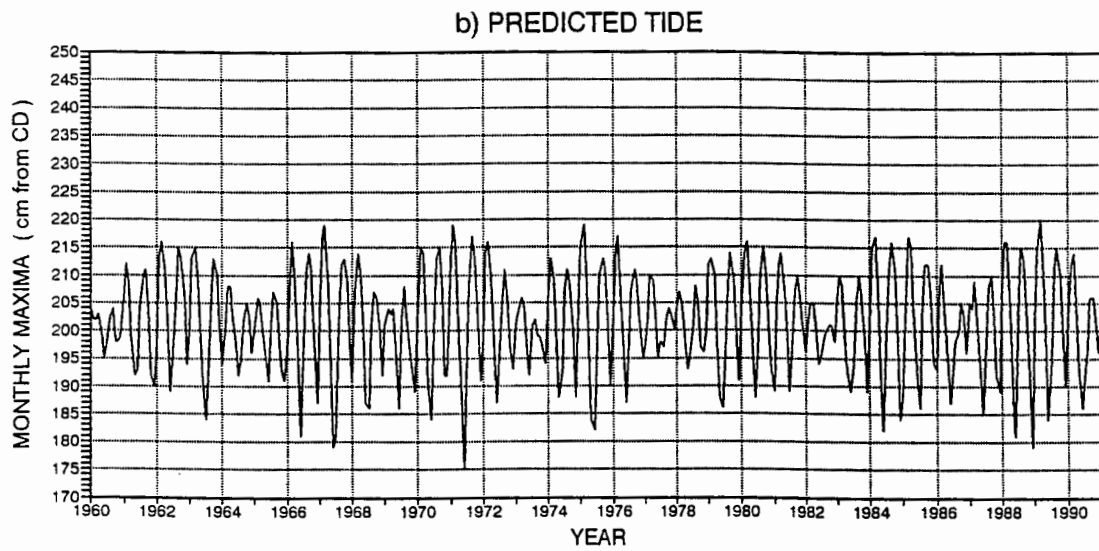
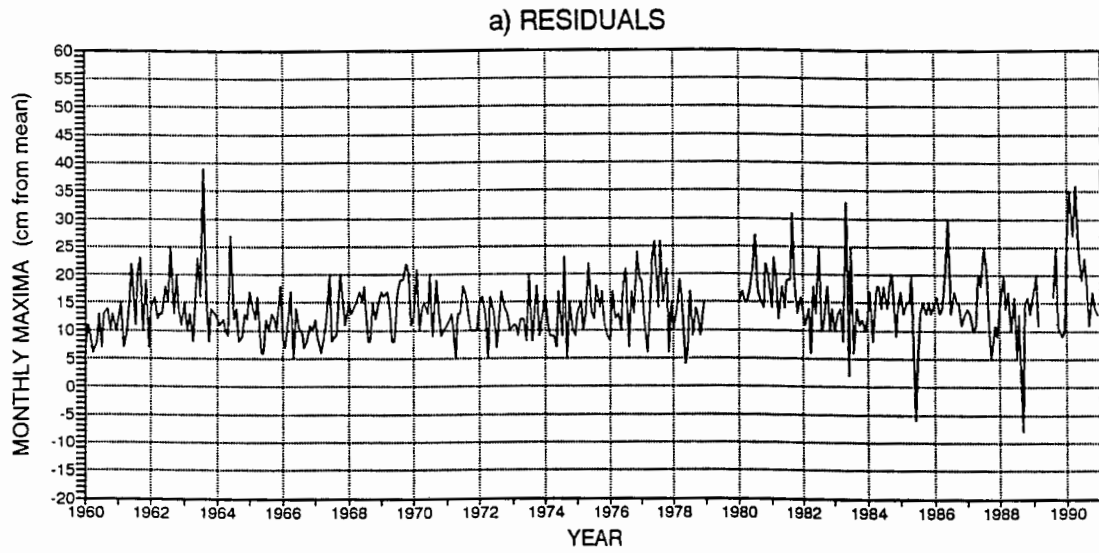


FIG. 4.5 a,b&c Monthly maxima from Simon's Bay, a) residuals b) tides and c) observed levels.

four yearly modulation of the order of 10 - 15 cm due to the coincidence of the moon's perigee, which completes one revolution in 8.8 years, with either equinox and results in a 4.4 year cycle. The well known 18.6 year cycle can just be distinguished, but it is only of the order of 2 cm. In the observed sea level record both cycles are clearly evident although with more 'noise' due to the additional effects of the residuals.

Seasonality of larger surges is present in the residual record where larger residuals are seen to occur during winter months. This characteristic does not generally feature in the observed sequence but the singular extreme surge of August 1963 gives some indication of the potential influence of residuals on sea level.

Both observed and residual series show a few particularly 'low' values during the eighties, these are due to incomplete data sets for those months.

Other Ports: For illustrative purposes four representative plots of monthly maxima are shown for Walvis Bay, Saldanha, Port Elizabeth and Durban.

In the observed sea level maxima (fig. 4.6), the equinoctial tidal signal is reasonably evident at all sites. The longer 4.4 yearly modulation is not so conspicuous, but just discernable (as for Port Elizabeth and Saldanha) at most Southern African ports. 'Low' maxima are again due to incomplete data sets.

The residual sequence (fig. 4.7) for Walvis Bay seems to show a datum shift downwards during the first half of 1981, although it is not immediately obvious from the observed levels alone. A decrease in values for winter months indicates the upwelling season which, for the Benguela north of 25°S, extends from March to November (Shannon 1985). The northern west coast ports are characterised by this winter upwelling, southern ports from Saldanha around to Port Elizabeth show high surges tending to occur in winter as a result of the passage of low pressure systems. The identification of cycles and trends at Durban is hampered by the lack of continuity in the sea level record.

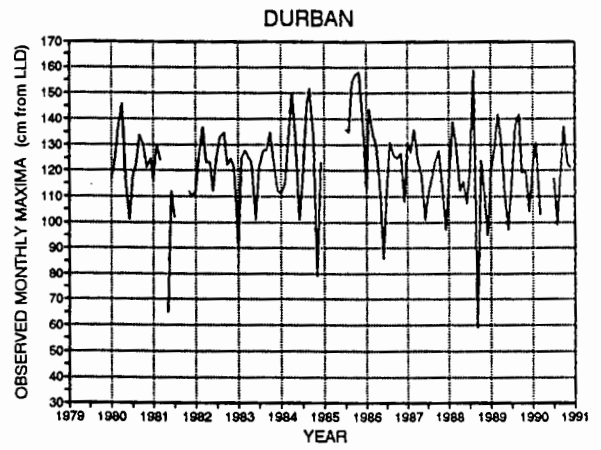
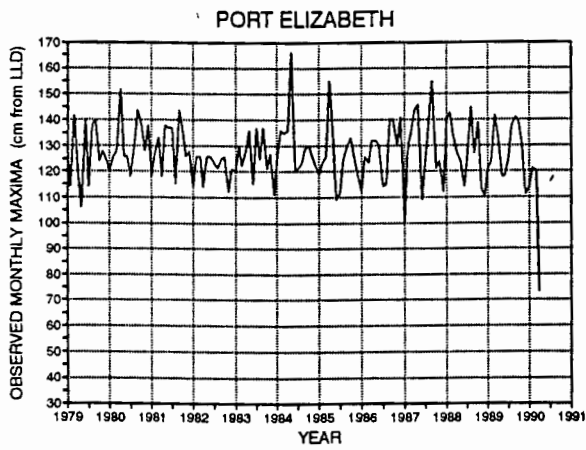
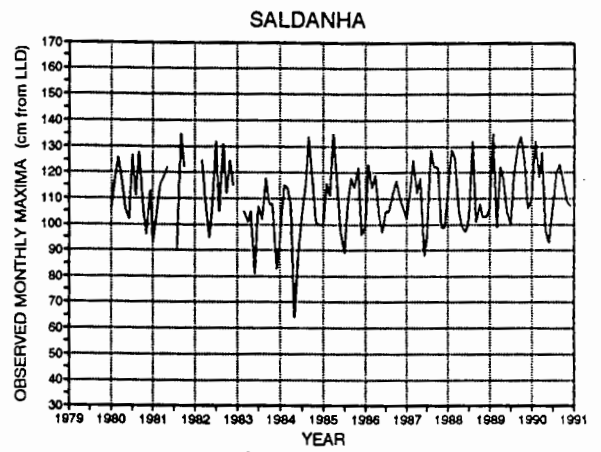
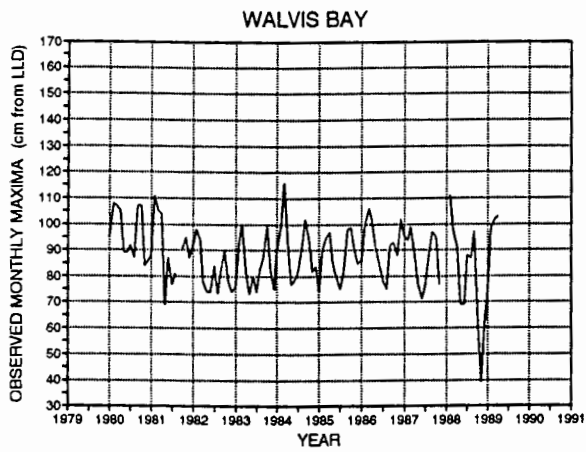


FIG. 4.6 Monthly maxima of observed levels at four ports.

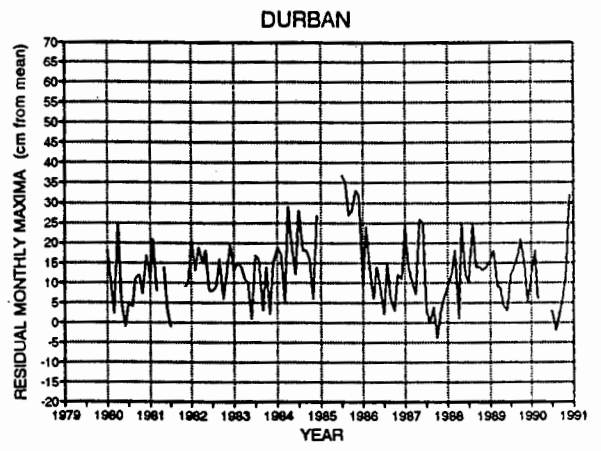
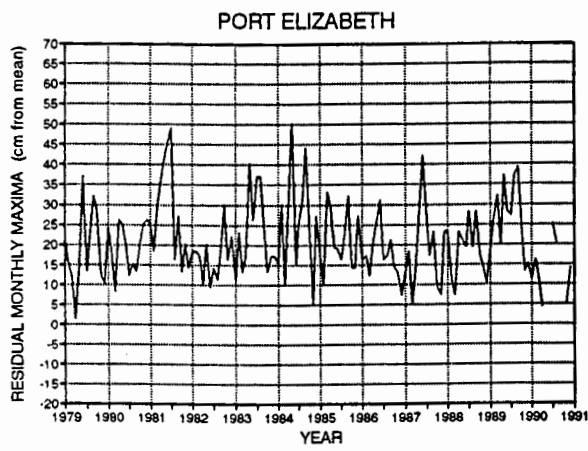
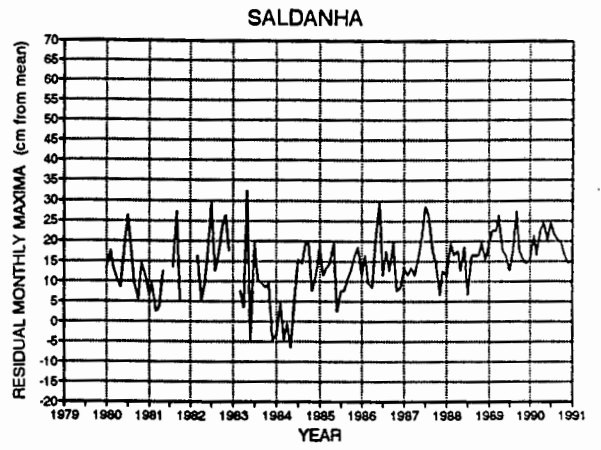
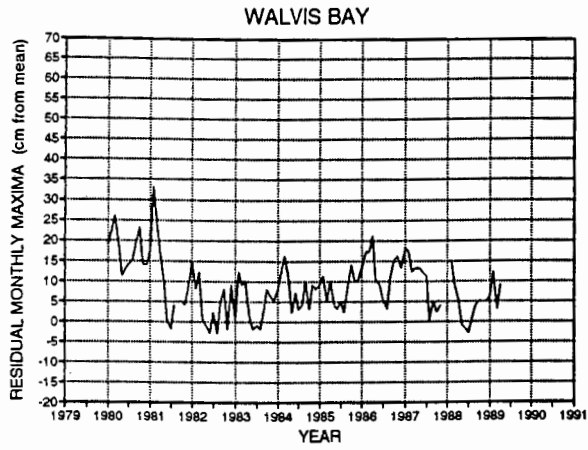


FIG. 4.7 Monthly maxima of residuals at four ports.

4.2.2 Composition of high sea levels.

Plotted for each monthly maxima observed event, the simultaneous hourly value of predicted tide and (Doodson) residual show the composition of the highest observed sea levels (fig. 4.8). Tidal values are in the upper third of their range, and residuals are in the upper two thirds of their distribution. Some events are composed of a tide and a 'negative' surge implying that for some months the highest monthly predicted tide is not achieved. The highest recorded surges at many ports (Luderitz, Port Nolloth, Saldanha, Granger Bay, Mossel Bay, and Knysna) did not result in a monthly observed extreme indicating that the tidal component must have been small i.e. occurring at neap tide.

4.2.3 Specific events at Simon's Bay and Port Elizabeth.

The seven highest recorded surges (fig. 4.9a) at Simon's Bay all occurred during winter months (May to September) and were meteorologically characterised by a low pressure system present to the south of Cape Town and then the associated passage of a cold front. Minimum pressures recorded at Cape Town were between 998 mb and 1012 mb, winds north or northwesterly 10-35 knots (Daily Weather Bulletins of August 1963, August 1977, September 1981, June 1986, June 1977, July 1980 and May 1983).

On three occasions the storm surge did not result in the highest observed sea level for that month, occurring on neap tides (May 1983, June 1986) or during the lower of two spring high tides (June 1977). The high surges of August 1963 and September 1981 resulted in two of the high observed levels. It is noticeable that all observed extreme examples (fig. 4.9b) occurred in months on or near equinox: April (1985), August (1963, 1988) and September (1970, 1980, 1981, 1984). Generally it can be noted that the highest extremes occur near equinoctial spring high tides reinforced by only a small or moderate residual component.

Five examples are given for Port Elizabeth (figs. 4.9 c&d). Only one 'event' the largest storm surge happened to (nearly) coincide with high spring tides (May 1984) which resulted in the largest observed level, other storm surges occurred

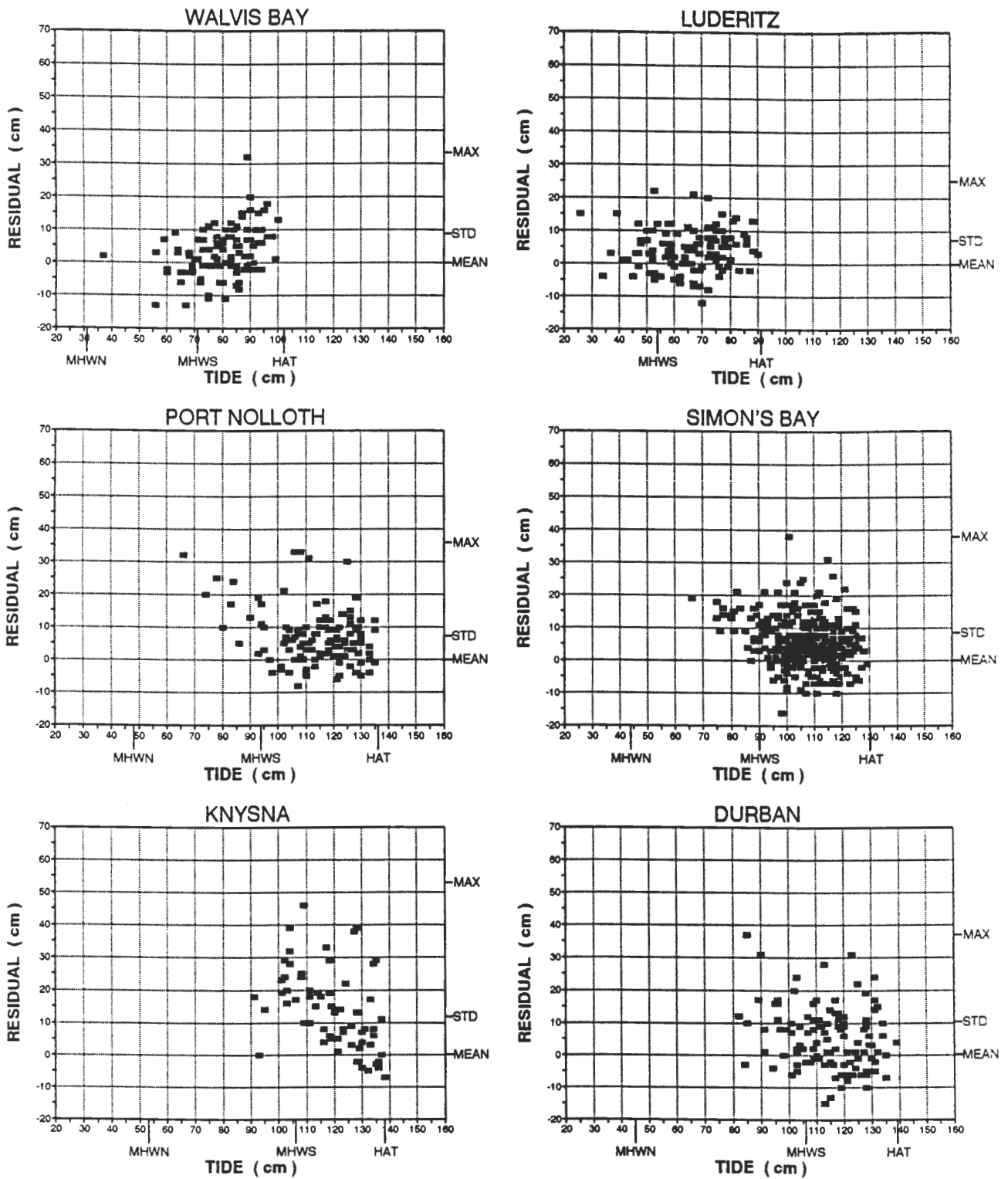


FIG. 4.8 Tide versus residual for each extreme event at six ports.

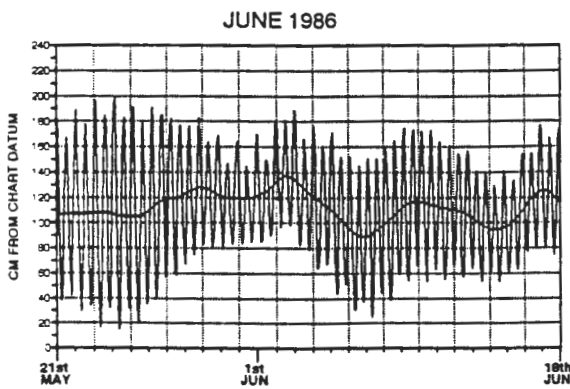
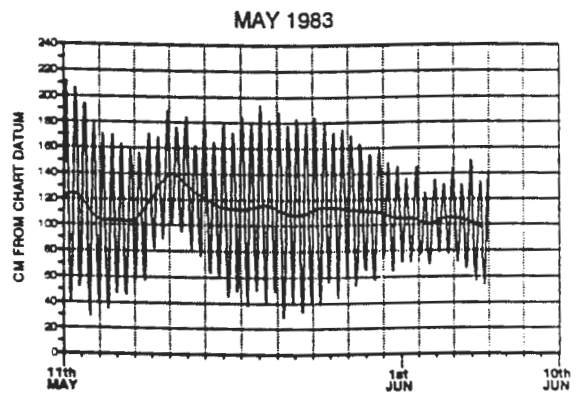
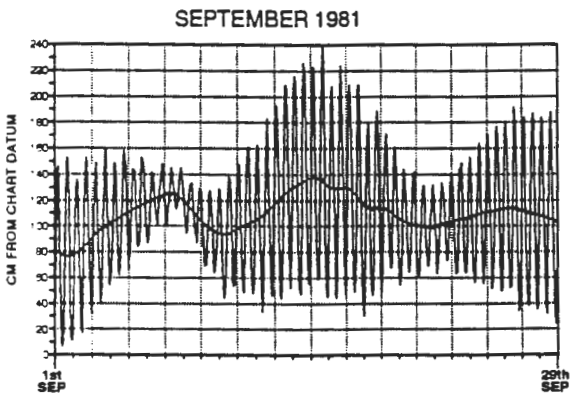
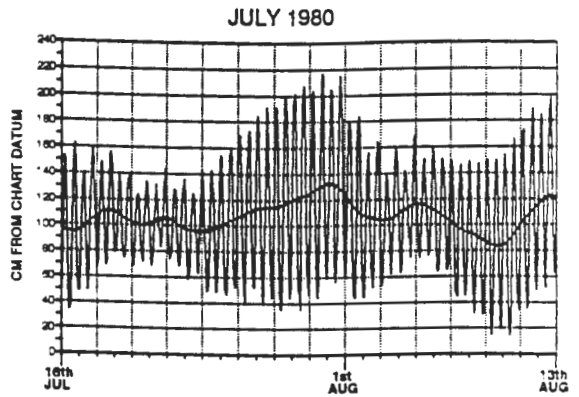
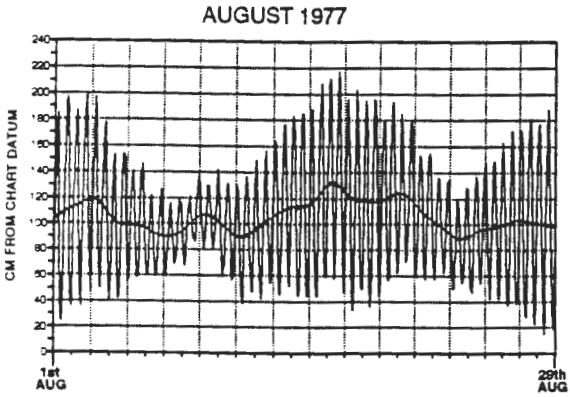
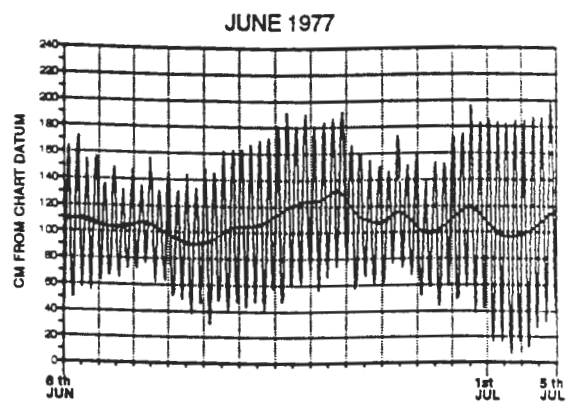
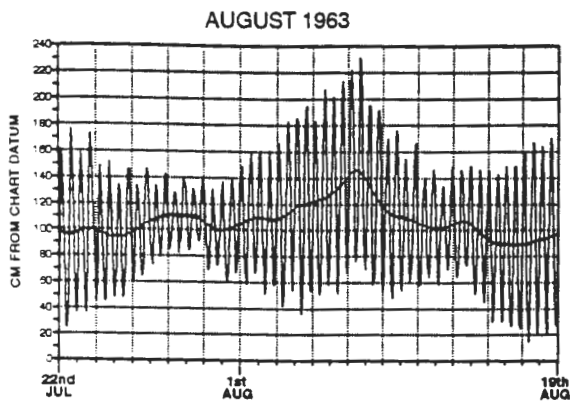


FIG. 4.9 a) Seven highest surge events at Simon's Bay.

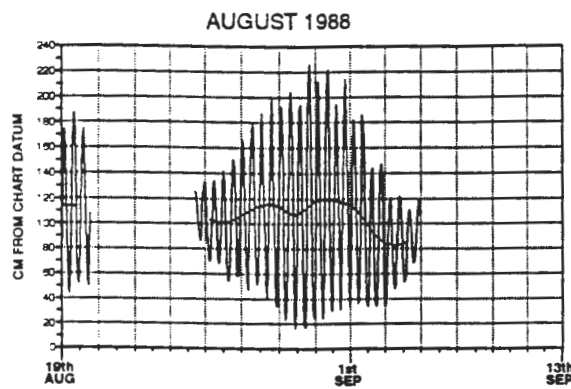
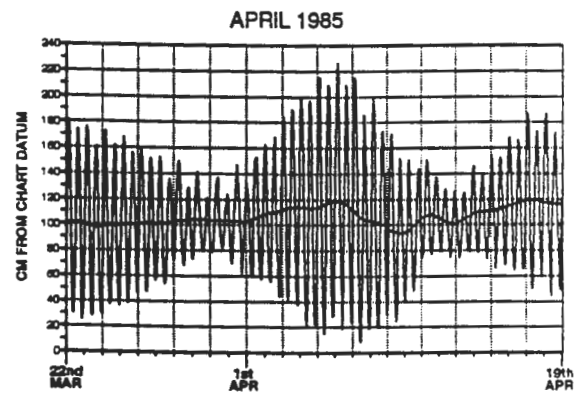
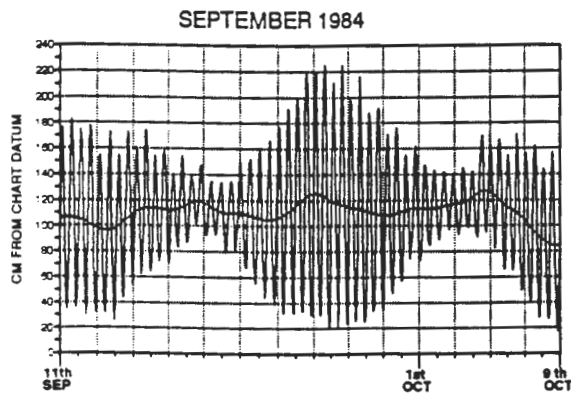
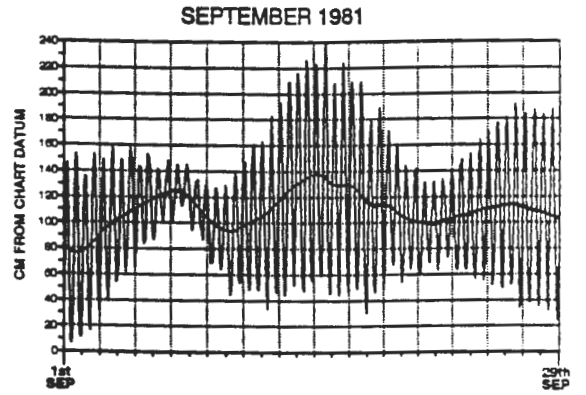
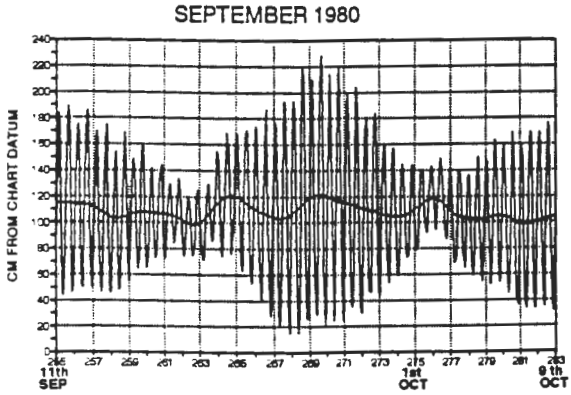
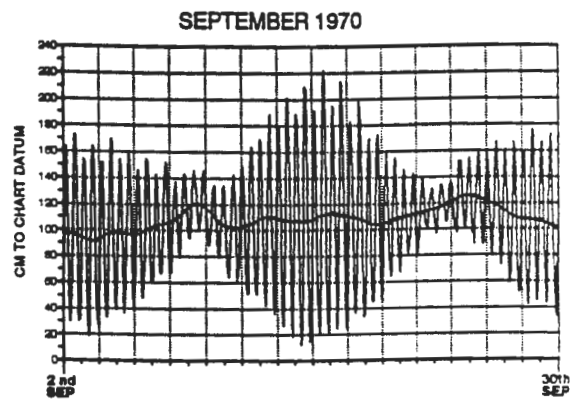
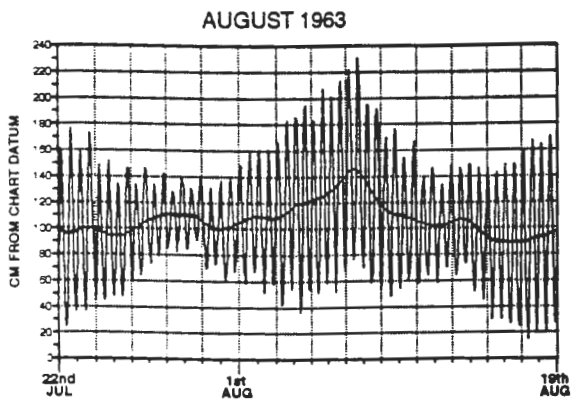


FIG. 4.9 b) Seven highest observed events at Simon's Bay.

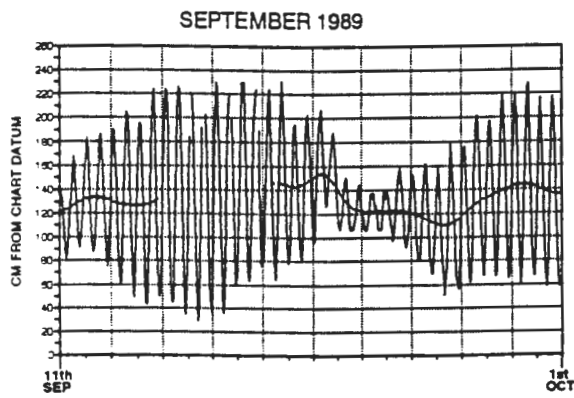
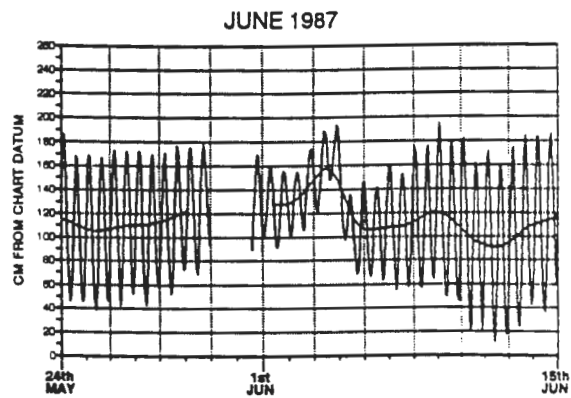
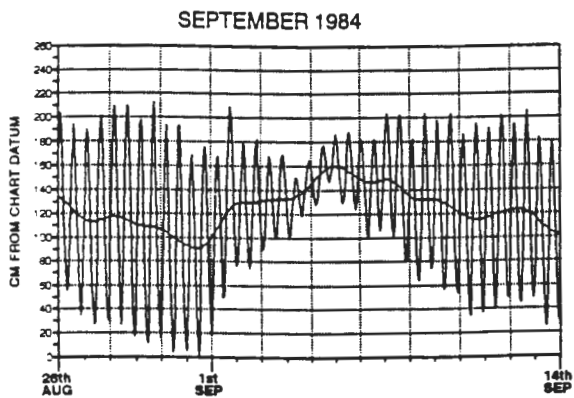
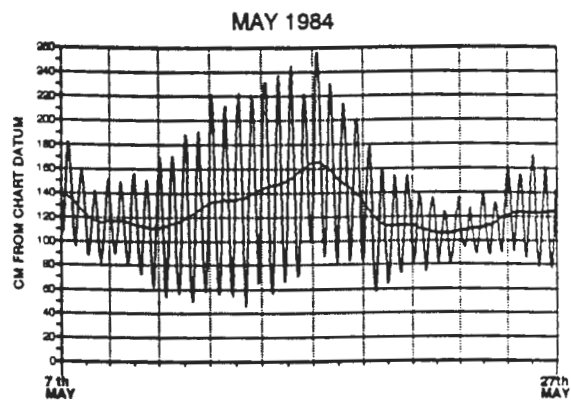
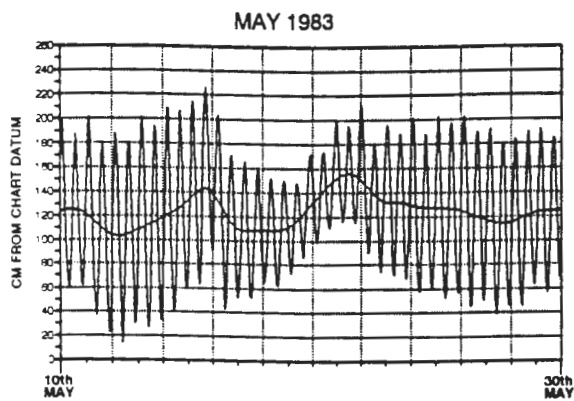


FIG. 4.9 c) Five highest surge events at Port Elizabeth.

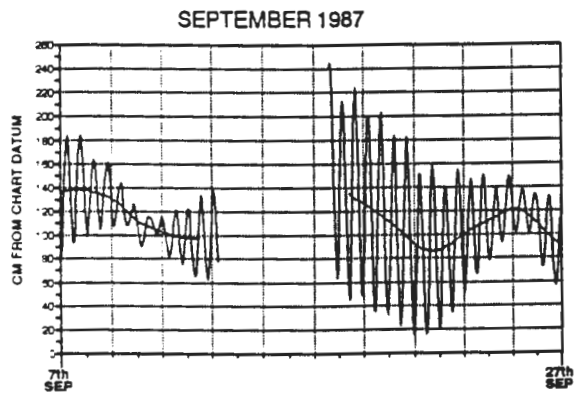
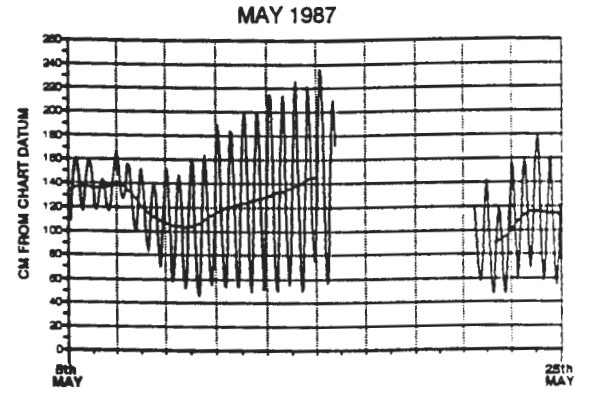
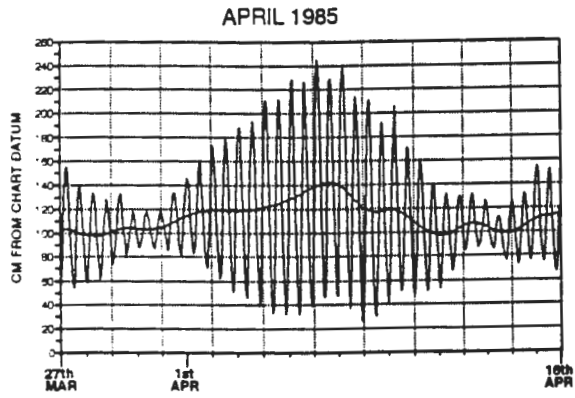
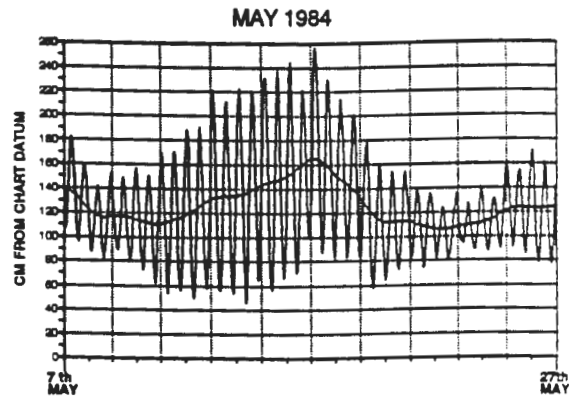
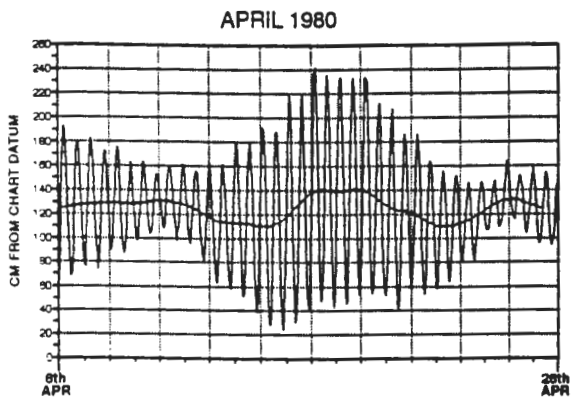


FIG. 4.9 d) Five highest observed events at Port Elizabeth.

during neaps (May 1983, September 1984, June 1987 and September 1989). The next four highest recorded levels (April 1980, May 1987, September 1987, and April 1985) tended to be composed of moderate surges on spring tides. This confirms that the composition of extreme sea levels is not dependent on large storm surges, but on the state of the tide in relation to springs and equinox.

4.2.4 Averaged monthly maxima.

All monthly maxima for each specific month (usually eleven one from each of the years 1980-1990) can be averaged to give a profile of the mean seasonal variations of the maxima during a year, in observed, residual and tidal signals.

The observed sea levels (fig. 4.10a) show expected seasonal behaviour corresponding to the dominant tidal equinoctial variations. This variation in range is up to 30 cm at Mossel Bay. Tidal averaged monthly maxima are given in fig. 4.10b, the slight difference between March and September equinoxes may be due to the proximity of perihelion in January (and the associated increase in tidal forcing) to the March equinox.

The variations in residual average monthly maxima (fig. 4.10c) are less smooth and much less in magnitude (note change in scale) but do show certain characteristics. Large storm surges (average monthly maximum residuals 'high') occur during winter at most south coast sites, with upwelling dominating in the summer after the southward shift of the passing mid-latitude storms. At the west coast ports of Walvis Bay and Luderitz the upwelling season is in winter. Mossel Bay is the most variable and this explains the clouding of the tidal equinoctial signal in the observed profile. Durban is far away from the influence of winter storms, but affected by a cyclone season from December to February.

4.3 EXTREME VALUE ANALYSIS AND EMPIRICAL DISTRIBUTIONS.

For details of the theory and equations refer to Chapter Three, section 3.4.2. Two empirical distributions were compiled according to the equations of

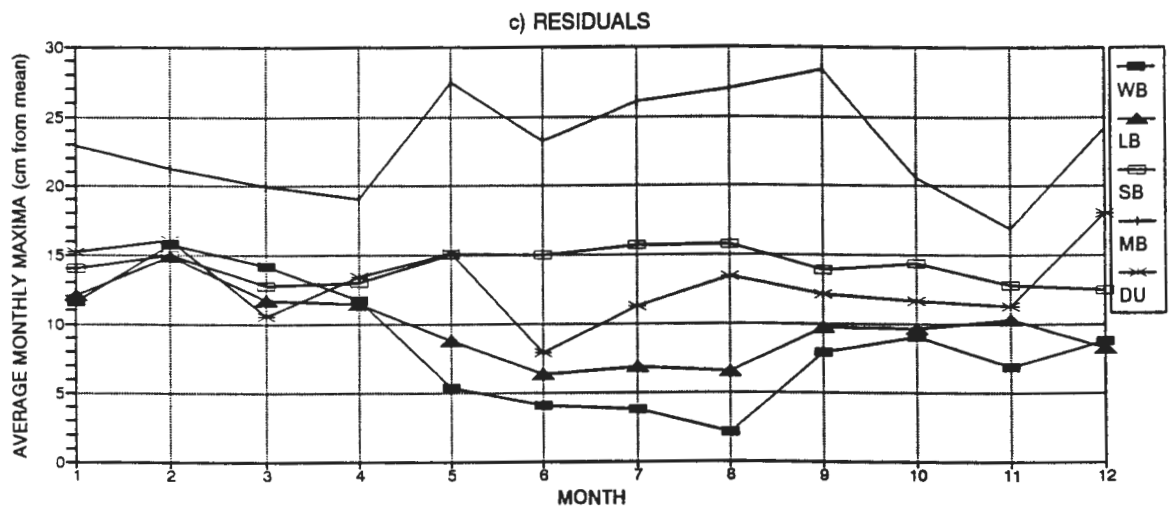
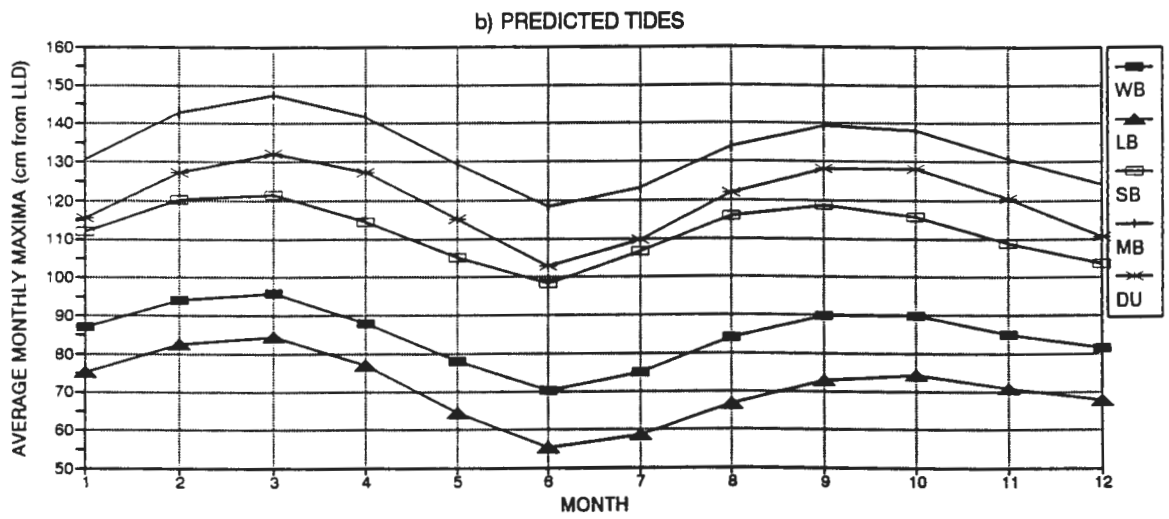
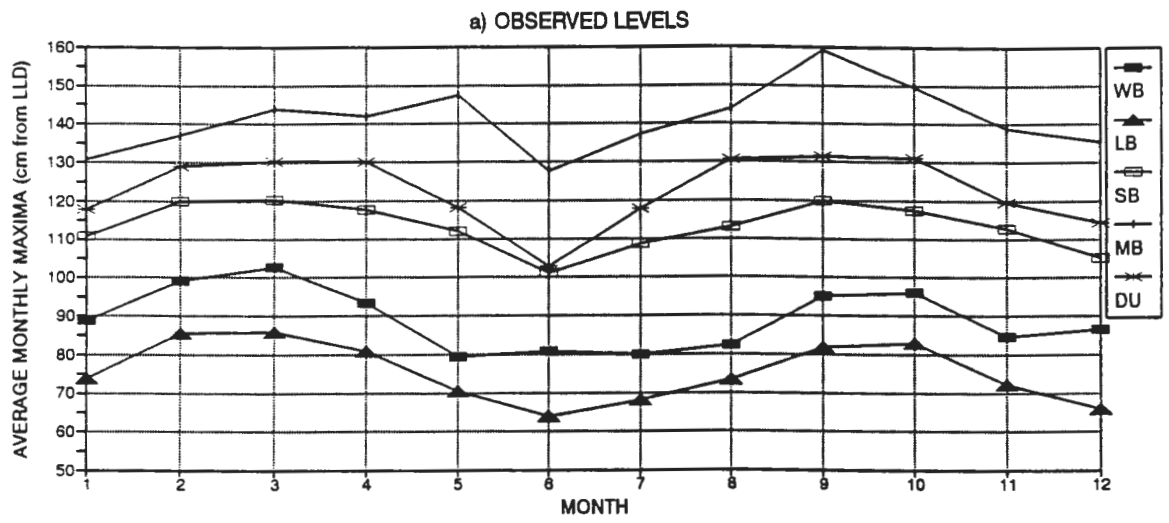


FIG. 4.10 a,b&c Average monthly maxima for six ports, a) observed levels b) tides and c) residuals.

Hazen and Gumbel which both derive probabilities for levels being greater than or equal to a particular extreme. Theoretical approximations to the asymptote are provided by Gumbel's Extreme Value theory (1958) and more generally by Jenkinson's Generalised Extreme Value (GEV) distribution (1955). These standard theoretical methods require at least twenty-five annual maxima hence were only applied to Simon's Bay which has an acceptable thirty year record of observed hourly levels; other Southern African ports typically have only eleven year records of data.

4.3.1 Simon's Bay.

The results of the empirical and extrapolation analyses of Simon's Bay annual maxima 1960-1990 are given in fig. 4.11. Both empirical distributions are clearly similar, although there is some minor deviation for the highest three levels with the Hazen plot being slightly steeper, i.e. estimated return periods are greater than for Gumbel. Hamon and Middleton (1989) noted the same effect with these two empirical formulae. From Jenkinson's theory k is derived from the ratio of annual to biannual standard deviation. Gumbel's extrapolation is equivalent to the special case of $k = 0$ in Jenkinson's GEV, but for Simon's Bay $k = -0.07256$ hence the Gumbel is not such a good fit as the GEV extrapolation. Nevertheless at the fifty year return period estimates differ by only 5 cm.

Using annual maxima a seasonal sampling bias may affect results, this problem is bypassed by the use of monthly maxima which also provides many more data points for the empirical distributions. Middleton and Thompson (1986) also used monthly maxima in the Gumbel approach for some of their analyses. Fig. 4.12 shows that the Gumbel empirical distributions of annual and monthly maxima for Simon's Bay 1960-1990 agree very closely. As a further comparison a 'short' 1980-1990 monthly maxima data set is used as this is more representative of the period available for the other Southern African sites. The shorter data set shows an overall decrease in return periods for particular levels, e.g. the level 231 cm is reduced from a ten year to a four year return period. An equivalent

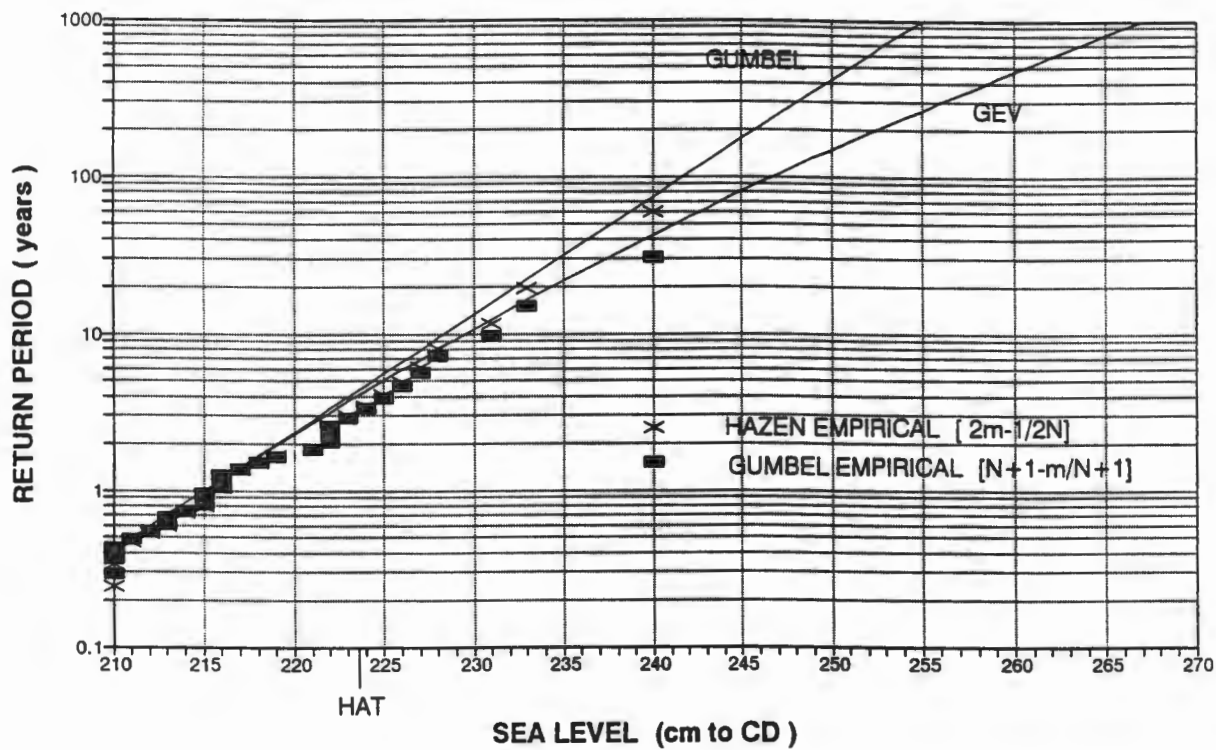


FIG. 4.11 Empirical distributions and Gumbel and GEV asymptotes for thirty annual maxima from Simon's Bay.

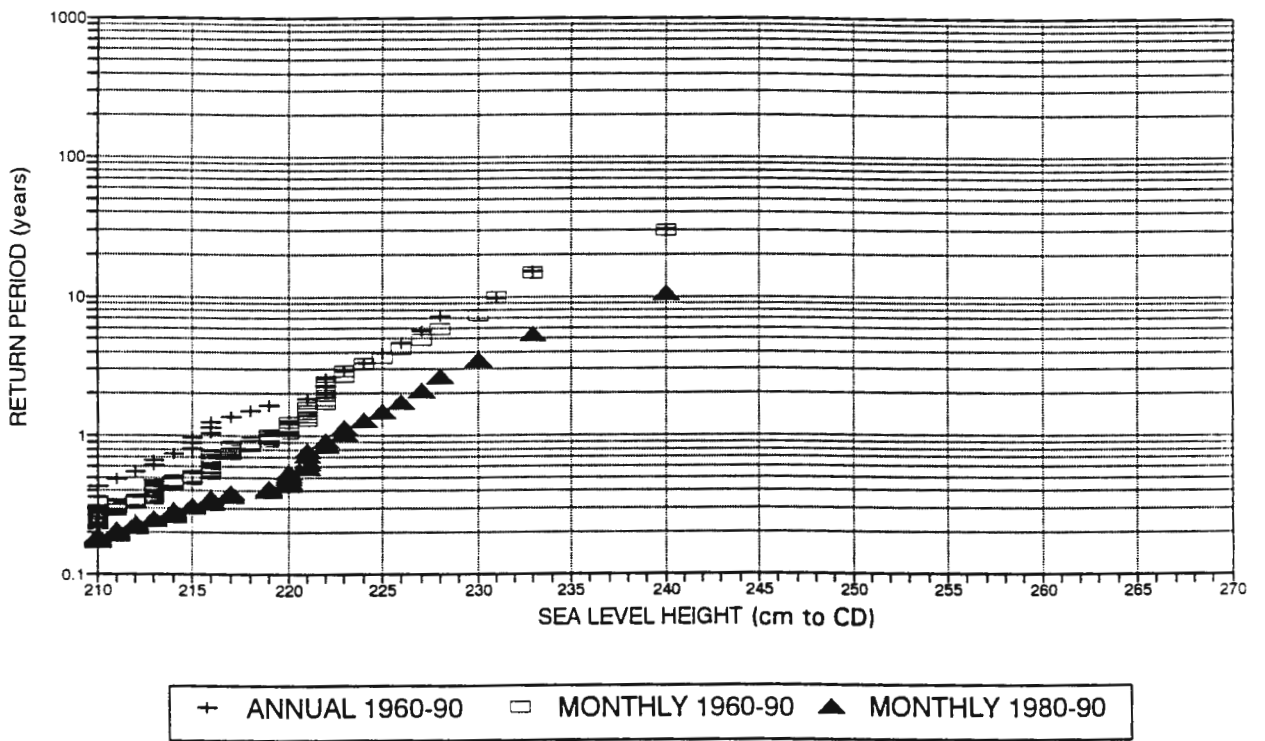


FIG. 4.12 Gumbel empirical distributions for three sub-sets of Simon's Bay data: annual maxima 1960-1990, monthly maxima 1960-1990 and monthly maxima 1980-1990.

interpretation is that the occurrence of higher extremes is more common in the period 1980-1990, the level corresponding to the ten year return period has increased 8 cm by using this shorter and more recent data set and the fifty year return period shows a difference of perhaps 10 - 15 cm.

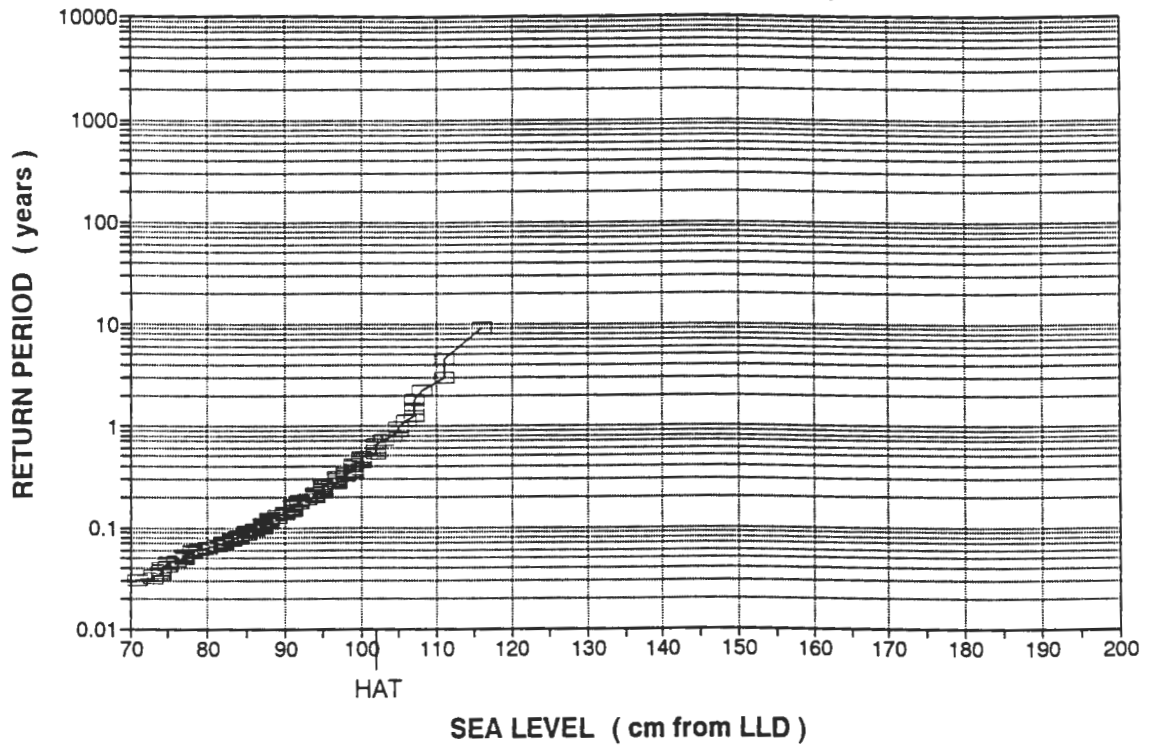
4.3.2 Port Diagrams.

The empirical results of Gumbel from monthly maxima are used in the further analysis of Southern African ports (figs. 4.13). Data availability negated the use of the extreme value analysis of Jenkinson (GEV) and Gumbel for these sites.

Simon's Bay produced a relatively smooth distribution and can be reasonably extrapolated by eye, however some other ports show notable deviations, Luderitz and Saldanha have particularly sharp vertical tails and Knysna has two distinct sections with the highest nine levels seeming to behave differently to bulk of observed extremes. The highest single observed sea level at Granger Bay appears to be greater than that suggested by the remainder of its distribution.

Fischer-Tippett classify distributions according to the overall curvature of the theoretical asymptote to the empirical distribution i.e. the k values. From the empirical analyses alone there seems little regional characterisation possible for the ten Southern African ports due to high sensitivity of the extreme positive tail of the sea level distributions, particularly with shorter data sets.

WALVIS BAY (1980-1990)



LUDERITZ (1980-1990)

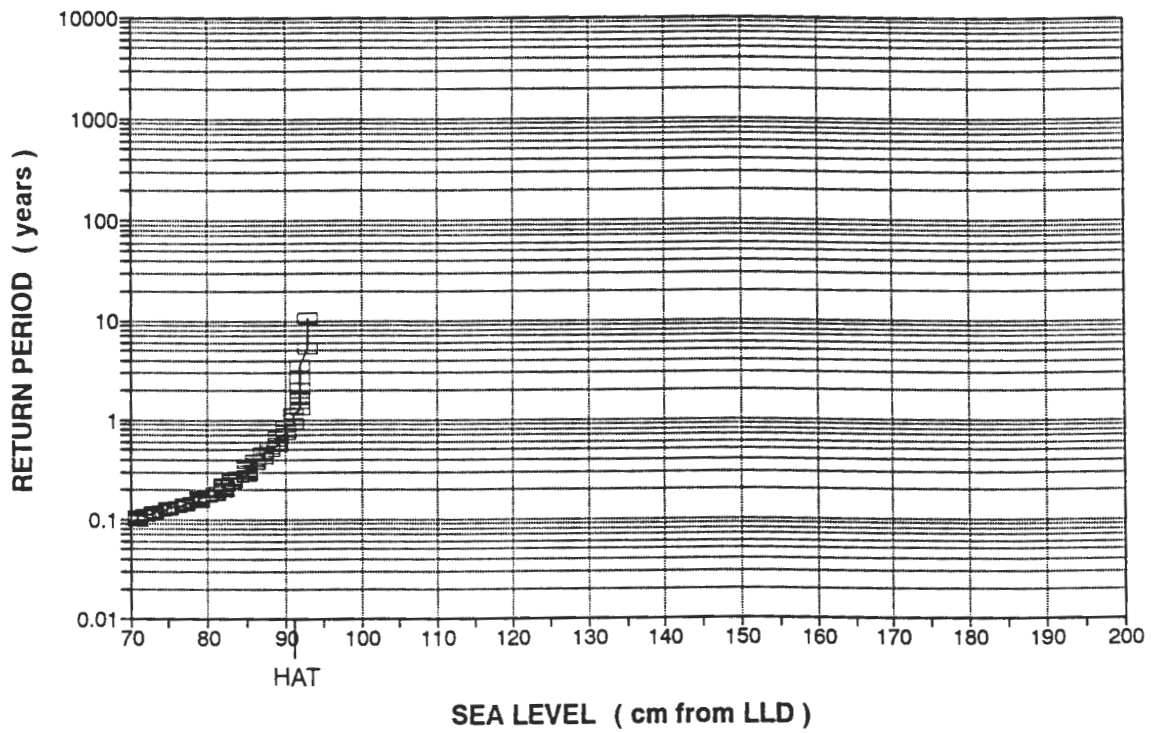
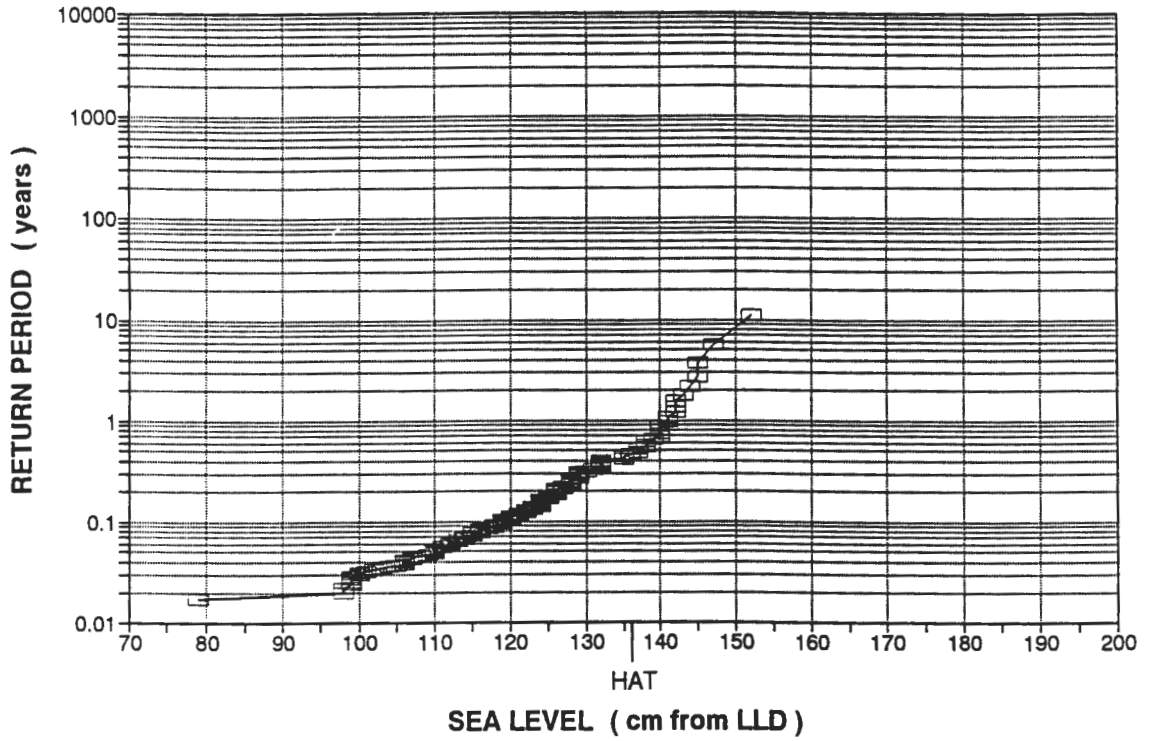


FIG. 4.13 Port Diagrams.

PORT NOLLOTH (1980-1990)



SALDANHA (1980-1990)

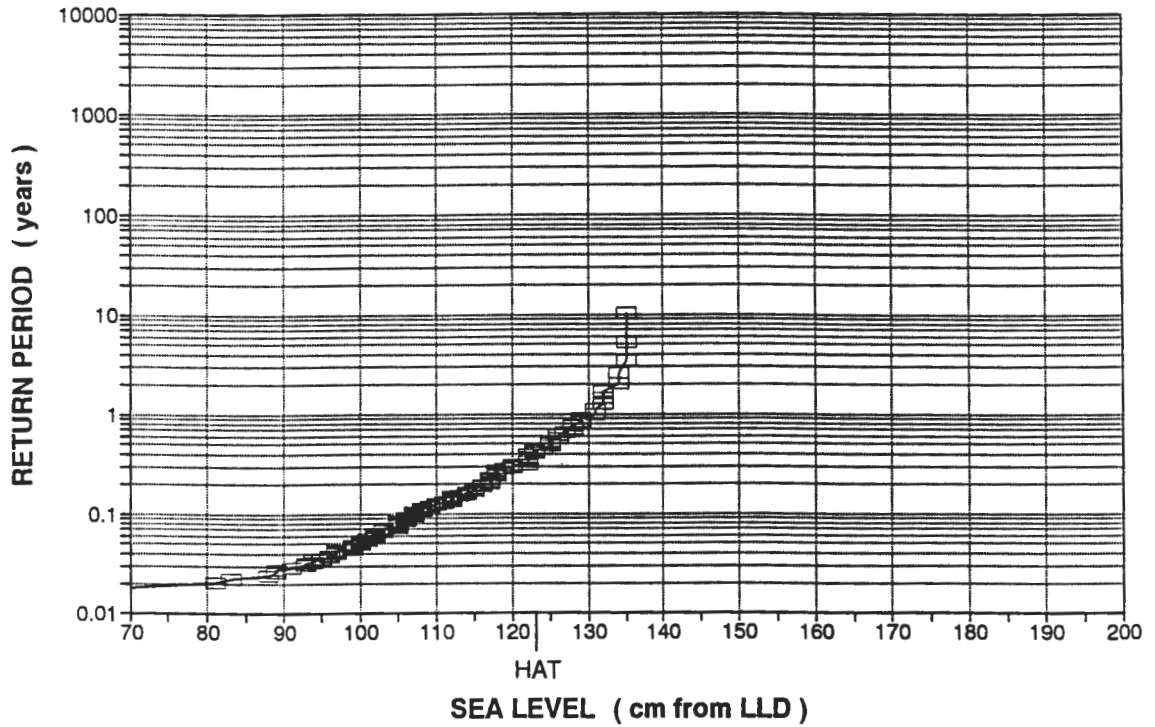
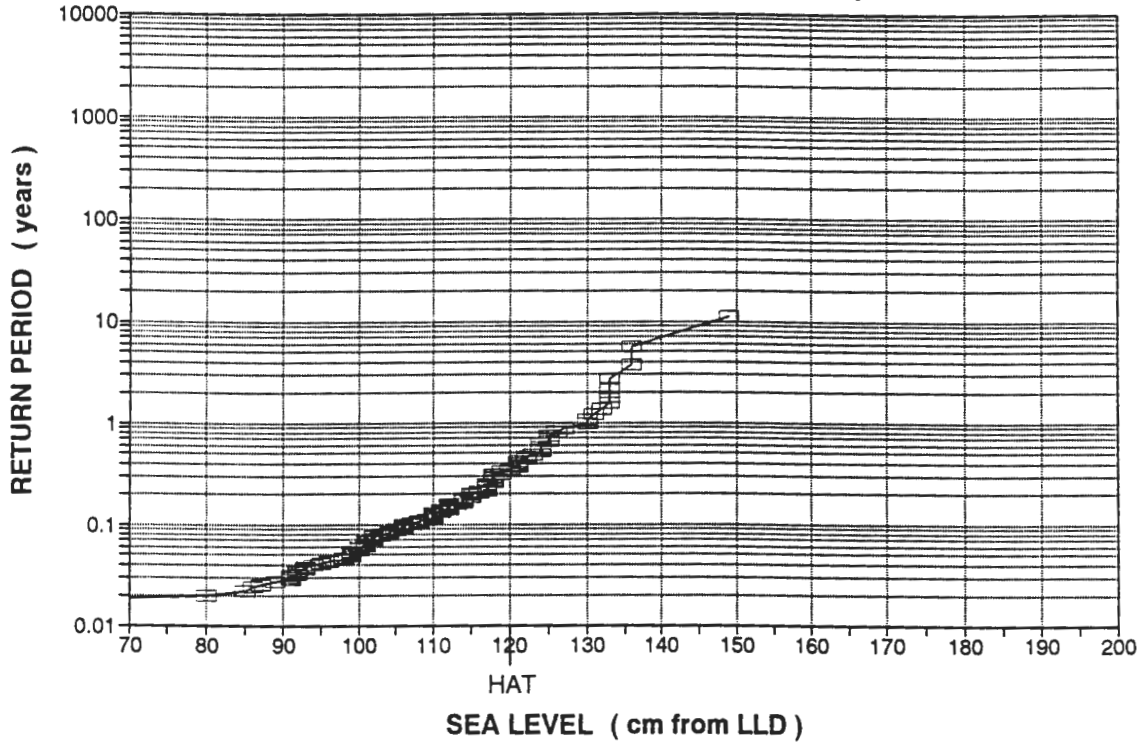


FIG. 4.13 Port Diagrams (continued).

GRANGER BAY (1980-1990)



MOSSEL BAY (1980-1990)

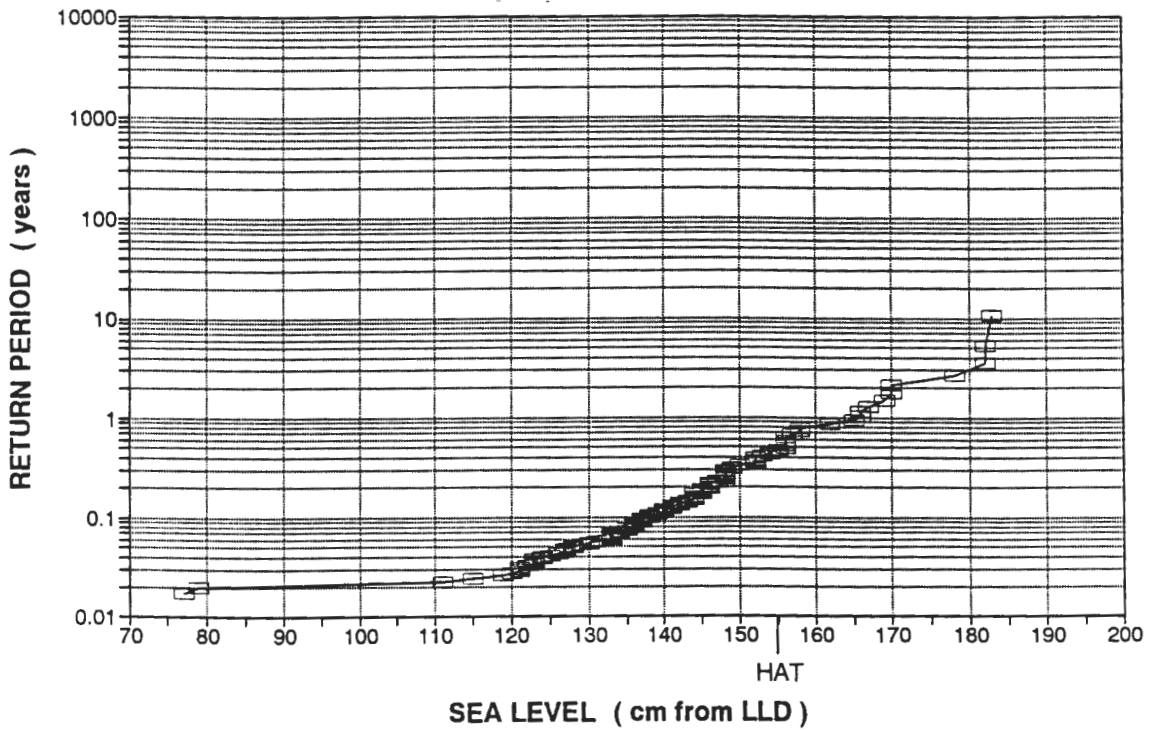
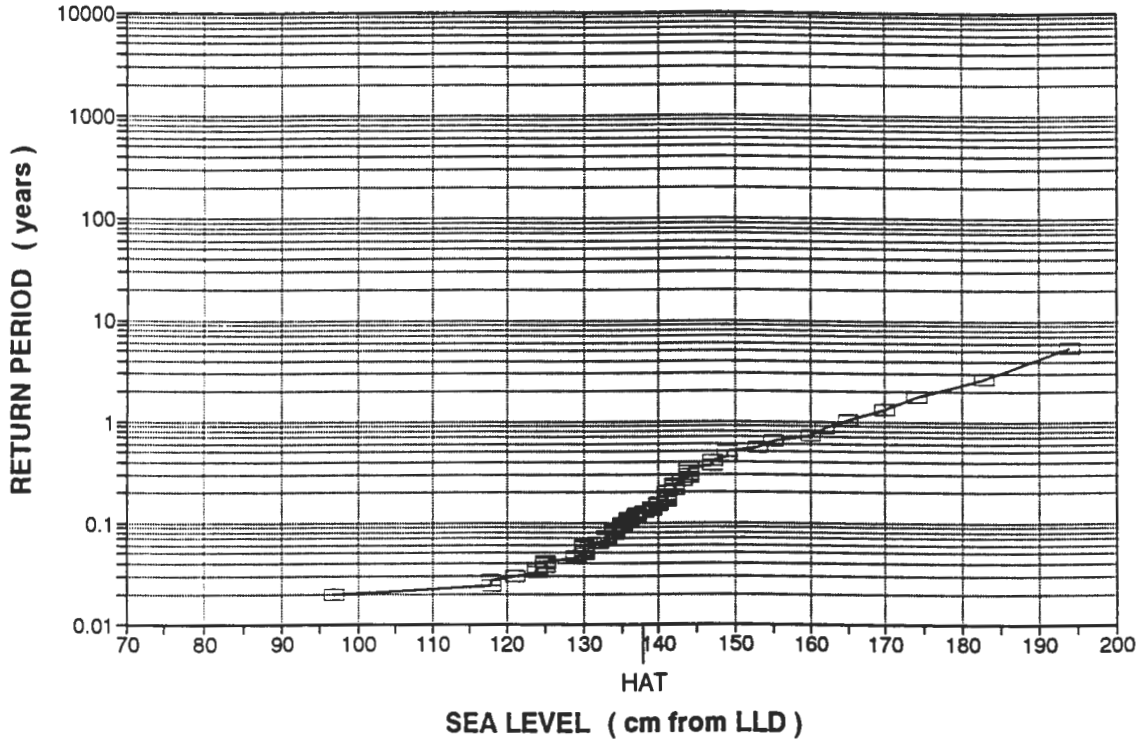


FIG. 4.13 Port Diagrams (continued).

KNYSNA (1980-1985)



PORT ELIZABETH (1979-1990)

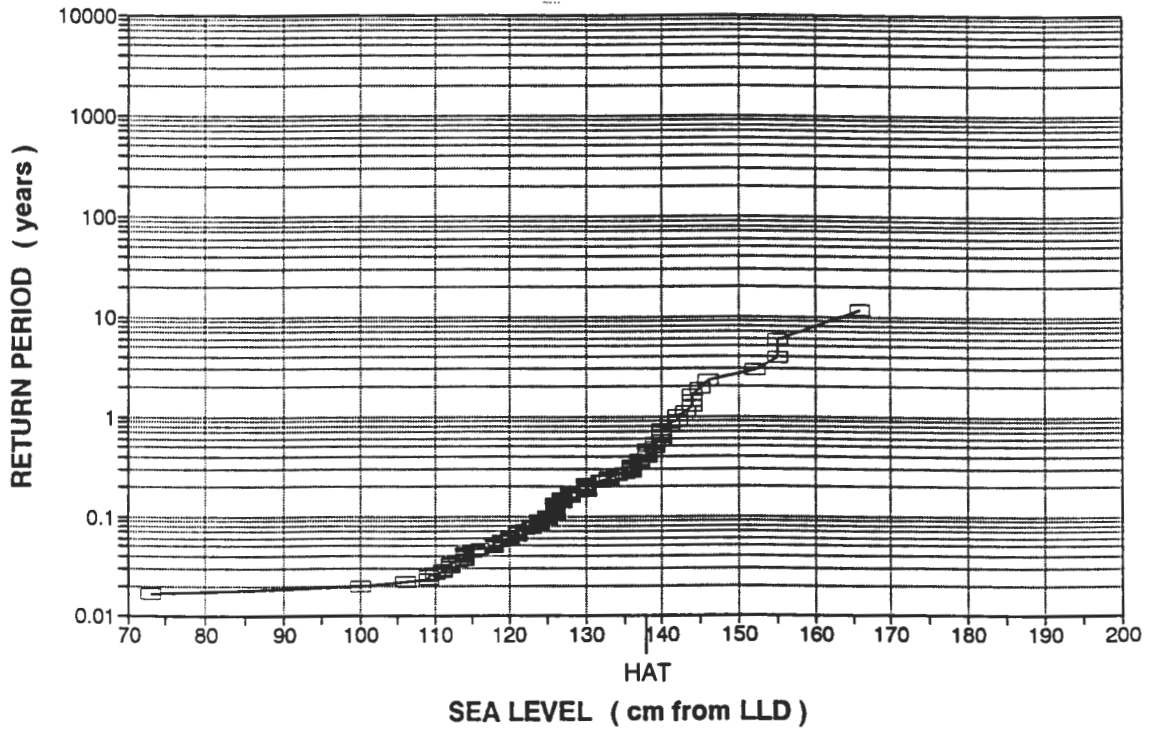


FIG. 4.13 Port Diagrams (continued).

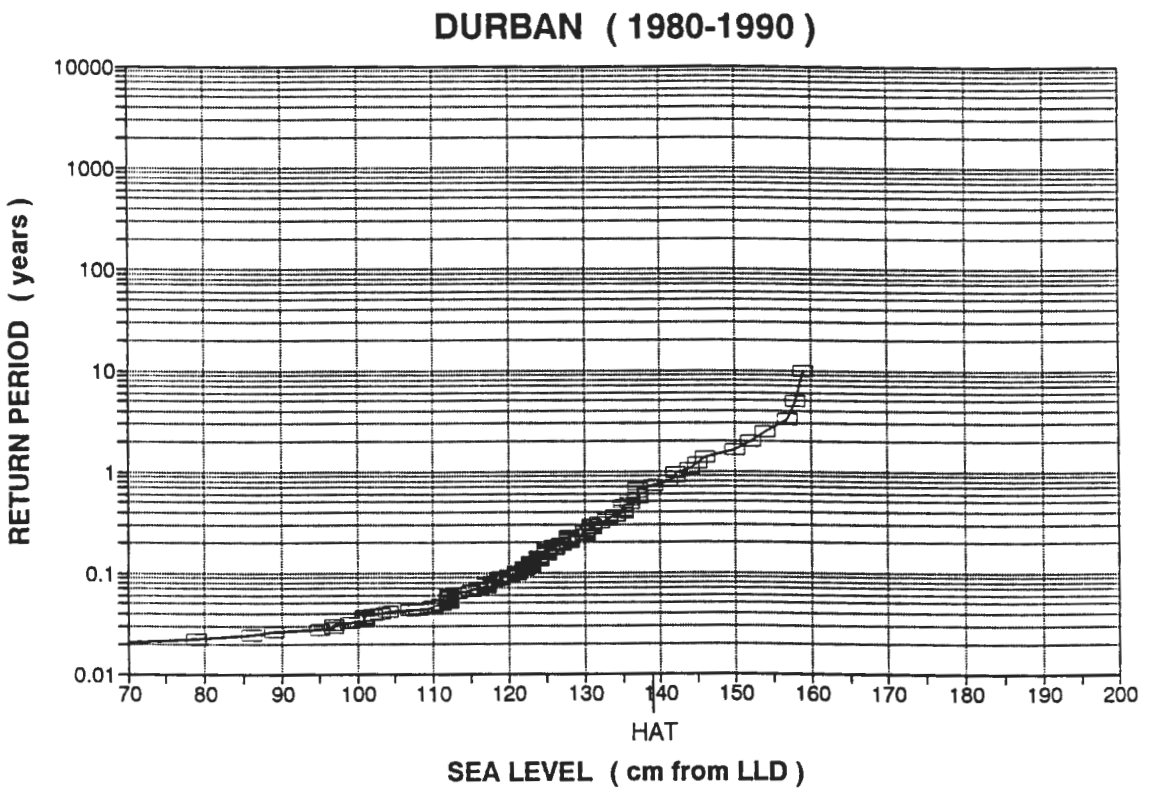


FIG. 4.13 Port Diagrams (continued).

Chapter 5

DISCUSSION

From the results presented in the previous chapter three key points emerge, and these are now further explored and discussed.

- The structure of Southern African sea levels, and that of its tidal and weather determined components, are each remarkably similar around the coast.
- Tides are the dominant contribution to extreme levels, hence the long term character of tidal variations is important in Southern African extremes.
- Tidal characteristics (particularly fortnightly, equinoctial and 4.4 yearly status) determine the expected sea level. From this lead, it is possible to construct exceedance charts of monthly probabilities for any year.

The overall form of observations is strikingly similar at all ports, especially considering the length of coastline covered (approximately 3000 km). The components of sea level are consistent, particularly the magnitudes (Table 4.1) and timing of the tides. Also the weather determined component which due to the travelling synoptic scale meteorology, causes much of the coast to experience the same transient features of pressure and wind. This is reflected in the uniformity of the frequency distribution graphs of residuals, fig. 4.3.

Fig. 5.1 shows the difference in times of arrival of the higher spring high tide of the 9th February 1993 between thirteen sites, obtained from the South

African Tide Tables. At first sight this figure suggests two distinct regions, the west and south coasts at least as far as Hermanus experiencing the high tide within the same eight minutes, and the high tides from Mossel Bay to Richard's Bay occurring some twenty-six to fifty minutes later. The seemingly unusual time lag at Knysna is explained by its location, inside a lagoon where a narrow inlet and shallow water (i.e. friction) delays the progress of the tidal wave (Pugh 1987, p.153). With the exception of Knysna, the two regions appear even more discrete.

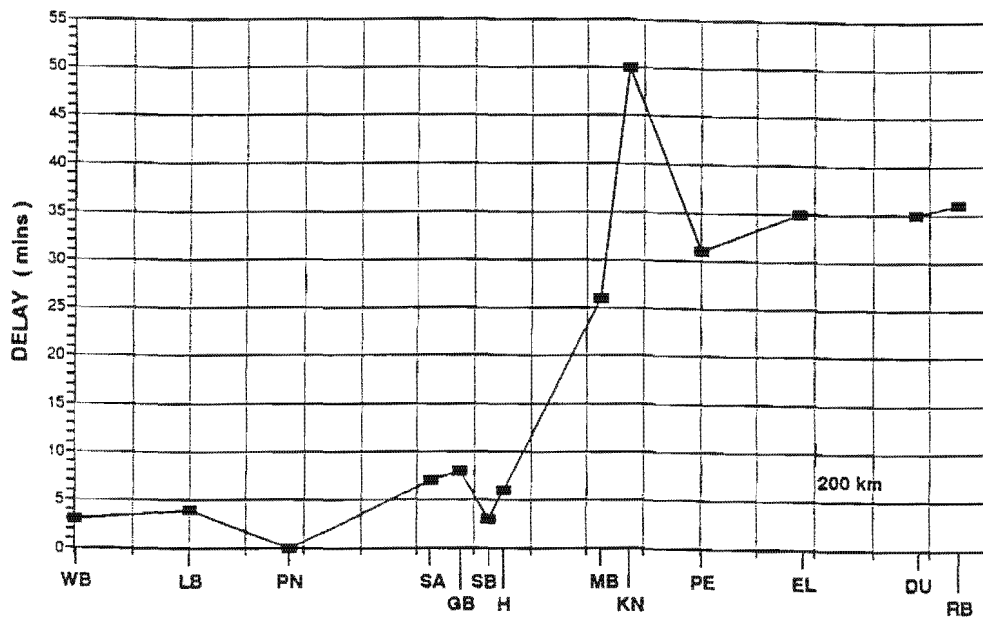


FIG. 5.1 Difference in time of arrival of the higher spring high tide of February 9th 1993, from South African Tide Tables. Port ID's from table 3.1, plus H = Hermanus, EL = East London and RB = Richard's Bay.

Fig. 5.2 is an example of a tidal chart for the M_2 constituent. The convergence of the solid lines (phase legs) indicates a point where there is no vertical displacement and around which the 'tidal wave' progresses. These are

amphidromes, and it can be seen that there are three influencing Southern Africa. In the South Atlantic is shown a system of two counter rotating amphidromic points, the tidal effect of these is felt on the west coast. For tides on the south and east coasts there is a different source situated in the Southwest Indian Ocean.

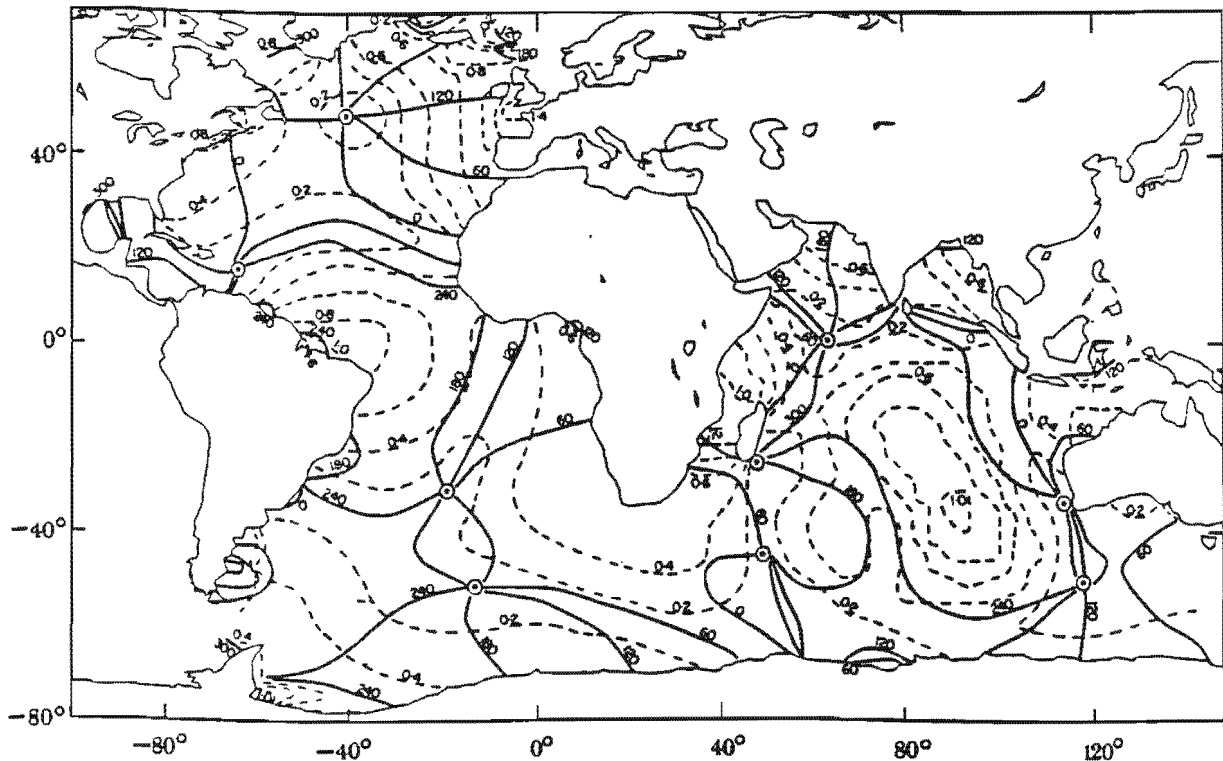


FIG. 5.2 Tidal chart of Atlantic and Indian oceans for M_2 after Cartwright et al 1988. Solid lines - phase lag, dotted lines - amplitude in metres.

In spite of the two region division the differences in time from fig. 4.1 are actually very small when taken as a percentage of the basic 12 hour 25 minute lunar semi-diurnal cycle (table 5.1), less than 5% for all ports except Knysna (6.73%). In other words the timing of the tides is essentially the same all around the coast and the small regional differences that do exist are explained by two 'source' amphidromic points.

Port	Time (SAST)	Difference (in minutes)	Difference (% of 12hr 25 min cycle)
WB	04:47	3	0.40
LB	04:48	4	0.54
PN	04:44	0	0.00
SA	04:51	7	0.94
GB	04:52	8	1.07
SB	04:47	3	0.40
H	04:50	6	0.81
MB	05:10	26	3.49
KN	05:34	50	6.71
PE	05:15	31	4.16
EL	05:19	35	4.70
DU	05:19	35	4.70
RB	05:20	36	4.83

Table 5.1 Timing of the higher spring high tide of 9th February 1993. Port ID's from table 3.1, plus H = Hermanus, EL = East London and RB = Richard's Bay.

This is the form of many indicators (means, maxima etc. Table 4.1 & fig. 4.1): small deviations and differences around the coast often with the same two region division, but within an overall 'sameness'. Two persistent features are the 'high' values at Knysna and 'low' values at Luderitz.

The lagoonal effects at Knysna delay tidal propagation but they also amplify variables such as means and maxima of observed and residual values (table 4.1). However it is not only the shallow water of the lagoon that enhances amplitudes, the proximity of correspondingly 'high' values at Mossel Bay and Port Elizabeth and their larger spread in frequency distributions (figs. 4.2, 4.3, 4.4) shows that the relatively shallow water of the extensive Agulhas Bank provides an additional magnifying effect. This phenomena, the transition and amplification of waves from ocean to shelf is discussed in detail by Pugh (1987, p163). From the location map (fig. 3.1) it should be noted that the continental shelf adjacent to Port Nolloth is wide compared to neighbouring ports. Consequently for sites from Walvis Bay to Simon's Bay many variables, e.g. maximum observed level, tidal standard deviation, M_2 amplitude, tidal range and others (table 4.1, fig. 4.1), all peak at Port Nolloth.

The particularly large values at Knysna have been explained in terms of its physical environment. The very low values characteristic of Luderitz (Table 4.1) can be similarly explained. In this case the presence of a semi-permanent upwelling cell (Shannon 1985) generally suppresses the sea levels and its components at this site.

Observed levels display a strong tidal signature not only evident in the hourly record as regular twice a day (semi-diurnal) and twice a month (spring-neap) components, but also on two longer time scales in monthly extremes: the equinoctial and 4.4 year cycles. The latter three variations can be seen as particularly important in the occurrence of observed extreme events. Springs occur twice a month soon after new and full moon, one 'set' often slightly larger due to the proximity of perigee. At the times of the March or September equinox solar semi-diurnal forces are at a maximum. The coincidence of the moon's perigee which completes one revolution around the earth in 8.8 years with either equinox results in the 4.4 yearly cycle.

These three cycles are known to be influential in the occurrence of extremes for semi-diurnal tidal regimes. Cartwright (1974) distinguished between maximum tide producing forces at a closest approach conjunction (perigee, perihelion, springs) and the maximising of semi-diurnal components at times of equinox and perigee-equinox coincidence (4.4 year cycle). The 18.6 year cycle is more predominant in diurnal or mixed regimes where declinational components are significant (Zetler and Flick 1985) and thus is not of great importance for the strongly semi-diurnal Southern African sites.

The tidal influence in the frequency distribution graphs of hourly observed data is clearly demonstrated (fig. 4.2). Typically there is a broad and slightly noisy profile common to all sites, with the prominence of the double peak diminishing gradually from west to east. The change in form of the observed frequency distributions around the coast is a reflection of the changes in the tidal profiles (fig. 4.4) which become broader and less sharp from between Simon's Bay/Mossel

Bay eastwards. This tidal regionality is due to the two different amphidromic tidal 'sources' and the shallow water effects of the Agulhas Bank. There is some asymmetry of the two peaks, Pugh (1987) suggested this phenomena is common in regions of shallow water. Pugh and Vassie (1978) related the feature to interaction of fourth- and semi-diurnal components and also found noticeable asymmetry at a port with relatively small non-linear (shallow water) tides. The irregularity in neap peaks around the coast of Southern Africa requires further investigation.

Of the seven examples of extreme observed events at Simon's Bay and five at Port Elizabeth (fig. 4.9 b&d) all were coincident with spring, and where applicable the higher spring high tides. The graphs of event composition (fig. 4.8) also show the importance of spring tides, with the majority of extremes at all ports containing a tidal component greater than mean high water springs (MHWS). The difference between MHWS and neaps (from table 4.1) indicates that for any Southern African port this 'spring factor' may add 40-50 cm to a sea level compared to the neap high tides.

For many ports (Luderitz, Port Nolloth, Saldanha, Granger Bay, Mossel Bay and Knysna) the highest few recorded residuals have not been sampled in the monthly extreme events (fig. 4.8), i.e. maximum residuals did not result in an observed monthly maxima. The potential for particularly high extremes at these sites composed of the high surge heights that have already been experienced (not necessarily exceeding previously recorded maxima) and near equinoctial spring high tides has not been realised in these records.

The profiles of averaged monthly maxima of observed levels (fig. 4.10) show the strong tidal equinoctial signal to be dominant at all ports. This average seasonal signal in the tides is nearly 30 cm, but with the additional contribution of a smaller and more 'random' average residual profile the observed levels show only a 20 cm average equinoctial modulation in its extremes.

In the observed monthly maxima time series for four ports (fig. 4.6) the equinoctial signal is very conspicuous and the 4.4 year cycle less so as the eleven

year data sets are too short. In the long thirty year record of monthly maxima from Simon's Bay (fig. 4.5) both cycles are clear in the observed record, with the equinoctial variation accounting for up to 50 cm and the 4.4 year cycle contributing about 10 cm.

The corresponding residual sequence (fig. 4.5a) seems less influential to the observed series with the exception of a particularly high residual in August 1963 that is also apparent as an observed extreme. The examples shown in fig. 4.9 include the circumstance of this particular extreme event: a surge of 39 cm occurred during spring high tides which had a maximum of 194 cm for that month. As a comparison, in September 1981 there was a surge of 30 cm, but this occurred during high equinoctial spring tides with a maximum of 207 cm. With the combination of tide and residual the resultant observed levels were 231 cm in August 1963 and 240 cm in September 1981. Thus although a large storm surge may last days and be superimposed on (semi-diurnal) high tides, unless it is coincident with the times when semi-diurnal tidal forcing is at a maximum (at least during springs near equinox) a high sea level extreme will not be attained.

It should also be remembered that sea level heights are measured by the use of a protected stilling well such that wind waves are effectively damped out, and usually sited within a harbour so that wave set up is unlikely to be recorded. 'Still' water levels are used here and do not take account of wave heights that may, during a storm, be considerable.

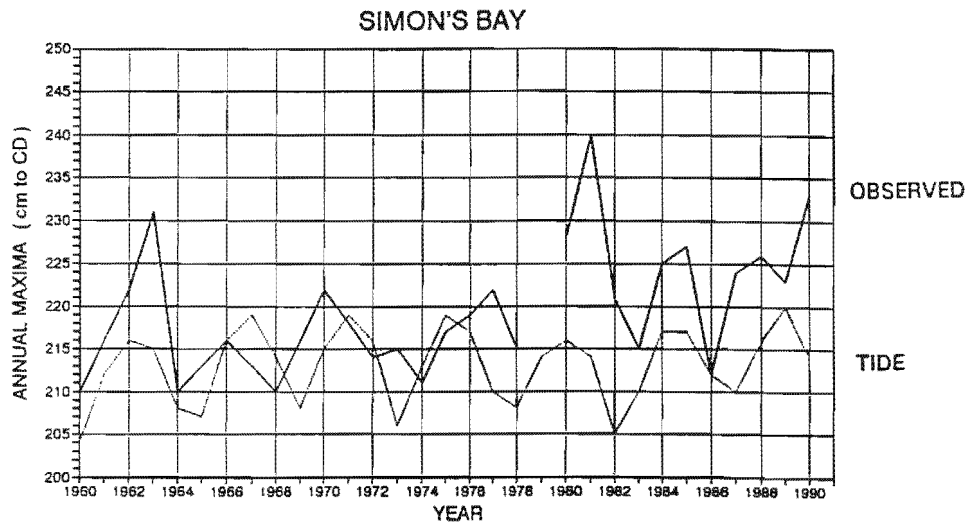
In summary: from looking at the representations of past monthly maxima data the occurrence of extreme events is seen to generally rely on the high state of the tide in relation to the spring, equinoctial and (to a slightly lesser extent) the 4.4 year cycles. Only a small or moderate surge is required to combine with such a high tide in order to produce an extreme observed level.

With the demonstrated importance of tidal characteristics in the structure of observed sea levels and particularly extremes, some attention must be given to the accuracy and quality of tidal predictions that have so far been used for analysis.

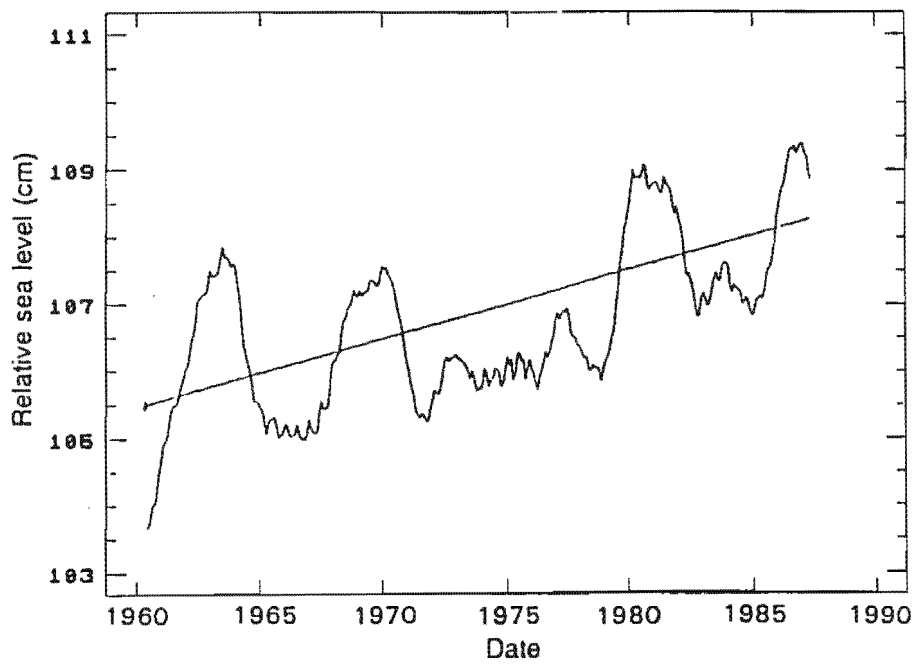
Certain control measures have already been stated (Chapter Three, section 3.2), primarily the quality control of the observed data, but also the need for selecting an analysis year with minimal gaps. These requirements ensure that a reasonable standard of input data is used in the harmonic analysis of one year of observed levels. However there is great reliance on the nature of the year chosen for analysis. Depending on 'storminess' and background interannual cycles, there will be variability in the constituent estimates and therefore also in the predictions.

Storminess at Simon's Bay can be broadly gauged by looking at the time series of monthly maxima residual and observed levels (fig. 4.5 a&c), where both series show more higher extremes occurring since the early eighties. Graff (1981) noticed a similar 'recent' increase in storminess for some British west coast ports, and Blackman and Graff (1978) suggested that trends in annual maxima generally reflect the trends in mean sea level albeit on a widely varying regional scale. For Simon's Bay, Hughes et al (1991) showed a clear but not statistically significant long term rising trend in sea levels of about 6 cm over the last thirty years (this included a factor for the relative movement of land, or isostatic adjustment of 15 mm/decade for South Africa). Fig. 5.3b shows this long term sea level and fig. 5.3a the corresponding annual observed and tidal maxima, the coincidence of peaks is striking. Simon's Bay observed annual maxima have appeared to increase roughly 12 cm over the last thirty years whilst the long term sea level rise accounts for only half that. It may be that other mechanisms are responsible for the increase in the occurrence of extremes e.g. warm water events or changing weather patterns, but it can be reasonably speculated as due to a local response to consequences of large scale global changes (Greenhouse warming etc.). Unfortunately, for the other Southern African sites records generally only exist during the eighties and so assuming some similarity to the trend at Simon's Bay any regional increase in storminess cannot be verified.

For the purposes of further examining the effects of storminess, fifteen different years were used for the generation of fifteen sets of harmonic constituents. An arbitrary selection of twenty-two of the larger constituents is



a)



b)

FIG. 5.3 Simon's Bay: a) Annual maxima observed and annual maxima tidal values and b) long term sea level variation and trend (after Hughes et al 1991).

Constituent	1980's ANALYSIS YEARS:										1960's ANALYSIS YEARS:						Mean	Std	Coeff. of variation		
	80/81	81	82	83	84/85	85	86	87	Mean	Std	Coeff. of variation	61	62	63	64	65				66	67
2 SA	3.2666	1.2645	3.2364	2.0908	4.5114	3.9908	1.8216	3.8448	3.003	1.155	38.448	2.7284	1.3329	1.6932	3.2148	5.3854	3.5649	3.4792	3.057	1.343	43.935
3 SSA	0.4168	1.6499	0.5277	0.8866	2.4358	1.7444	0.5299	2.0368	1.278	0.783	61.230	1.1531	0.3487	0.9435	1.2225	2.3888	0.7782	1.9499	1.255	0.698	55.642
4 MSM	0.4490	0.8463	0.8815	1.3146	1.7974	1.4326	0.8507	0.9339	1.063	0.424	39.869	0.3390	0.8040	2.7705	2.8151	0.7538	0.8858	0.3743	1.249	1.075	86.088
5 MM	0.9794	0.8562	0.8662	1.3288	2.6244	1.6694	0.7260	1.5957	1.331	0.631	47.429	2.0989	0.6299	2.7380	2.4621	1.6368	2.4456	0.4387	1.779	0.919	51.664
6 MSF	0.3729	0.8666	0.6058	1.3513	2.1166	0.9538	0.8713	0.7987	0.992	0.534	53.814	1.3652	0.8367	1.2552	1.5088	0.6083	1.2954	1.3832	1.179	0.328	27.861
7 MF	1.7594	0.6871	0.8558	0.6650	1.7879	0.4341	0.9062	1.2624	1.045	0.509	48.676	0.2787	0.5345	1.3964	1.8063	1.1215	0.6752	0.4566	0.896	0.560	62.559
11 Q1	0.9821	0.8070	0.6940	0.7761	0.6956	1.0497	1.1770	1.0356	0.902	0.182	20.199	0.9889	0.8871	0.8631	0.7370	0.7134	0.8151	0.9442	0.850	0.102	11.986
13 O1	1.6294	1.6171	1.8166	1.8755	1.6429	1.7475	1.6275	1.6727	1.704	0.098	5.771	1.5900	1.5708	1.7497	1.8452	1.7399	1.7522	1.6435	1.699	0.100	5.879
19 P1	1.6178	1.4853	1.6803	1.6511	1.6066	1.6546	1.4576	1.5920	1.593	0.081	5.062	1.5607	1.5361	1.5768	1.3039	1.5529	1.6263	1.6391	1.543	0.112	7.252
20 S1	0.0873	0.1694	0.2775	0.4647	0.5427	0.7041	0.9015	0.7273	0.484	0.289	59.677	0.6307	0.6662	0.8914	1.2170	0.6076	0.4729	0.7524	0.748	0.244	32.569
21 K1	6.0046	6.0493	6.0291	6.1692	6.0456	6.0557	5.9217	5.9651	6.030	0.073	1.210	5.8673	5.9570	5.7769	5.5972	5.9511	5.8621	5.9073	5.846	0.125	2.144
31 2N2	1.8240	1.6712	1.7462	1.5739	1.2190	1.8845	2.1448	2.4623	1.816	0.373	20.517	1.9001	1.6015	1.6450	1.7338	1.5024	1.5851	2.0168	1.712	0.185	10.809
32 MU2	2.0571	1.9225	1.9544	1.7679	2.0827	1.7193	1.6389	1.4150	1.820	0.228	12.522	1.9855	2.1197	1.9921	1.8866	1.8244	1.8015	1.8652	1.925	0.113	5.866
33 N2	11.8176	11.4845	11.7168	11.3248	10.9468	11.2825	11.3940	11.4962	11.433	0.269	2.355	11.4516	11.3978	11.3685	11.5017	11.2153	11.1492	11.1474	11.319	0.146	1.294
34 NU2	2.6219	1.8690	2.0253	2.2794	2.2848	1.7214	2.1942	2.0021	2.125	0.281	13.247	2.0306	2.1267	2.0762	2.0824	2.0699	2.0720	2.1304	2.084	0.035	1.686
36 M2	51.8341	51.5211	51.8967	52.4339	51.3616	52.9844	52.6683	52.2771	52.122	0.565	1.084	51.0000	50.9321	50.6859	50.9068	50.8627	50.8348	50.7235	50.852	0.113	0.222
38 MKS2	0.7945	1.4252	0.4184	0.4790	1.5459	1.3128	0.3652	0.4260	0.846	0.503	59.464	0.2728	0.2960	0.3408	0.2494	0.1747	0.3634	0.3386	0.291	0.065	22.461
40 L2	1.7551	1.3496	1.5909	1.4015	1.2048	1.2271	1.4935	1.4801	1.438	0.184	12.792	1.5956	1.6575	1.5430	1.3794	1.4345	1.2051	0.7322	1.364	0.317	23.214
41 T2	1.4037	1.1731	1.5006	1.0914	2.2444	1.3526	1.7394	1.1157	1.453	0.387	26.611	1.4577	1.2701	1.2758	1.3223	1.3438	1.3878	0.9421	1.273	0.165	12.968
42 S2	23.2168	23.2332	22.9873	23.1294	22.7726	23.4457	23.2321	23.3295	23.168	0.209	0.900	22.6582	22.5493	22.6030	22.7297	22.6177	22.6297	22.9773	22.681	0.142	0.625
44 K2	6.6648	6.5164	6.7057	6.5812	5.9624	5.9551	6.6445	6.5560	6.448	0.308	4.779	6.4180	6.6294	6.3265	6.5930	6.4252	6.5073	6.2894	6.456	0.128	1.984
53 M4	0.6864	0.6336	0.6621	0.6642	0.5789	0.5049	0.4158	0.5321	0.585	0.095	16.190	0.6438	0.6311	0.7535	0.7265	0.8116	0.7864	0.7465	0.728	0.068	9.356

TABLE 5.2 An arbitrary selection of twenty-two of the larger constituents, and variations in the estimates of their amplitudes with analysis year, for two decades 1960's and 1980's at Simon's Bay. All amplitudes, means and standard deviations are in centimetres.

given in table 5.2, corrected amplitudes (to the same time zero) are given for each analysis year and are in two sections, seven years in the 1960's and eight in the 1980's. A years worth of data was required for the analysis programs and in most cases it was convenient to use January to January. However two periods were used outside this convention: April to April 1980/81 and March to March 1984/85.

The 1980's data set shows a slightly greater mean amplitude for most constituents, although there is considerable variability from year to year in both decadal sections. The mean of the Z_0 component has increased from 106.2 cm for the 1960's data set to 108.0 cm in the 1980's, which is comparable with the unadjusted rate of long term sea level rise indicated in fig. 5.3b.

Within the TOGA package standard deviations are calculated for each of the sine and cosine components of the constituent frequencies, they have a relatively constant standard deviation for each set of harmonics (different sets ranging from approximately 0.123 to 0.156 cm) which seems to be derived from residual RMS of the least squares fit. From table 5.2, each constituent's sample standard deviation is also relatively small and constant in absolute terms, but as a percentage of the average value these coefficients of variation become significant.

Consider the predictions for 1993 (fig. 5.4) using the constituents derived from the analysis years 1966, 1980/81, 1984/85, 1986 and heights given in the South African Tide Tables. It is seen that the lowest estimates of tidal heights are from 1966, and the highest predictions are from 1980/81 and 1986, and which are low, high and low periods respectively in terms of long term sea level (fig. 5.3b). From the Simon's Bay time series (fig. 4.5) 1986 is not as 'stormy' as 1980/81 and also low in the tidal 4.4 year cycle hence predictions based on 1986 are slightly smaller. Overall differences in the monthly maxima predicted heights range over about 15 cm but are consistent from one to another.

The accuracy of tidal parameters was discussed in Pugh (1987, p.132) for the port of Lerwick, Scotland. Annual analyses over eight years showed the M_2 amplitude to have a STD equal to 0.5% of mean, the other five constituents considered ranged from 0.4% (S_2) to 6.6% (M_4) as a percentage of mean values.

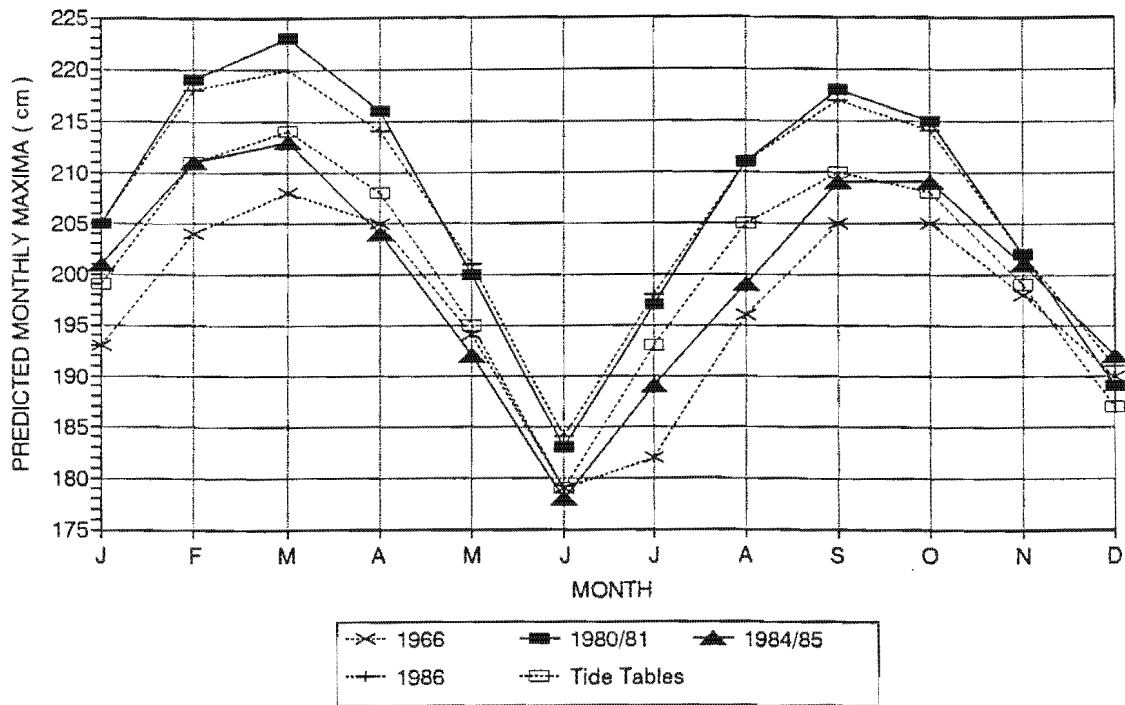


FIG. 5.4 Monthly maxima tidal predictions for 1993 at Simon's Bay using four different analysis periods and South African Tide Tables.

Pugh's results are somewhat less than half of those found for Southern Africa and were nevertheless considered 'not negligible'. Pugh suggested three reasons for the variability of the tidal parameters:

- analysis limitations due to non-tidal energy (surges) at tidal frequencies.
- possible inconsistencies in equipment or hardware (e.g. charts accurate to only two minutes, corresponding to 1° of phase).
- real changes and oceanographic modifications in actual tidal behaviour.

But these are unlikely to be solely responsible for such great variability in the constituent amplitudes shown in table 5.2.

The year used for generation of the Simon's Bay tidal predictions was 1980/81. It is a 'high' year in terms of long term sea level and is at the beginning of a period of increased storminess, but this was balanced by being a complete and contemporary data set with no gaps.

There is much variability of tidal predictions, dependant on the nature of year chosen for analysis. Long term sea level changes can be accounted for in the

Z_0 constituent, but it is uncertain what causes the great diversity in the amplitudes for the remaining constituents. However the overall form and all cycles are persistent in the predictions, albeit with some difference (approximately 15 cm) in peak magnitudes. Further investigation needs to be done on fine tuning this tidal prediction process.

Before proceeding to the third key point in this discussion, that of using the dominant tidal characteristics to determine expected sea levels for Southern African ports, it is appropriate to comment on and discuss the results of the classical annual maxima methods of analysis and its advantages and disadvantages in terms of the Southern African data sets.

The theoretical extrapolations of Gumbel (1958) and Jenkinson (1955) applied to Simon's Bay annual data (1960-1990) agree well with the distribution derived empirically. However, several authors stated reservations and drawbacks on the method of using annual extremes arising from the assumption that annual maxima should be randomly distributed in order to apply the extreme value analysis.

An actual separation of between one and twenty-three months is possible for maxima, should a storm season extend from the end of one year to the beginning of the next. Ackers and Ruxton (1975) solved this by using a July - June year to cover the European winter storm season. In Southern Africa the graphs of average monthly maxima show a lack of major seasonality in residuals, but the profile of observed levels is highly bi-modal influenced more by the tides than surges. Observed extremes tend to occur near March and September so likely separations are between six and eighteen months. Although a problem in annual maxima, seasonality is bypassed by the use of monthly maxima for the empirical distributions.

It is assumed in the statistics that an extreme is equally likely to occur on any hour of any day of the year, but if there is a high sea level it is likely that the adjacent hourly readings or adjacent high tides will also be high. At Port Elizabeth

surges may stay positive for up to 10 days (fig. 4.9c) and combine with many high tides.

Additionally secular changes and cycles in mean sea levels alter extreme distributions but can be simply accommodated using 'reduced' or referenced maxima to a specific year (Suthons 1963). At Simon's Bay with the longest record of thirty years, the increase in long term sea level is estimated to be 2 cm per decade (Hughes et al 1991) and is not statistically significant. The increase in storminess is greater and unfortunately it is also difficult to quantify. Future increases in sea level can be accounted for in the Port Diagrams simply by a translation of the distribution by the projected amount. The main problem in extrapolation is the limitation of data with which to quantify past trends and to predict future changes. Outliers are known to affect results, due to the sensitivity of the statistics to the highest extreme (e.g. Smith 1986). They can also change the shape and direction of the empirical tail considerably.

Lennon (1963) commented on the underutilisation of data involved where one sea level height is used for approximately every 8766 measured and of his shorter data sets of fourteen and eighteen years he noted it "placed a considerable strain on the statistical techniques employed and introduced a consequent anxiety over validity of results obtained". Blackman and Graff (1979) restricted their extrapolations to four times the length of the original data set, which for Simon's Bay would allow for estimations of levels up to the 120-year return period.

Replacing annual maxima with monthly extremes does not visibly alter the empirical distributions for the period 1960-1990 at Simon's Bay (fig. 4.13). The use of monthly maxima provides many more data points specifically of use to the other Southern African ports where data sets are shorter (usually 1980-1990) and the use of theoretical extrapolation techniques is precluded.

However the shorter (1980-1990) Simon's Bay data set shows the empirically derived ten year return period increased by about 10 cm (fig. 4.13). This agrees with the suggested increase in storminess for Simon's Bay as shown by the increase in the number of high annual maxima and consequently is thought

to be a 'real' shift in the Port Diagram. Unfortunately this cannot be verified by any of the other ports because of data limitation.

The form of the Port Diagrams (fig. 4.14) are not usually individually uniform. Deviations from a smooth distribution seem particularly significant at Luderitz and Saldanha where the tail end tends to the vertical and Knysna where the distribution is in two differently sloping parts.

The vertical tail on the distributions implies a ceiling to the maximum attainable level. The severity of the cut off at Luderitz suggests links to the semi-permanent upwelling cell which in some way may suppress extremes but as a similar feature is present at Saldanha an alternative physical process is indicated.

Tide-surge dependence is known to heavily influence the probability distribution (Pugh 1987, Tawn 1988 b). Non-linear hydrodynamical processes lead to the high surges occurring on the rising tide with high tide somehow inhibiting the occurrence of high positive surges. This would explain the shape of distributions at Luderitz and Saldanha although its absence at other Southern African sites is not consistent for a shallow water phenomena e.g. Knysna where the extreme distribution could only be explained as surges favouring times of peak high tides within the lagoon. Any interaction would be evident in the shape of the residual versus tide graphs (fig. 4.8) by the clustering or absence of points representing high surges and high tides. Graff and Ovadia (1980) showed distinct inversely proportioned surge - tidal heights at Liverpool. There appears no conspicuous sampling bias in Southern African sea level extremes.

Regionality is again evident in the Port Diagrams, it can be seen that the empirical tails extend beyond the level of highest astronomical tides (HAT's), by approximately 30 cm on the south and east coasts and about half that on the west coast. At Luderitz the highest observed level is only 2 cm above HAT. This strongly suggests that an interaction is taking place but it has not been possible to provide a reasonable physical explanation.

It is felt that, with the exception of Luderitz where some unknown process is thought to interfere with the occurrence of high sea levels, the uneven tails of

the Port Diagrams must be due primarily to the lack of sufficiently long data sets. Annual maxima methods are known to be sensitive to the highest extremes (Graff 1981) and even with relatively large data sets many authors' results illustrate irregularity in the tail of the empirical distributions (Suthons 1963, Hamon and Middleton 1989, Ackers and Ruxton 1975). Jenkinson (1955) showed this to be the case with several environmental variables. Lennon (1963) suggested the frequency distributions of sea levels are unlikely to be of 'simple form' due to the complexity of the processes and interplay involved.

There is only limited use for the Port Diagrams because of the difficulty in estimating a reasonable visual extrapolation due to the great diversity in individual form, especially at the tail end which is also unfortunately the area of most interest. Nevertheless, the good results of Simon's Bay and the potential for further investigation highlights the need for continuous and accurate long term measurement of sea levels at all ports, for the reliable monitoring of extremes and secular trends.

With the knowledge that tides are the key component in the occurrence of observed extremes a joint probability type approach is developed to produce a first order estimation of the likelihood of exceedance for each month of a year.

The highest astronomical tide for a particular month is known. Therefore the probability of a high sea level being exceeded in that month depends on the likelihood of the necessary residual being exceeded. The residual probability is calculated using the frequency distribution of all residual values measured during that particular month in all available years. Although the residual data set for each month may be small it is representative, can be easily and quickly updated, and the problem of seasonality is bypassed. Thus a probability can be readily calculated for the exceedance of a sea level during that month, for the extreme occurring at the time of highest spring high tide.

By using a monthly time scale for this procedure equinoctial variations are incorporated. In order to take account of the 4.4 year cycle results are calculated

for three scenarios: high, medium and low years. Fig. 5.5 shows predicted monthly maxima tides at Simon's Bay for the nineties, the years chosen as typical for high and low extremes within the 4.4 year cycle were 1993 and 1995 respectively. The average of monthly maxima were used to represent a medium year.

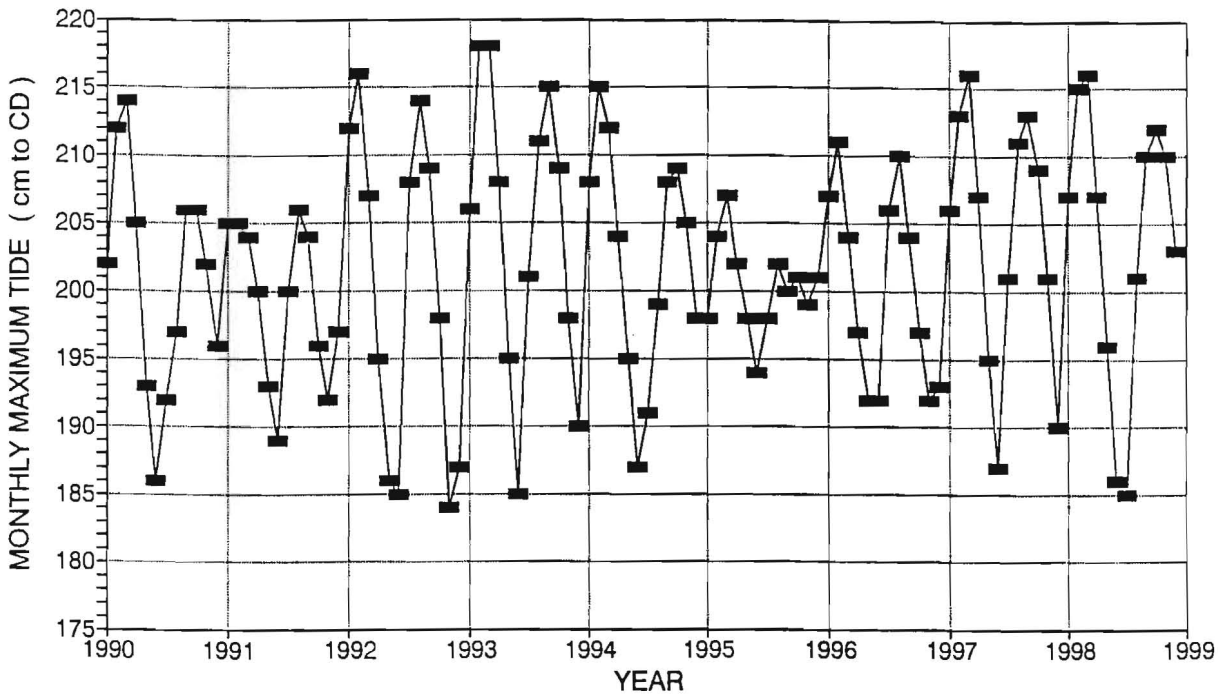


FIG. 5.5 Monthly maxima in predicted tides for 1990-1998 at Simon's Bay.

The known highest monthly astronomical tides shown in fig. 5.5 combined with the the corresponding monthly residual probabilities enable exceedance charts to be constructed. These present the percentage chance of exceedance for sea level heights in each month of three 'representative' years. The three exceedance charts for Simon's Bay are given in fig. 5.6 a-c, and clearly show two interesting points. A decreasing spread of probabilities with decreasing 4.4 year magnitude, and February and March as constant danger months. Consider the sea level height 230 cm (i.e. HAT plus 10 cm) which has only been exceeded in four months in the last thirty years (twice in 1990). For a high year (1997 will be the next) the

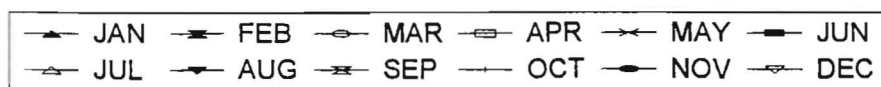
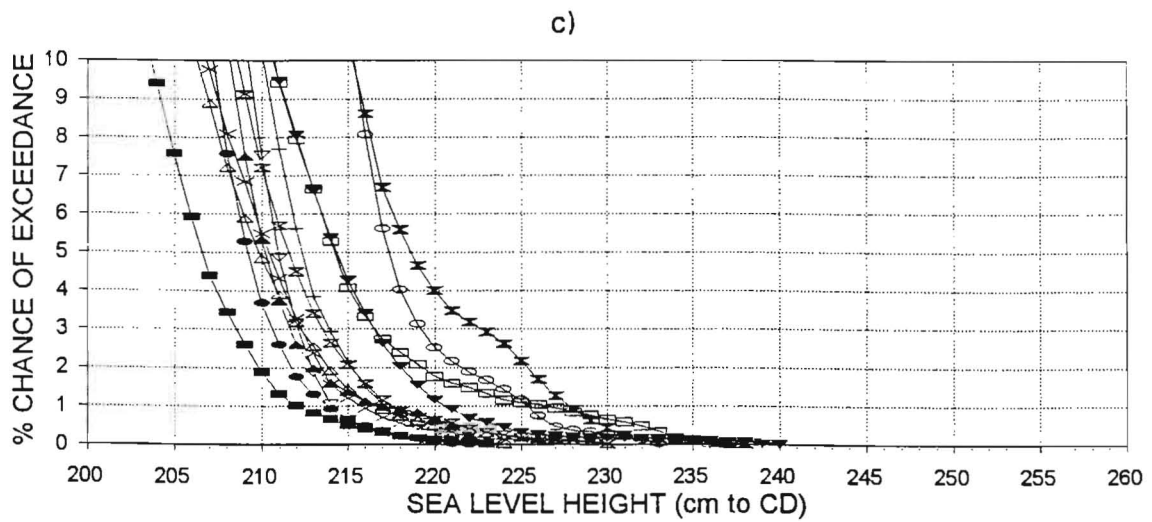
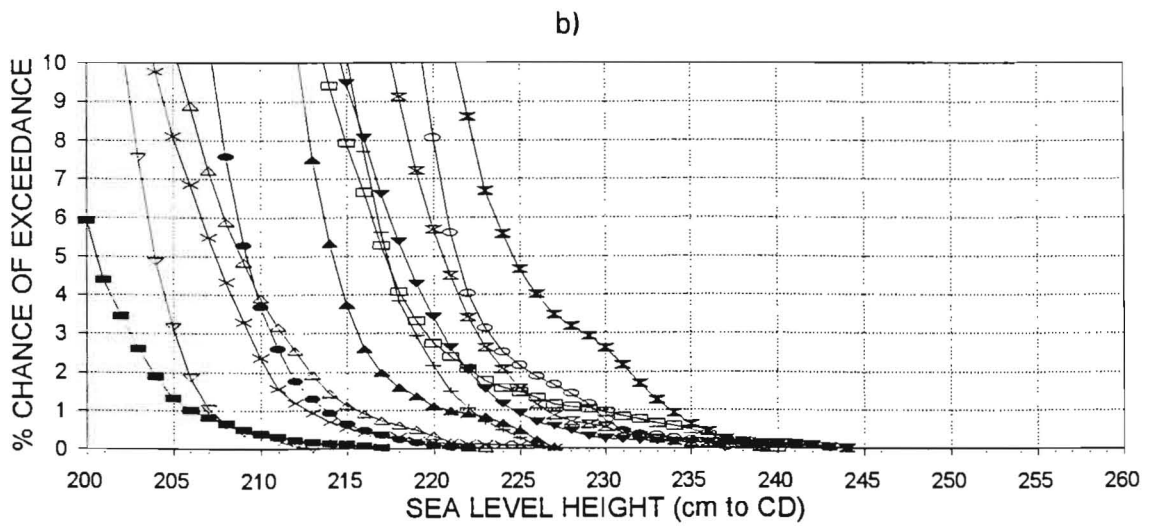
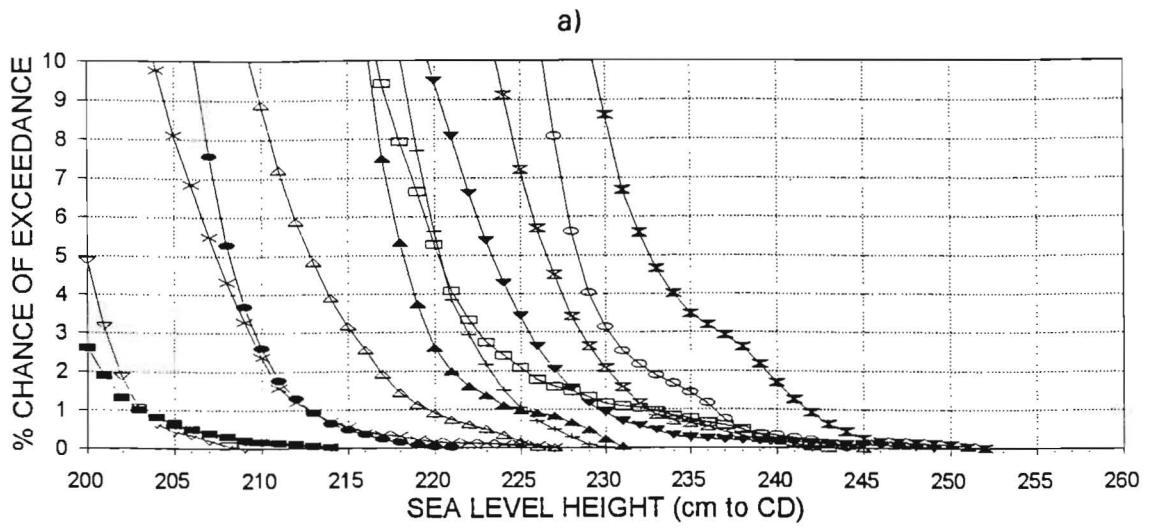


FIG. 5.6 Exceedance charts for Simon's Bay a) a 'high' year: 1993, b) an 'average' year and c) a 'low' year: 1995.

percentage chance of exceedance in February and March are approximately 8.5% and 3% respectively, September is 2%, and April and August around 1%. In an average year February will have 2.5% chance of exceedance, March and April about 1% and September and August dropped to less than 1%. For a low year (1995), all months have a less than 1% chance of exceeding 230 cm.

The noticeable emphasis on February as being most likely to produce extreme sea levels can be explained in part by the seasonal profiles of extremes (fig. 4.10) which show Simon's Bay average monthly maxima tides in February (and March) to be slightly greater than those in September and other months. The exceedance probabilities also depend on residual frequencies which, again from fig. 4.10, show average residual maxima for Simon's Bay to be high during winter months (May - August) and in February. The low predicted tides in winter negate most of the influence of the high winter residuals, whilst February's residual effect is noticeable because its tides are considerable.

For completeness table 5.3 gives the percentage chances of exceedance for the sea level height corresponding to HAT (220 cm above CD) for each month of the years 1990 - 1998. The spread of values between and within years is variable, also shown in fig. 5.6. The months without a likelihood indicate HAT would not be exceeded by the monthly highest tide combined with the largest experienced surge. There is always a possibility that a storm surge may occur exceeding the previously recorded maximum.

The objectives of this thesis were threefold, firstly a basic exploration of the sea level, tidal and residual data, secondly a thorough study of their monthly maxima and thirdly the compilation of Southern African Port Diagrams. These objectives have been fulfilled and some interesting points have emerged. In conclusion the additional findings are now summarised.

The character of sea levels, tides and residuals around the coast of Southern Africa exhibit great similarity. However small regional differences do exist between the west and south coasts and two common features within this are the

	Y E A R								
	1990	1991	1992	1993	1994	1995	1996	1997	1998
JAN	1.1	2.0	18.2	2.6	5.3	0.7	3.7	2.6	3.7
FEB	22.6	4.7	48.8	62.0	42.0	4.0	17.6	28.9	42.0
MAR	18.4	1.7	2.5	40.9	11.1	2.5	1.7	29.3	29.3
APR	2.7	1.5	0.9	5.3	2.4	1.8	1.1	4.1	4.1
MAY	0.1	0.1		0.2	0.2	0.4	0.1	0.2	0.2
JUN						0.1	0.1	0.9	
JUL		0.7	4.9	0.9		0.5	3.2	9.5	
AUG	0.3	3.4	15.6	9.5	0.6	1.2	8.1	14.0	0.9
SEP	2.6	1.6	5.7	20.8	4.5	0.6	1.6	5.6	7.2
OCT	2.2			5.6	5.6	0.3		0.2	13.2
NOV	0.3				0.9	0.1			5.3
DEC									0.2

TABLE 5.3 Percentage likelihood of exceeding HAT (220 cm above CD) for each month 1990-1998 at Simon's Bay.

consistently lower values at Luderitz (due to a semi-permanent upwelling cell) and higher values at Knysna (due to shallow water lagoonal effects).

Tides are the dominant contribution to sea level extremes. Three modulations in the long term tidal variations are particularly important: fortnightly, equinoctial and 4.4 year cycles. From this information and the fact that tides are deterministic, a prediction technique has been developed.

Probabilities of exceedance are calculated for specific months and can be presented as an exceedance chart for a particular year. This explicit prediction is potentially more useful than traditional return periods for certain activities in the coastal environment such as harbour management and mariculture. It is relatively simple to undertake, uses all available data and is suitable for short data sets.

Although developed as a first order estimation, this method could potentially be expanded in future work. The probability of the extreme is for the highest monthly tide, but to improve the accuracy of the likelihoods a tidal probability could be derived in the same manner as the residual frequencies.

Other issues have arisen in this thesis and need further investigation. There is great variability in the tidal constituents derived from different analysis periods. It is not known what causes this discrepancy, although it seems in part to reflect changing storminess and interannual long term sea levels.

Two ports in particular warrant future research. Luderitz appears anomalous in several respects, highlighted by the Port Diagram that shows the highest observed levels to be only 2 cm above HAT. An unknown process inhibiting extremes is suggested, possibly with connections to the local upwelling cell. Knysna displays some interesting and unusual behaviour, presumably due to the deep lagoon. Its Port Diagram seems to suggest a process is taking place that 'enhances' extremes i.e. some interaction causing the surges to develop more strongly at high tide.

REFERENCES

- ACKERS, P. and RUXTON, T.D. (1975) Extreme levels arising from meteorological surges. Proc. 16th Coastal Eng. Conf., Copenhagen, 1974, Vol. 1 Amer. Soc. of Civ. Engrs., New York, 69-86.
- BLACKMAN, D.L. and GRAF, J. (1978) The analysis of annual extreme sea levels at certain ports in southern England. Proc. Instn. Civ. Engrs., Part 2 1978, Vol. 65, 339-357.
- BRINK, K.H. (1990) On the damping of free coastal trapped waves. J. Phys. Oceanogr., Vol. 20, 1219-1225.
- BRUNDRIT, G.B. and SHANNON, L.V. (1989) Cape storms and the Agulhas Current: a glimpse of the future ? S. Afr. J. Sci., Vol. 85, 619-620.
- CALDWELL, P.C. and KILONSKY, B.J. (1988) Manual for the TOGA Sea Level Center / National Oceanographic Data Center software package.
- CARTWRIGHT, D.E. (1974) Years of peak astronomical tides. Nature, Vol. 248, No. 5450, 656-657.
- CARTWRIGHT, D.E. (1980) The historical development of Tidal Science, and the Liverpool Tidal Institute. Oceanography The Past, ed. Sears and Merriman, Springer-Verlag, New York, 240-251.
- CARTWRIGHT, D.E., SPENCER, F.R.S., VASSIE, J.M. and WOODWORTH, P.L. (1988) The tides of the Atlantic Ocean, 60°N to 30°S. Phil. Trans. Roy. Soc. Lond., Vol. 324, 513-563.
- DAMES and MOORE (1979) KNPS: Tsunami Risk Evaluation. Report 9629-009-45, Escom (unpublished).
- DEACON, M. (1971) Scientists and the sea. Academic Press, London.
- DE CUEVAS, B.A. (1985) Characteristics of sub-tidal coastal trapped disturbances in sea level along the coasts of Namibia and South Africa. M.Sc. thesis, Univ. of Cape Town, S.A.
- DEFANT, A. (1961) Physical Oceanography, Vol. 2. Pergamon Press, London.

- JURY, M.R., SHILLINGTON, F.A., PRESTIDGE, G. and MAXWELL, C.D. (1986) Meteorological and oceanographic aspects of a winter storm over the south-western Cape Province, South Africa. *S. Afr. J. Sci.*, Vol. 82, 315-319.
- KING, C.A.M. (1962) *An introduction to oceanography*. McGraw Hill, New York.
- LENNON, G.W. (1963) A frequency investigation of abnormally high tidal levels at certain west coast ports. *Proc. Instn. Civ. Engrs.*, Vol. 25, 451-484.
- LENNON, G.W. (1965) The treatment of hourly elevations of the tide using an IBM 1620. *Int. Hydr. Rev.*, Vol. 42, No. 2, 125-148.
- MARKANDAY, S. and SRIVASTAVA, P.S. (1980) *Physical oceanography in India: An historical sketch*. *Oceanography The Past*, ed. Sears and Merriman, Springer-Verlag, New York, 551-561.
- MERRY, C.L. (1982) Variations in mean sea level on the South African coast. 7th Conf. of S.A. Surv., Jhb.
- MIDDLETON, J.F. and THOMPSON, K.R. (1986) Return periods of Extreme sea levels from short records. *J. Geophys. Res.*, Vol. 91, 11707-11716.
- PUGH, D.T. (1987) *Tides, Surges and Mean Sea Level*. John Wiley and Sons, New York.
- PUGH, D.T. and VASSIE, J.M. (1978) Extreme sea levels from tide and surge probability. *Proc. 16th Coastal Eng. Conf., Hamburg. Amer. Soc. civ. Engrs, New York.*, Vol. 1, 911-930.
- ROBINSON, A.R. (1964) Continental shelf waves and response of sea level. *J. of Geophys. Res.*, Vol. 69, No. 2., 367-368.
- ROSENTHAL, G. and GRANT, S. (1989) Simplified tidal prediction for the South African coastline. *S. Afr. J. Sci.*, Vol. 85, 104-107.
- SCHUMANN, E.H. (1983) Long period coastal trapped waves off the southeast coast of Southern Africa. *Cont. Shelf Res.*, Vol. 2., No. 2/3, pp. 97-107.
- SCHUMANN, E.H. and BRINK, K.H. (1990) Coastal trapped waves off the coast of South Africa: Generation, propagation and current structures. *J. Phys. Oceanogr.*, Vol. 20, 1206-1218.

- SHANNON, L.V. (1985) The Benguela ecosystem Part I. Evolution of the Benguela, physical features and processes. *Oceanogr. Mar. Biol. Ann. Rev.*, Vol. 23, 105-182.
- SHANNON, L.V., BOYD, A.J., BRUNDRIT, G.B. and TAUNTON-CLARK, J. (1986) On the existence of an El Nino type phenomenon in the Benguela system. *J. Mar. Res.*, Vol. 44, 495-520.
- SHILLINGTON, F.A. (1984) Long period edge waves off southern Africa. *Cont. Shelf Res.*, Vol. 3, No. 4, 343-357.
- SMITH, F.G.W. (1973) *The seas in motion*. Thomas Y. Crowell, New York.
- SMITH, R.L. (1986) Extreme value theory based on the r largest annual events. *J. Hydrology*, Vol. 86, 27-43.
- SUTHONS, C.T. (1963) Frequency of occurrence of abnormally high sea levels on the east and south coasts of England. *Proc. Instn. Civ. Engrs.*, Vol. 25, 443-449.
- TAWN, J.A. (1988 a) An extreme value theory model for dependent observations. *J. Hydrology*, Vol. 101, 227-250.
- TAWN, J.A. (1988 b) Extreme value theory with oceanographic applications. Ph.D. thesis, Univ. of Surrey, U.K.
- TAWN, J.A., and VASSIE, J.M. (1989) Extreme sea levels: the joint probabilities method revisited and revised. *Proc. Instn. Civ. Engrs.*, Part 2 1989, Vol. 87, 429-442.
- TAWN, J.A., and VASSIE, J.M. (1990) Spatial transfer of extreme sea level data for use in the revised joint probability method. *Proc. Instn. Civ. Engrs.*, Part 2 1990, Vol. 89, Technical note 535.
- DAILY WEATHER BULLETINS. Weather Bureau, Dept. of Envir. Affairs, S.A., published monthly.
- WARNER, B. and WARNER, N. (1984) *Maclear and Herschel letters and diaries at the Cape of Good Hope 1834 - 1838*. A.A. Balkema, Cape Town.
- WHP (1976) Koeberg Nuclear Power Station. Report on extreme water levels. Watermeyer Halcrow & Partners, Johannesburg (unpublished).

- WILKINSON, J.H. (1965) The algebraic eigenvalue problem. Clarendon press, Oxford.
- WIJNBERG, A.R. (1993) Design sea levels for Southern Africa. Ph.D. thesis, Univ. of Cape Town, S.A.
- WOOD, F.J. (1986) Tidal dynamics. D. Reidel, Dordrecht.
- YANG ZUOSHENG, EMERY, K.O., and XUI YUI (1989) Historical development and use of thousand-year-old tide-prediction tables. *Limnol. Oceanogr.*, Vol. 34, No. 5, 953-957.
- ZETLER, B.D., and FLICK, R.E. (1985) Predicted high tides for mixed tide regimes. *J. Phys. Oceanogr.*, Vol. 15, 357-359.

ACKNOWLEDGEMENTS

I am grateful to Capt. Mike Thompson and the Hydrographic Department of the South African Navy for the tidal data which they supplied and additional assistance in solving minor problems in data verification.

I would also like to thank my supervisor Professor Geoff Brundrit for advice and suggestions, particularly for his guidance during the final stages of this thesis.